



U.S. Department
of Transportation

**National Highway
Traffic Safety
Administration**



DOT HS 813 434

April 2023

A Modeling Study on Child Occupant Safety With Unconventional Seating Configurations

DISCLAIMER

This publication is distributed by the U.S. Department of Transportation, National Highway Traffic Safety Administration, in the interest of information exchange. The opinions, findings, and conclusions expressed in this publication are those of the authors and not necessarily those of the Department of Transportation or the National Highway Traffic Safety Administration. The United States Government assumes no liability for its contents or use thereof. If trade or manufacturers' names or products are mentioned, it is because they are considered essential to the object of the publications and should not be construed as an endorsement. The United States Government does not endorse products or manufacturers.

NOTE: This report is published in the interest of advancing motor vehicle safety research. While the report may provide results from research or tests using specifically identified motor vehicle models, it is not intended to make conclusions about the safety performance or safety compliance of those motor vehicles, and no such conclusions should be drawn.

Suggested APA Format Citation:

Wu, J., Boyle, K., Orton, N. R., Manary, M. A., Reed, M. P., & Kliunich, K. D. (2023, April). *A modeling study on child occupant safety with unconventional seating configurations* (Report No. DOT HS 813 434). National Highway Traffic Safety Administration.

Technical Report Documentation Page

1. Report No. DOT HS 813 434	2. Government Accession No.	3. Recipient's Catalog No.	
4. Title and Subtitle A Modeling Study on Child Occupant Safety With Unconventional Seating Configurations		5. Report Date April 2023	
		6. Performing Organization Code	
7. Authors Jingwen Hu, Kyle Boyle , Nichole Ritchie Orton , Miriam A. Manary, Matthew P. Reed , Kathleen D. Klinich		8. Performing Organization Report No. UMTRI 2022-XX	
9. Performing Organization Name and Address University of Michigan Transportation Research Institute 2019 Baxter Rd. Ann Arbor, MI 48109		10. Work Unit No.	
		11. Contract or Grant No. DTNH2215D00017/693JJ920F000158	
12. Sponsoring Agency Name and Address National Highway Traffic Safety Administration 1200 New Jersey Avenue SE Washington, DC 20590		13. Type of Report and Period Covered Final	
		14. Sponsoring Agency Code	
15. Supplementary Notes The authors would like to acknowledge Jen Bishop and Brian Eby with their assistance in testing, and Yushi Wang for modeling.			
16. Abstract <p>This study uses computer models to study how unconventional seating positions and orientations such as those conceptualized to be offered in vehicles with Automated Driving Systems (ADS) may affect occupant response metrics of children restrained by child restraint systems (CRS) equipped with internal harnesses (CRS harness-restrained) or vehicle lap-shoulder belts, with and without belt-positioning boosters.</p> <p>We first conducted a literature review to frame a simulation plan, including selections of surrogate vehicles, potential seating arrangements, impact scenarios, anthropomorphic test device (ATD) models, and CRS models that are relevant to the selected ATD occupant models. Due to lack of impact tests with child ATD and CRS in farside, oblique, and rear impacts, we conducted 16 sled tests with CRS harness-restrained ATDs and belt-restrained ATDs in conventional and unconventional vehicle seat orientations in frontal, farside, oblique, and rear impact conditions, and used the sled tests to validate a set of computational models. A total of 550 Mathematical Dynamic Models (MADYMO) simulations were then conducted with the CRABI 12MO in rear-facing CRS, the H33YO in both rear-facing and forward-facing CRS, the H36YO in a backless booster, and the H310YO with and without a booster across a range of conventional and unconventional seating locations and orientations under five impact directions and various CRS installation methods. We did not find major safety concerns in ATDs that were restrained using a CRS equipped with an internal harness based on the nature of ATD contacts. This is the first study using different child ATDs and CRSs to investigate child occupant responses in a wide range of impact directions and seating orientations. Results from the sled tests and simulations provide a better understanding of child occupant responses in those crash conditions, but also identified several limitations of using frontal ATDs in other crash directions.</p>			
17. Key Words automated vehicles, child restraint systems, unconventional seating, sled tests, computational modeling		18. Distribution Statement This document is available to the public from the National Highway Traffic Safety Administration, National Center for Statistics and Analysis, crashstats.nhtsa.dot.gov	
19. Security Classif. (of this report)	20. Security Classif. (of this page)	21. No. of Pages 98	22. Price

Table of Contents

Introduction.....	1
Literature Review	3
Overview.....	3
Methods.....	3
Results.....	4
ADS-Equipped Vehicles.....	4
ADS-Related Possible Unconventional Seating.....	5
Crash Scenarios Associated With Conventional and Future ADS-Equipped Vehicles.....	6
Vehicle Interior Models, Child Occupant Models, and CRS Models Available.....	8
Child Occupant Modeling Studies.....	10
Child ATD Testing.....	17
Child Injury Measures and IARVs.....	27
Summary of the Literature Review.....	27
Simulation Conditions	29
Vehicle Models.....	29
Seating Arrangements and Occupant Seating Locations.....	29
Crash Configurations and Severities.....	30
ATD, CRS, and Vehicle Seat Models.....	31
Validation Testing.....	33
Sled Test Matrix.....	33
Sled Pulses.....	34
Data Collection.....	35
Results.....	36
Frontal Impacts.....	36
Oblique Impacts.....	37
Side Impacts.....	37
Rear Impacts.....	38
Model Validation.....	40
Kinematics Validation.....	40
CORA Scores for ATD Head Excursion Time Histories.....	45
ATD Injury Measure Validation.....	46
Simulations of ATDs in Harnessed CRS.....	47
Simulation Matrix.....	47
Injury Measures and Contact Definition.....	47
Data Analysis.....	48
Simulation Results.....	48
CRABI 12MO in RFCRS.....	48
H33YO in RFCRS.....	51
H33YO in FFCRS.....	54
Simulations of Vehicle Belt-Restrained ATDs	57
Simulation Methods.....	57

Simulation Results	57
H36YO in Booster	57
H310YO With and Without Booster.....	61
Discussion.....	65
Safety Concerns	65
Head Contacts for Older Children in Farside Impacts.....	65
Injury Concerns for Children Restrained by Harnessed CRS.....	65
Rear and Rear-Oblique Impacts.....	66
Conventional Seating Versus Unconventional Seating	66
Potential Countermeasures.....	67
Belt-Restrained Older Children in Farside/Oblique Impacts.....	67
Children Using Harnessed CRS in Farside/Oblique Impacts	67
Limitations	67
Summary.....	69
References.....	70
Appendix A: ADS-Equipped Highly Automated Vehicles.....	A-1
Appendix B: Differences in Benches	B-1
2014 Bench	B-1
2015 Bench	B-2
2018 Bench	B-2
Appendix C: Overlay Plots From Validation Tests	C-1

List of Figures

Figure 1. Exemplar vehicles with high-level ADS	5
Figure 2. Five different seating positions from the study	5
Figure 3. Six feasible seat configurations in passenger scenarios used in Nie et al.,2020	6
Figure 4. Distribution of planar crashes by PDOF based on NASS-CDS	7
Figure 5. Distribution of crash types and percentage of crash avoided with CCAT	8
Figure 6. Exemplar vehicle interior models available at UMTRI	9
Figure 7. MADYMO (Siemens) and FE (Humanetics) child ATD models	9
Figure 8. Examples of CRS models in the field.....	10
Figure 9. UMTRI’s improved, scalable MADYMO child ATD model	12
Figure 10. Pareto-optimal designs for children, midsize male adults, and infants in RFCRS.....	13
Figure 11. Optimized child seat model development and validation.....	14
Figure 12. Simulation and testing results with H36YO in frontal crashes	14
Figure 13. Examples of CRS scans in one of the ISO envelopes	15
Figure 14. Exemplar head trajectories of children overlaid in vehicle second-row geometries...	17
Figure 15. Comparison of Dodge Grand Caravan and Ford Fiesta interiors relative to the forward-facing vehicle seats	29
Figure 16. Proposed crash scenarios, seating configurations, and seating locations	30
Figure 17. Scaled FMVSS No. 213 frontal pulse and NCAP side impact pulses.....	31
Figure 18. Illustration of vehicle seat mounted rear-facing on FMVSS No. 213 bench	34
Figure 19. Comparison of UMTRI sled approximation of FMVSS No. 213 pulse, a completely compliant pulse, the FMVSS No. 213 corridor, and an average of the FMVSS No. 213 corridor.....	35
Figure 20. Example screen shots of six camera views used in study: rear, rear oblique, lateral, front oblique, front, and overhead.....	36
Figure 21. Comparison of peak head excursion from tests NT1419 (left) and NT2102 (right) ...	37
Figure 22. Extreme rotation of RF H33YO, H36YO, and H310YO during lateral tests.....	38
Figure 23. Comparison of model and test for CRABI 12MO in infant seat at time of peak excursion in various impact conditions.....	40
Figure 24. Comparison of model and test for H33YO in rear-facing convertible at time of peak excursion in frontal impact	41
Figure 25. Comparison of model and test for H33YO in forward-facing convertible at time of peak excursion in frontal impact	42
Figure 26. Comparison of model and test for H36YO in backless booster in various impact conditions.....	43
Figure 27. Comparison of model and test for H310YO in frontal impact conditions	44
Figure 28. Model-predicted CRS/injury measures for CRABI 12MO in RFCRS by effective crash angle	49
Figure 29. Factor effects on HIC of CRABI 12MO in RFCRS.....	50
Figure 30. Factor effects on chest acceleration for CRABI 12MO in RFCRS	50
Figure 31. Factor effects on CRS rotation for CRABI 12MO in RFCRS	51
Figure 32. Model-predicted injury measures for H33YO in RFCRS at various impact directions.....	52
Figure 33. Factor effects on HIC15 for H33YO in RFCRS	52
Figure 34. Factor effects on chest acceleration for H33YO in RFCRS.....	53

Figure 35. Factor effects on chest deflection for H33YO in RFCRS	53
Figure 36. Model-predicted injury measures for H33YO in FFCRS at various impact directions.....	54
Figure 37. Factor effects on HIC15 for H33YO in FFCRS	55
Figure 38. Factor effects on chest acceleration for H33YO in FFCRS	55
Figure 39. Factor effects on chest deflection for H33YO in FFCRS.....	56
Figure 40. Model-predicted injury measures for H36YO in booster at various impact directions.....	58
Figure 41. actor effects on HIC15 for H36YO in booster	58
Figure 42. Factor effects on chest acceleration for H36YO in booster	59
Figure 43. Factor effects on chest deflection for H36YO in booster.....	59
Figure 44. Factor effects on ATD to vehicle contact scaler for H36YO in booster	60
Figure 45. ATD to vehicle contact distribution and exemplar contact cases for H36YO in booster.....	60
Figure 46. Model-predicted injury measures for H310YO at various impact directions	61
Figure 47. Factor effects on HIC15 for H310YO	62
Figure 48. Factor effects on chest acceleration for H310YO	62
Figure 49. Factor effects on chest deflection for H310YO.....	63
Figure 50. Factor effects on ATD to vehicle contact scaler for H310YO	64
Figure 51. ATD to vehicle contact distribution and exemplar contact cases for H310YO	64
Figure A-1. ADS-equipped highly automated vehicles	A-3
Figure B-1. 2014 version of the updated 213 bench used for the test series	B-1
Figure B-2. 2015 Version of the updated 213 bench	B-2
Figure B-3. 2018 version of the updated 213 bench.....	B-3
Figure B-4. Comparison of the 213 bench used for booster metrics (left) and misuse (right) ...	B-4
Figure B-5. Overlay of the 2018 bench and 2020 drawing.....	B-5
Figure C-1. Head resultant acceleration for tests with CRABI 12MO and H33YO.....	C-1
Figure C-2. Head resultant acceleration for tests with H36YO and H310YO.....	C-1
Figure C-3. Chest resultant acceleration for tests with CRABI 12MO and H33YO	C-2
Figure C-4. Chest resultant acceleration for tests with H36YO and H310YO.....	C-2
Figure C-5. Neck resultant force for tests with CRABI 12MO and H33YO.....	C-3
Figure C-6. Neck resultant force for tests with H36YO and H310YO.....	C-3
Figure C-7. Neck resultant moment for tests with CRABI 12MO and H33YO.....	C-4
Figure C-8. Neck resultant moment for tests with H36YO and H310YO.....	C-4

List of Tables

Table 1. A List of Vehicles With High-Level ADS.....	4
Table 2. Delta V Percentiles for Each Planar Crash Mode Based on NASS-CDS.....	7
Table 3. Child Modeling Studies for Crash Safety in the Literature	11
Table 4. Crash Tests With Child ATDs Between 2000 and 2020	18
Table 5. FMVSS No. 213 Injury Criteria	27
Table 6. H3 Child ATD IARVs	27
Table 7. Sled Test Matrix.....	33
Table 8. Frontal Injury Reference Measures.....	36
Table 9. Oblique Injury Reference Measures	37
Table 10. Side Impact Validation Test Injury Measures	38
Table 11. Rear Impact Validation Test Injury Measures	39
Table 12. CORA Scores for Head Excursions*	45
Table 13. Comparison of HIC 36 and Chest Acceleration Between Tests and Simulations	46
Table 14. Simulation Matrix for Harnessed Occupants.....	47
Table 15. Effective Crash Angle for Each Combination of Impact and Vehicle Seat Orientation.....	48
Table 16. Simulation Matrix for Belted Occupants	57

Introduction

New automated technologies continue to be developed by traditional automakers and other companies that allow designers to reimagine the interior cabin designs of future vehicles where traditional human drivers may no longer be needed. While these new technologies offer opportunities for enhancing vehicle safety through crash prevention, they may also provide unusual challenges when protecting occupants in the remaining crashes that do occur. For example, conventional vehicles are designed to protect occupants in mostly forward-facing vehicle seating positions, but vehicles equipped with Automated Driving Systems (ADS) may operate bi-directionally and may offer unconventional seating. This unconventional seating may not be in two or three distinct rows and may be rear-facing, lateral-facing, or angled relative to the vehicle's direction of travel. In this study, we specifically focus on child occupants in concept vehicles envisioned to be operated solely by ADS.

Currently, Federal Motor Vehicle Safety Standard (FMVSS) No. 213, Child Restraint Systems, specifies a number of child anthropomorphic test devices (ATD) to assess the child restraint systems (CRSs) for the full range of child occupant sizes. These ATDs include the CRABI 12-month-old (12MO), Hybrid III 3-year-old (H33YO), Hybrid III 6-year-old (H36YO), and Hybrid III 10-year-old (H310YO). However, FMVSS No. 213 only defines tests for forward-facing vehicle seats in a simulated frontal crash condition, although a side impact test procedure has been recently adopted.¹ Most child restraint manufacturers do not permit installation of their products in non-forward-facing vehicle seats. Given the potential for new and varied vehicle seating positions that may occur in vehicles with ADS, research to study the effect of unconventional seating on child occupant kinematics and injury potential would be helpful. The variability of occupant seating positions may challenge existing CRSs. Changes to the vehicle interior may also require reconsidering occupant restraint strategies, including potential changes to the CRSs, seat belts, and vehicle interior. The suitability of currently available ATD and/or human body models for simulating the responses beyond pure frontal crash loading may also need to be determined. Therefore, it is critical to study child-specific safety considerations from unconventional vehicle seating positions, orientations, and seating environments.

The objective of this study was to use computer models to study how unconventional seating positions and orientations may affect occupant response metrics of children restrained by CRSs equipped with an internal harness or the vehicle lap-shoulder belt, with and without belt-positioning boosters.

Specifically, the following tasks were performed:

- 1) Conducted a literature review to help select surrogate vehicles, potential seating arrangements, impact scenarios, ATD models relevant to the selected impact scenarios, and CRS models relevant to the selected ATD occupant models.
- 2) Conducted sled tests with CRS harness-restrained ATDs and belt-restrained ATDs seated in conventional and unconventional vehicle seat orientations in various impact conditions, and used the sled tests to validate a set of computational models.

¹ 49 CFR. § 571.213a Standard No. 213a; Child restraint systems - side impact protection. www.ecfr.gov/current/title-49/subtitle-B/chapter-V/part-571/subpart-B/section-571.213a.

- 3) Studied occupant response metric differences of ATDs in harnessed CRSs across a range of conventional and unconventional seat positions and orientations in various restraint and impact conditions.
- 4) Studied occupant response metric differences between belt-restrained children with and without booster seat across a range of conventional and unconventional vehicle seat positions and orientations in various impact conditions.

Literature Review

Overview

This study began with an in-depth literature review of topics relevant to a computational study on child passenger safety in unconventional seating. The following topics were reviewed.

- The types, sizes, and shapes of ADS-equipped vehicles being conceptualized, developed, or proposed
- Unconventional seating positions and orientations that could be used by ADS-equipped vehicles
- Crash scenarios associated with current vehicles and those that could be relevant for future ADS-equipped vehicles
- Vehicle interior models, child occupant models, and CRS models available in the field
- Computational modeling studies related to child passenger safety
- Crash tests with child ATDs and CRSs
- Child injury measures and associated injury assessment reference values (IARVs)

Through the literature review, we also discussed the following items.

- The process to identify the potential seating arrangement and the likely crash scenarios associated with ADS-equipped vehicles.
- The relevance of vehicle, child occupant, and CRS models to the crash scenarios selected and model validation.
- The suitability of the existing occupant models for evaluating the occupant response in non-traditional automotive seating postures and configurations.
- The appropriate injury criteria and associated IARVs for child ATDs.

This literature review only focused on unconventional seating and ADS-related child ATD and CRS testing and modeling. There are extensive publications related to biomechanical aspects of pediatric human modeling and material property testing, which were not considered in this review but could be referred to review articles specifically focusing on those areas (Arbogast & Maltese, 2015; Brolin et al., 2015).

Methods

The literature databases searched in this study included PubMed (covering the majority of biomedical literature), Scopus (covering the majority of engineering literature), and papers published at Enhanced Safety of Vehicles (ESV) conferences (not covered by PubMed and Scopus). A separate effort was made to identify relevant technical reports published by NHTSA. Due to the proprietary nature of automated vehicle designs, the list of automated vehicles and the associated companies were collected through a Google search for news and documents rather than scientific publications.

For the review of previous child/CRS modeling efforts and previous crash tests, we searched the PubMed database using the following key words. The number of publications found from each search is indicated in parentheses afterward.

- Rear-facing child (127)
- Booster seat (206)

- Forward-facing child (109)
- Child restraint model vehicle (156)
- Child rollover crash (45)
- Child rear impact (119)

The publications were reviewed and the ones related to child and CRS modeling and testing were included in the literature review.

When reporting direction of impact simulations or tests, researchers have had variable definitions of the angle of impact and the description as front, oblique, side, or rear impacts. For the purposes of this literature review, we use the following definitions.

- Frontal: 0 +/-20°
- Oblique: 45 +/-25° (20 to 70°, 250 to 340°)
- Side: 90 +/- 20° (70 to 110°)
- Rear: 180 +/-70° (110 to 250°)

Results

ADS-Equipped Vehicles

When vehicles can be operated with a high level of automation, unconventional seating arrangements could allow occupants a wider range of interactions and activities. Based on SAE International’s J3016_202104 standard, these vehicles correspond to Level 4 or Level 5 of driving automation. Based on CB Insight’s investment, acquisition, and partnership data, more than 40 companies world-wide are developing road-going Level 4 or Level 5 self-driving vehicles. They are a diverse group, ranging from automotive industry companies to leading technology brands and telecommunications companies. Table 1 presents a list of automated vehicles, and Figure 1 shows a few exemplar and popular vehicles/prototypes with high-level ADS, which range from passenger cars to small shuttle buses and heavy trucks. A full illustrated list of vehicles with high-level of ADS can be found in Appendix A. Even among the passenger cars, they range from the size of a compact car and midsize sedan to a larger minivan, and the majority are conventional vehicle models with add-on ADS. Vehicles with high-level ADS, even within the passenger cars, are very diverse.

Table 1. A List of Vehicles With High-Level ADS

Sedans & Minivans	Shuttles	Heavy Trucks
Tesla Model S	Cruise/GM Origin	Plus.ai
APTIV/Lyft BMW	Volkswagen SEDRIC	Volvo Vera
Ford Argo AI	May Mobility/Toyota	Freightliner Inspiration
Waymo/Alphabet Inc.	Polaris GEM	Tesla Semi
Volkswagen I.D.	Easy Mile	Ford F-Vision
Nissan Easy Ride	Olli 2.0 by Beep	Tu Simple
Voyage	SAIC	Future Truck by Mercedes-Benz
Drive.ai	Autonom NAVYA/Beep	Daimler/Torc Robotics
Smart vision EQ fortwo	Optimus Ride	Starsky Robotics
Uber ATG	Navya Trapezio	Embark Trucks



Figure 1. Exemplar vehicles with high-level ADS

ADS-Related Possible Unconventional Seating

In vehicles equipped with high-level ADS, new seating arrangements, such as the carriage-style face-to-face configuration (often used in trains) and a campfire face-to-face with inward and angled seats, may become more widely available in the high-sales residential vehicle market.

However, several studies have investigated people’s preferences for seating in hypothetical vehicles, which could be considered as reasonable predictions for future ADS-equipped vehicles. Researchers from Stanford University (Ive et al., 2015) conducted a study with 17 university students through visualization, think-aloud exercises, and semi-structured interviews, to relate their current behavior in conventional vehicles with their imagined experience in an autonomous vehicle (considered throughout the report to be equivalent with the term ADS used in the current study). They explored how occupants will sit, what activities they will engage in, and how they will relate with each other socially in autonomous vehicles. Although their results showed a wide range of responses, the removal of the driving task may increase interactions between occupants, encourage adjusting seats to face one another, and impact perceptions about the vehicle as a tool for traveling to a destination changing to a destination in itself.

A study by Chalmers University in Sweden (Jorlöv et al., 2017) recruited 52 participants 11 to 63 years old, and used a questionnaire and a structured interview to explore their preferred seating positions within a simplified physical environment representing a highly automated vehicle. As shown in Figure 2, the study found that in a total of 13 groups, the most preferred position for longer family drives was the “living room position” with the front seats rotated 180° (C), followed by the living room positions E and D (12, 6 and 5 tests, respectively). In 4 tests, participants wanted to sit facing forward (A), and one preferred the conversation position (B).

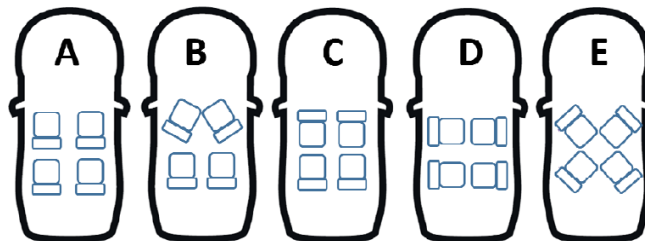


Figure 2. Five different seating positions from the study (Jorlöv et al., 2017)

A study by Monash University in Australia (Koppel et al., 2019) conducted online surveys with 552 participants on their seating preferences in a fully automated vehicle across seven hypothetical traveling scenarios. Essentially the same seating configurations and positions were used as those shown in Figure 2. Across all scenarios, participants were most likely to prefer a conventional seating configuration (i.e., all seats facing forward; between 40.0 and 76.3%), followed by the living room style with and without angled seats (C and E in Figure 2).

To expand Koppel’s study, Lopez-Valdes et al., (2020) conducted another online survey with 730 participants on their seating preferences in fully automated vehicles across three hypothetical scenarios, riding by oneself, with an unknown person, and with a partner. Conventional seating configurations were always preferred regardless of scenarios, and the face-to-face seating configuration was the second most preferred. Those riding with a partner tended to prefer the conversation position.

A recent study by Tsinghua University in China (Nie et al., 2020) also conducted online surveys with 1,018 respondents on their seating preferences in highly automated vehicles. Among the six seat configurations shown in Figure 3, the most preferred seating configuration was conventional seating facing forward (B), followed by face-to-face configurations with (F) and without angle (A). The rear seat was also preferred for both the conventional (65.6%) and face-to-face (77.6%) seating configurations, largely because they viewed rear seats as being safer than front seats in a crash.²

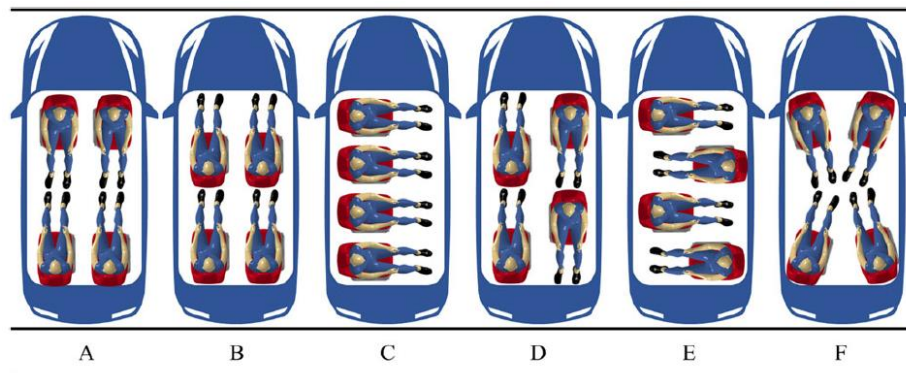


Figure 3. Six feasible seat configurations in passenger scenarios used in Nie et al.,2020

Crash Scenarios Associated With Conventional and Future ADS-Equipped Vehicles

Previous field data analyses have shown consistent trends of frontal crashes accounting for the most injuries in motor vehicle crashes, followed by side impacts. Rear impacts are also common, but have relatively lower impact severity (delta V) and associated injuries. For example, a previous UMTRI study (Hu et al., 2014) analyzed the National Automotive Sampling System-Crashworthiness Data System (NASS-CDS) database and generated distributions of longitudinal and lateral delta Vs in crashes, which can be used to define crash simulations that reflect the real-world crash scenarios for conventional vehicles. The distribution of crashes by principal direction of force (PDOF) is shown in Figure 4, and the delta V percentiles are shown in Table 2. (Left and right sides referred here are relative to a conventional forward-facing occupant

² Note that Nie et al., 2020, did not specify the crash scenario.

coordinate system.) Frontal and frontal oblique impacts account for the majority of vehicle planar impacts. More crashes are associated with a significant portion of frontal impact than rear impact, and rear-oblique impacts are rare. Crashes from the left side are slightly more frequent than those from the right side. The delta V percentile results shown in Table 2 indicate that the impact velocity of 48 km/h defined in FMVSS No. 213 corresponds to a greater than 98th percentile frontal impact delta V. The delta Vs in side and rear impacts are generally lower than frontal crashes by about 10 to 20 percent, when dealing with percentiles over 90th.

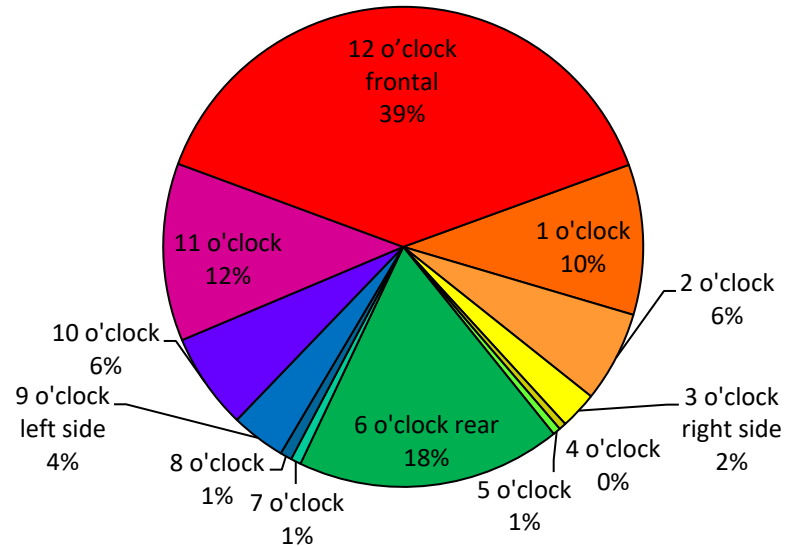


Figure 4. Distribution of planar crashes by PDOF based on NASS-CDS

Table 2. Delta V Percentiles for Each Planar Crash Mode Based on NASS-CDS (Unit:km/h)

Percentile	Frontal 11,12,1 o'clock	Right 2,3,4 o'clock	Left 8,9,10 o'clock	Rear 5,6,7 o'clock
50th	18	17	16	16
75th	25	24	22	21
80th	28	26	23	23
90th	34	31	29	27
95th	40	37	34	34
98th	47	43	41	42
99th	55	49	45	46

Currently available real-world crash-injury data for highly automated vehicles are significantly limited by sample size. The only study found including crash data for automated vehicles is from Wang and Li (2019). Wang’s study used California’s Report of Traffic Collision Involving an Autonomous Vehicle (AV)³ database, which includes AV crash data from 2014 to 2018. This study is the most current and complete AV crash database in the United States. Among the 113 crashes involving AVs, 69 were rear-end impacts, 25 were side impacts, 10 were angled

³ The term “autonomous vehicle” referred to in this study is equivalent to the term “vehicles with ADS” in this report.

collisions, and 9 were run-off-road. Because AVs can be both striking and struck vehicles, the exact crashing mode distribution for the AVs are not available. Among all 113 cases, AVs were at fault for 15 of them.

A previous UMTRI study (Klinich et al., 2016) analyzed crash distribution change using NASS-GENES and NASS-CDS data by assuming a vehicle with comprehensive crash avoidance technology (CCAT) would not cause crashes with other vehicles. As shown in Figure 5, if a vehicle does not cause any crash, it would be involved in 63 percent fewer crashes on average, including 93 percent fewer frontal impacts and 85 percent fewer rollovers; side and rear impacts would comprise a greater proportion of the remaining crash population. Although this study assumed idealized conditions, the trends shown indicate that highly automated vehicles would be involved in crashes at lower rates than human-operated vehicles. Although they could potentially be involved in a lower proportion of frontal crashes, the proportion of side and rear impacts could be higher compared to the current crash distribution, because crash avoidance technologies are more effective for frontal crashes.

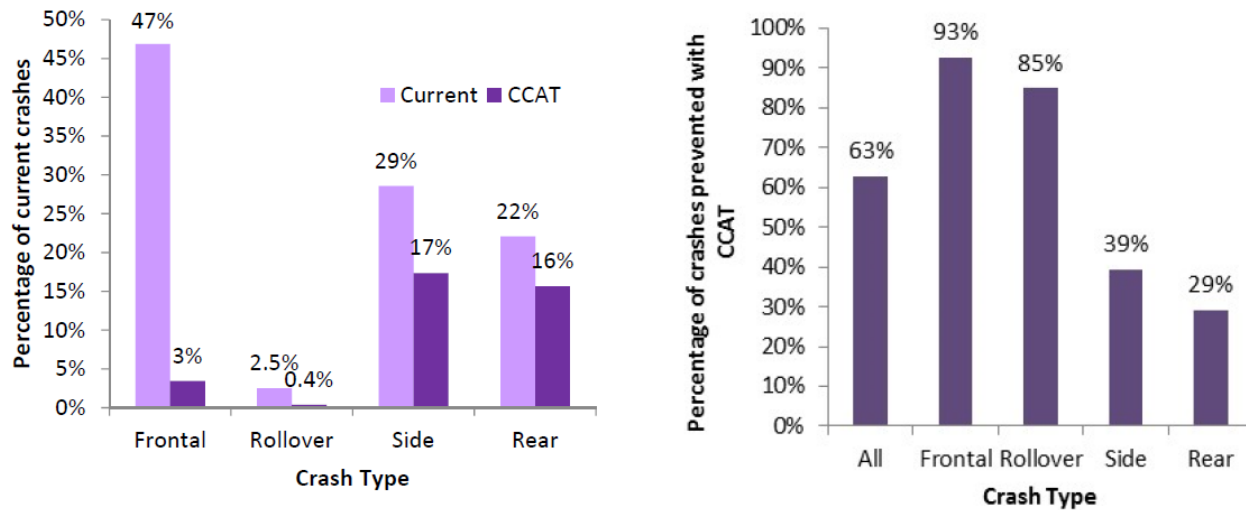


Figure 5. Distribution of crash types and percentage of crash avoided with CCAT (Klinich et al., 2016)

Vehicle Interior Models, Child Occupant Models, and CRS Models Available

A large set of finite element (FE) vehicle models are publicly available at NHTSA’s website and at the Center for Collision Safety and Analysis at George Mason University, which cover a wide range of vehicle types (sedan, SUV, minivan, and pickup truck) and vehicle sizes (compact car, midsize sedan, large SUV, etc.). In previous studies, UMTRI has gathered 3D vehicle interior laser scanning data for about 100 vehicles. UMTRI also has developed a set of MADYMO vehicle interior models with facet mesh surfaces that are validated against crash tests in frontal and frontal oblique impacts. Figure 6 shows a few examples of the NHTSA FE vehicle models, UMTRI MADYMO vehicle models, and UMTRI vehicle scans. A wide selection of options is available from which to select the vehicle interior geometries to be used in this study.

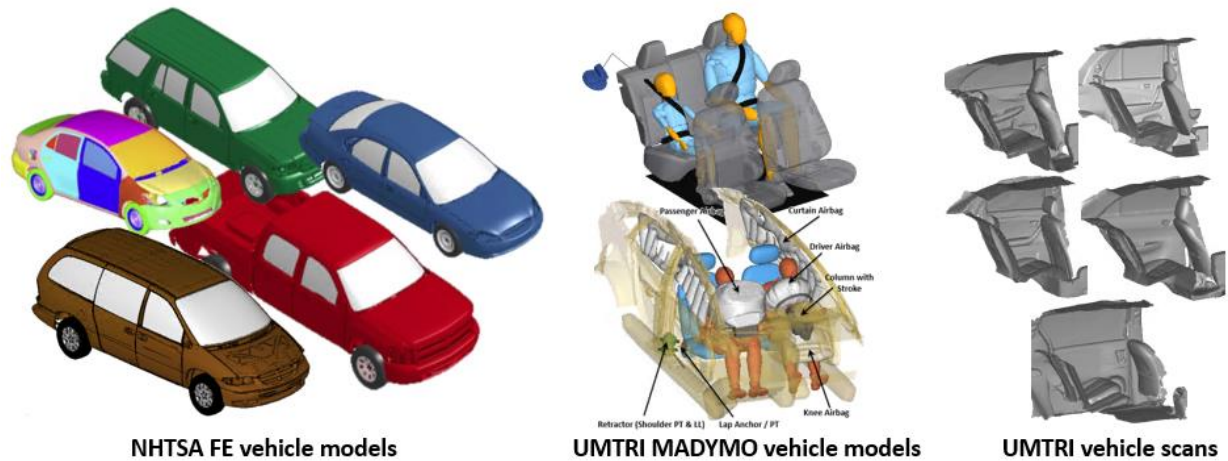


Figure 6. Exemplar vehicle interior models available at UMTRI

As shown in Figure 7, a many child occupant models are available for crash simulations. These include a full set of MADYMO models covering the majority of child ATDs (Hybrid III family, P-series, and Q-series), a full set of FE child ATD models from Humanetics (Hybrid III family and Q-series), an H36YO model publicly available through Ansys (formerly known as Livermore Software Technology Corporation (LSTC)), and MADYMO and FE child human models with various ages and sizes published by different companies, universities, and consortiums. UMTRI maintains a 6YO child model with a modified, more-biofidelic pelvis, and parametric child ATD models representing children 6 to 12 years old. The 6YO and 10YO child models have been validated against frontal crash tests with various restraint configurations. UMTRI has access to commercialized models through paid licenses. However, these models may lack validity to simulate farside, rear, and oblique crashes.

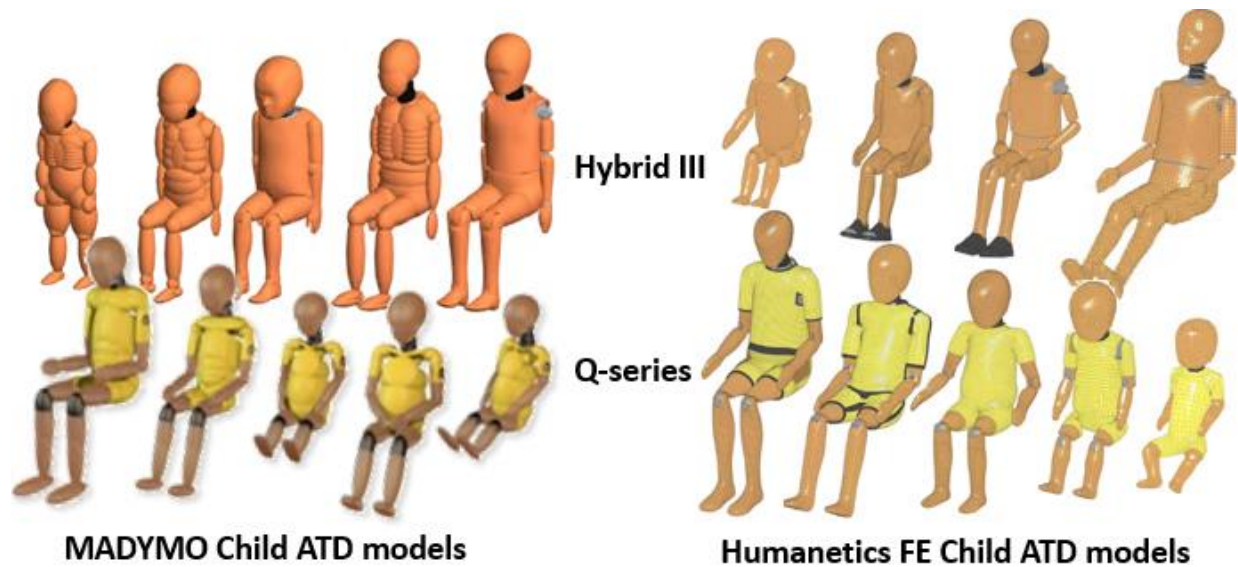


Figure 7. MADYMO (Siemens) and FE (Humanetics) child ATD models

Based on the literature search, we found only one set of FE CRS models that are publicly available. The PIPER project,⁴ funded by the European Union, has published a rear-facing-only infant CRS, a forward-facing harnessed CRS model, and a high-back booster seat model. However, those models have minimal documentation and validation. UMTRI has its own set of CRS models, including an infant seat MADYMO model in facet mesh, an FE convertible child seat model, and a backless booster seat model in MADYMO (Figure 8). Some other studies also developed and validated their own CRS models along with ATD models (Deo, 2005; Hulme et al., 2004; Ibrahim et al., 2009; Kapoor et al., 2008; Mizuno & Namikiri, 2007; Park et al., 2004; Wang et al., 2006), but those models are not publicly available. In addition, they were developed over 10 years ago, and may not represent features found in current CRS products sold in the United States.

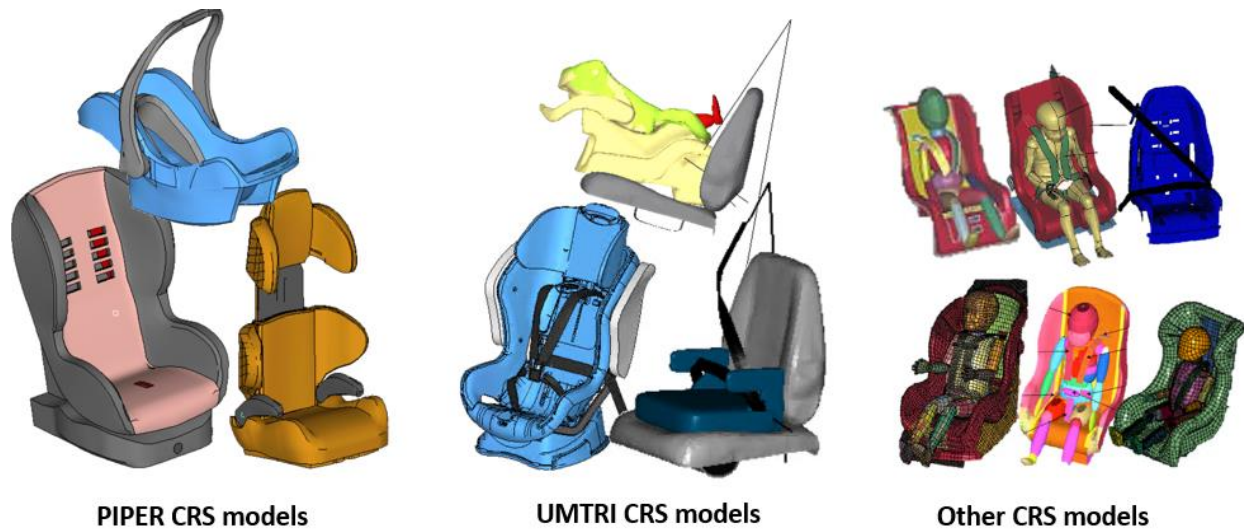


Figure 8. Examples of CRS models in the field

Child Occupant Modeling Studies

Table 3 shows the publications related to child occupant modeling reviewed in this project, categorized by impact direction and age of the ATD/human model. The majority of these studies focused on frontal impacts. However, the ATD and human models used in these studies varied significantly.

Frontal Impact

Park et al., (2004) used FE simulations to optimize a forward-facing (FF) CRS with an H33YO model. The model was validated against a sled test, and material and shell thickness optimization was conducted to achieve the final design.

A 3YO child FE model was developed by scaling the Total Human Model for Safety (THUMS) midsize male model (Mizuno et al., 2005). Two types of FF-CRS, a 5-point harness and a tray shield CRS, were used in an ECE R44 sled test performed for validation. In general, the responses from the child FE model are consistent with the H33YO testing results. In both CRS types, the spine flexed more in the child FE model, which cannot be simulated by the H33YO. However, the head excursions were similar between the human model and ATD tests. A follow-

⁴ <http://piper-project.org/>

on study was conducted by Mizuno and Namikiri, (2007) in which both the THUMS 3YO model and an H33YO model were used with three FFCRS: a 5-point harness, a tray shield, and an ISOFIX⁵ CRS. The simulation results are consistent between these two studies. This study also found that a slack seat belt and a loose 5-point harness increased the injury risks, while ISOFIX CRS provided the best protection among the three CRS designs.

Table 3. Child Modeling Studies for Crash Safety in the Literature

Occupant	Frontal	Side	Oblique
CRABI 12MO	Hu, 2013, RF-infant		
Q1.5/HBM1.5	He et al., 2018, shield FFCRS		
PIPER 1.5-6YO	Belwadi et al., 2019, convertible Bohman et al., 2020, 3 boosters Johannsdottir 2019, FFCRS and booster Maheshwari et al., 2018, 4 boosters		
Q3	Andersson 2012a, booster Rola and Wdowicz 2018, convertible Kapoor et al., 2008a, FFCRS	Kapoor et al., 2008b, FFCRS	Andersson, 2012a, booster
THUMS 3YO	Mizuno et al., 2005, 3 FFCRS Mizuno & Namikiri, 2007, FFCRS Kapoor et al., 2008, FFCRS	Andersson et al., 2012b, booster	
H33YO	Park et al., 2004, FFCRS* Kapoor et al., 2006, convertible Kapoor et al., 2008, FFCRS	Kapoor et al., 2008b, FFCRS	
H36YO	Cruz-Jaramillo et al., 2018, booster Hu et al., 2017, booster Hu et al., 2016, booster Hu et al., 2014, booster Hu & Jayakar 2014, convertible Hu et al., 2012, booster Wu et al., 2012	Hu et al., 2014, booster	Hu et al., 2014, booster
H310YO	Hu et al., 2014	Hu et al., 2014	Hu et al., 2014

* Exact child ATD model was not specified.

Kapoor et al. (2006) conducted front crash FE simulations using an H33YO in a convertible CRS model under Canadian Motor Vehicle Safety Standard 208. The forward-facing setup was validated against a crash test with a reasonable correlation. The comparison of rear-facing and forward-facing configurations showed that rear-facing ATDs sustained significantly lower levels of neck injury measures while exhibiting similar levels of head injury criteria as the forward-facing ATD. The same group conducted another study (Kapoor et al., 2008) using the same CRS but with three occupant models (H33YO, Q3, and THUMS 3YO models) to investigate the effects of load-limiting in Lower Anchors and Tethers for Children (LATCH) on occupant injury risks. Load-limiting in the upper tether and lower anchors can reduce the head injury criteria by ~60 percent to 70 percent, while controlling forward head excursion within the limits defined by FMVSS No. 213. However, such load-limiting designs could potentially increase risk of head contact in smaller vehicles, so should be considered with caution.

⁵ ISOFIX is a system, mostly used in Europe, for the connection of child restraint systems to vehicles. The system has two vehicle rigid anchorages, two corresponding rigid attachments on the child restraint system, and a means to limit the pitch rotation of the child restraint system.

Hulme et al. (2004) developed a scientific visualization toolkit called NYSCEHIII CRS visualization module (NCVM), and used a MADYMO H33YO model and a FFCRS model to simulate a frontal crash.

To evaluate the kinematics of the Q3 MADYMO model and a modified version of Q3 model, Andersson et al. (2012a) reconstructed three frontal and frontal oblique crashes through stochastic simulations of 3YO children seated in booster seats and a wide range of crash speeds (30 to 92 kph). In high-severity pure frontal crashes, the Q3 model predicted non-head impact adequately. However, in oblique frontal crashes, the Q3 model did not sufficiently predict the head excursions. As a result, greater flexibility of the thoracic spine and redistributed mass may be needed to further improve the Q3 biofidelity.

Through a NHTSA-funded project, UMTRI researchers developed a 6YO ATD MADYMO model (Figure 9) that incorporated improved pelvis and abdomen geometry and properties (Hu et al., 2012). We developed and tested these components physically in a modified H36YO. The model was validated against four sled tests under two test conditions with and without submarining using a multi-objective optimization method. A sensitivity analysis using this validated child dummy model showed that dummy knee excursion, torso rotation angle, and the difference between head and knee excursions were good predictors of submarining. In addition, restraint system design variables, such as lap belt angle, D-ring height, and seat coefficient of friction, had important effects on predicted head and abdomen injury risks. The study concluded that child dummies and dummy models capable of accurately simulating belt interaction, including submarining, are crucial for future restraint system design optimization for young school-aged children. A follow-up study developed and validated a scalable MADYMO model representing children from 6 to 12 YO (Figure 9) using a similar multi-objective optimization technique.

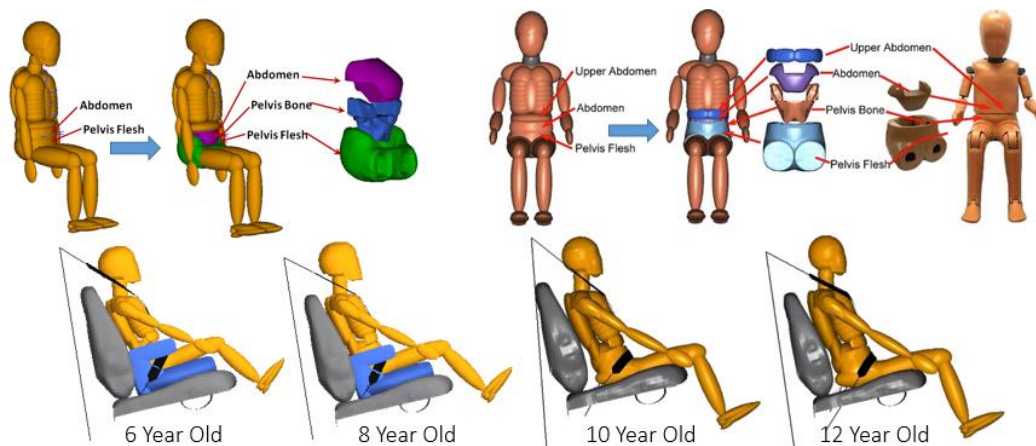


Figure 9. UMTRI's improved, scalable MADYMO child ATD model

In a series of NHTSA-funded studies (Hu, Wu, Klinich, et al., 2013; Hu, Wu, Reed, et al., 2013), UMTRI researchers conducted sensitivity analyses and design optimizations for older children, adults, and infants in a RFCRS to investigate whether the optimal rear-seat restraint systems for different age groups are consistent. A total of 10,000+ simulations were conducted using a set of validated MADYMO models, an automated simulation framework, and occupant belt-fit and posture prediction models from our previous studies. The optimal designs for 6-year-old children, adults, and infants in a RFCRS are shown in Figure 10. The optimal belt geometry and

seat design for the smallest belted children can provide “acceptable” but not “optimal” protection to adults and infants in a RFCRS. In particular, the more-vertical lap belt orientation that best prevents submarining for belted children is sub-optimal for adults and infants in RFCRS, and the short seat cushion that best prevents adverse “submarining” kinematics for belted children, by reducing slouching, would increase RFCRS rotation in frontal crashes. These findings suggest that adaptive or adjustable restraint systems could simultaneously improve the rear-seat occupant protection for all age groups.

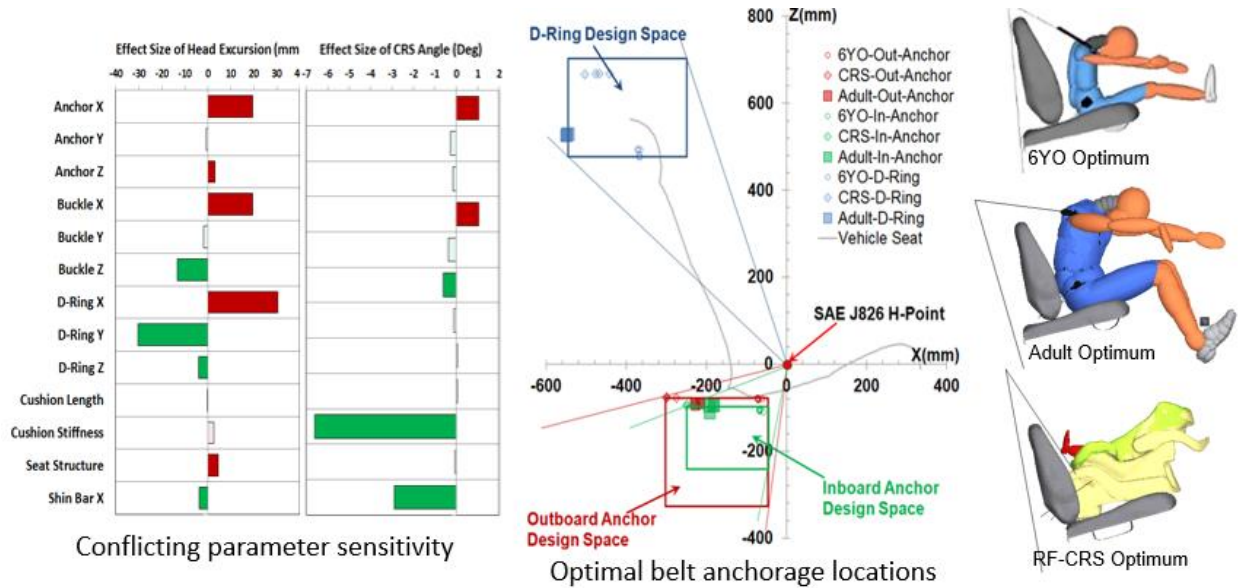


Figure 10. Pareto-optimal designs for children, midsize male adults, and infants in RFCRS

Hu and Jayakar (2014) developed an FE model of a convertible child seat (Figure 11) and validated the model against four sled tests with different restraint conditions (lap belt with and without tether, LATCH with and without tether) along with an H36YO model. The simulated results of ATD kinematics and restraint forces correlated well to the test data. A parametric study showed that lowering the height of child seat base can reduce both the overall child seat weight, as well as the ATD head/knee excursions in frontal crashes. Overall, the modified design reduced the ATD head and knee excursions in FMVSS No. 213 test conditions under all four restraint conditions.

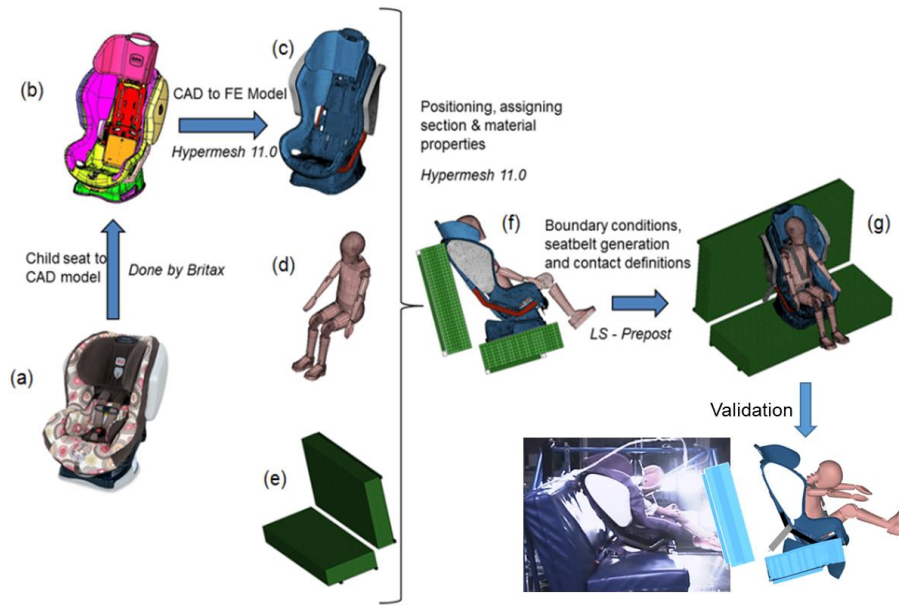


Figure 11. Optimized child seat model development and validation (Hu & Jayakar, 2014)

Through a NHTSA-funded rear-seat occupant protection study (Hu et al., 2017), UMTRI researchers developed and validated a series of rear-seat compartment and restraint models, evaluating the H36YO with and without a backless booster and three other adult ATD models. Sled tests and simulations using an H36YO in frontal and frontal oblique impacts showed that a backless booster seat is necessary to prevent submarining in a severe frontal or frontal oblique impact. Farside oblique impacts induced higher head excursions than pure frontal or nearside oblique impacts. ATD neck tension is often high without an air bag and seat belt load limiter, and a properly designed rear-seat air bag and load limiter can effectively reduce head, neck, and chest injury measures. Figure 12 shows examples of simulation and testing results with baseline and optimal restraints in frontal crashes.

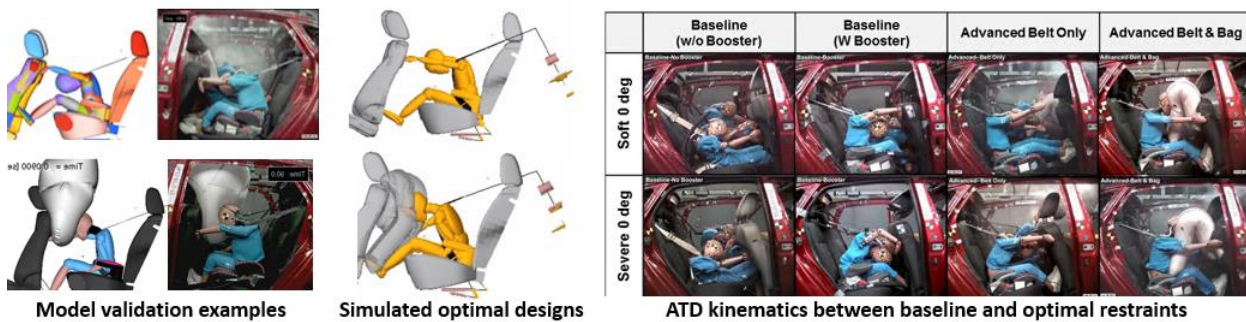


Figure 12. Simulation and testing results with H36YO in frontal crashes (Hu et al., 2017)

Another study used modeling to evaluate the International Organization for Standardization (ISO) 13216-3:2006(E) CRS envelopes relative to rear seat compartments from vehicles and CRSs in the U.S. market (Hu et al., 2015). This study assessed whether it was feasible to adapt the ISO compatibility evaluations for U.S. vehicles and CRSs. Geometry models for 26 vehicles and sixteen convertible CRS designs developed previously at UMTRI were used. Geometry models of three FFCRS and three RFCRS envelopes provided by the ISO were developed. The

virtual fit process closely followed the physical procedures described in the ISO standards. Examples of CRS scans in one of the ISO envelopes are shown in Figure 13. The CRS scans can potentially provide a geometric basis for building CRS models in this proposed study. Klinich et al. (2018) performed a NHTSA-funded follow-on task to develop envelopes suitable for assessing vehicle/child restraint compatibility for CRSs and vehicles found in the U.S. market. To construct additional CRS models for the study, 11 rear-facing-only, 5 convertible CRS, and 1 booster were scanned and added to the CRS database.



Figure 13. Examples of CRS scans in one of the ISO envelopes (Hu et al., 2015)

FE frontal crash simulations were conducted using an H36YO model in a vehicle rear seat with and without a booster (Cruz-Jaramillo et al., 2018). Although no model validation was performed, the simulation results showed that a backless booster could effectively reduce ATD HIC and excursions.

FE frontal crash simulations with the MADYMO Q1.5 and 1.5YO child facet human model were conducted with a shield CRS (He et al., 2018). The Q1.5 and the CRS models were validated against sled tests. The simulations showed that the Q1.5 has a stiffer thoracic and lumbar spine than the human model, which resulted in different kinematics between the ATD and human model.

MADYMO frontal crash simulation were conducted using a Q3 model seated in both RFCRS and FFCRS under three impact speeds (Rola & Wdowicz, 2018). Although no validation was provided, the simulation results showed benefits of RFCRS over FFCRS in reducing the majority of injury metrics for the head and neck.

Frontal crash simulations using the PIPER 6YO and Q6 models were conducted with four boosters and the FMVSS No. 213 bench (Maheshwari et al., 2018). They found that the PIPER model has a more flexible neck and shows higher chest deflection than those from Q6. Later on, the same group (Belwadi et al., 2019) scaled the 6YO PIPER model child FE model into 18, 24, 30, 36, 42, 48 MO children, and conducted frontal crash simulations with a convertible seat in both rear-facing and forward-facing configurations. Although there is no validation for the scaled models, the simulation results demonstrated the benefit of rear-facing orientation compared to forward-facing for children up to 4 years of age.

Johannsdottir (2019) used the scaled PIPER FE child models to reconstruct two crashes, one with a 26 MO child in a FFCRS, and the other with a 5 YO child in a booster. Both of them involved CRS misuse. Simulation results showed that most misuse scenarios increase the

potential child occupant injury risks, while proper use of CRS can reduce the injury risks substantially.

To investigate booster design on child occupant kinematics, Bohman et al., (2020) conducted parametric FE frontal crash simulations using the PIPER 6YO model and three backless boosters with and without ISOFIX attachment and varied shoulder belt routings. Three sled tests with the Q10 were also conducted for validation and comparison purposes. Overall, the human and ATD responses showed consistent sensitivity to the booster design. Interestingly, different boosters providing similar initial static belt fit could result in different occupant responses during a crash. Specifically, compression of the booster cushion may lead to a delayed belt-to-pelvis engagement, which may affect the torso pitching motion as well. The belt routing above or under the guide also affected the shoulder belt interaction, and in turn the torso kinematics in a frontal crash.

Side and Oblique Impacts

Andersson, Pipkorn, and Lövsund (2012b) used the THUMS 3YO model developed previously to study the effects of crash-related parameters on head and chest injury risks in nearside impacts. A full vehicle model was used, and the THUMS 3YO model was seated on a backless booster. The simulation results showed that a properly-designed curtain air bag, side air bag, and belt pre-tensioner have the potential to reduce child occupant injury measures. They concluded that lateral movement management is of greater importance for smaller occupants in nearside impacts.

Kapoor et al. (2008) conducted nearside impact simulations using the H33YO and Q3s models in a FFCRS. The H33YO model was validated against sled tests under an acceleration pulse with a closing speed of 24.1 km/h, in the presence of a rigid wall and absence of a vehicle body. They found that rigid ISOFIX with two base attachments and one top attachment could effectively reduce ATD lateral motion and injury measures compared to LATCH installation with flexible lower anchors and top tether. Although H33YO and Q3s provided considerably different neck forces, the general trends provided in terms of the installation methods are consistent.

The scalable MADYMO child ATD model was used in another NHTSA-funded UMTRI study (Hu et al., 2014) to estimate the distributions of possible head impact locations as a function of crash type, vehicle interior characteristics, and child size. The goal was to find child head impact locations for a range of crash scenarios to determine which should be padded and where a side curtain should be deployed to protect child occupants. Geometries of the second-row compartment from five vehicles were laser scanned to provide high-resolution data for assessing probable head contact zones. Simulations of crashes ranging from pure frontal to pure side impact (9 o'clock to 3 o'clock) with varied sizes of children with and without backless boosters were conducted using Uniform Latin Hypercube sampling (ULHS), UMTRI's ATD positioning procedure based on child volunteer postures, and an automated belt-fitting and crash simulation system. Examples of the simulation results are shown in Figure 14, in which the head contact zones with respect to interior components were identified. The findings of this study provided a reference for future vehicle rear compartment design to reduce head injuries for older children.

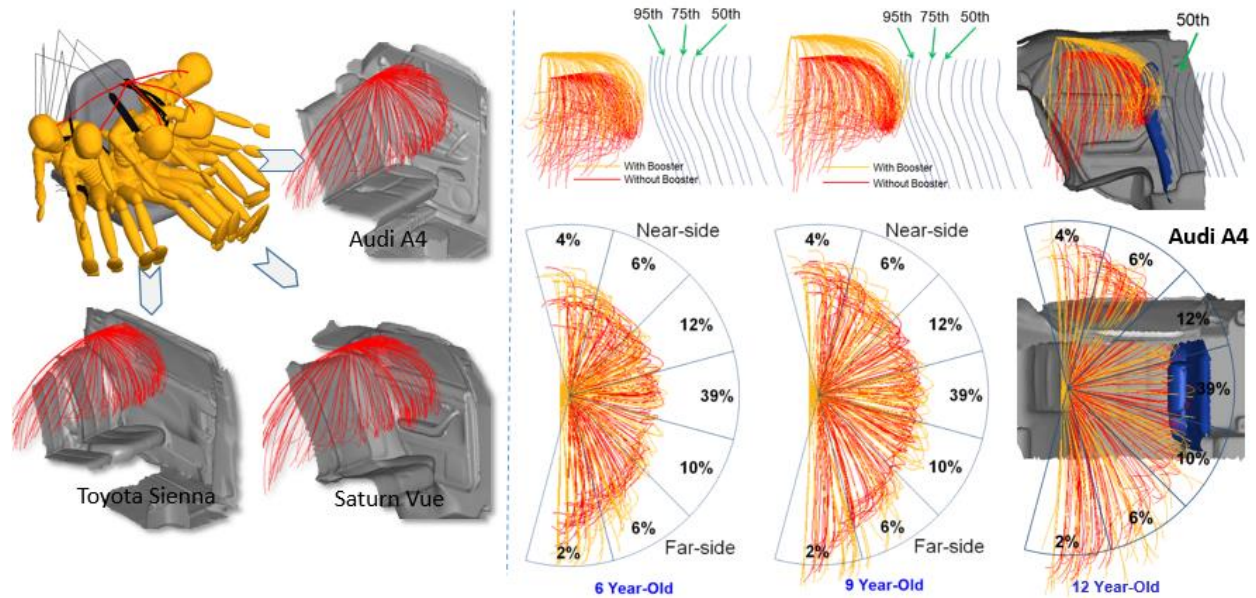


Figure 14. Exemplar head trajectories of children overlaid in vehicle second-row geometries

Summary of Previous Modeling Studies

- The majority of the previous studies focused on frontal crashes, while farside and oblique impact simulations are rare.
- None of the previous modeling studies examined rear impacts for child passenger safety.
- Model validations were focused on frontal impacts, while no farside or oblique models were validated against dynamic test data.
- H3 ATDs are the most commonly used.
- In general, H3 ATDs, Q-series ATDs, and human models provided consistent trends in terms of CRS designs and other impact parameters, although studies have shown that human models are generally more flexible than the ATDs.
- Rear-facing has shown consistent benefit over forward-facing in frontal impacts.

Child ATD Testing

Literature documenting dynamic testing of CRS using pediatric ATDs performed since 2000 is summarized in Table 4. Studies are categorized by the ATD used and impact direction. Bold text indicates testing performed on a laboratory bench, while normal text indicates testing performed on a vehicle seat. An overview of each study follows the table.

Table 4. Crash Tests With Child ATDs Between 2000 and 2020

Occupant	Frontal	Side	Oblique	Rear
CRABI 6MO	Charlton et al., 2004	Charlton et al., 2007 Bilston et al., 2005 Charlton et al., 2004	Bilston et al., 2005	O'Donel 2017 Williams et al., 2015
CRABI 12MO	Manary et al., 2006 Mansfield et al., 2020 Sherwood et al., 2004, 2005, and 2007 Tylko et al., 2013 Wietholder et al., 2016 Maltese & Horn, 2019	Hauschild et al., 2013 Ghati et al., 2009 Tylko et al., 2015 Sullivan et al., 2014 Brelin-Fornari et al., 2014		Manary et al., 2006 Mansfield et al., 2018
P1.5/Q1.5 CRABI 18MO	He et al., 2018 Manary et al., 2018 Sherwood et al., 2007	Charlton et al., 2007		
P3/Q3/Q3S	Johansson et al., 2009 Juste-Lorente et al., 2018 Sherwood et al., 2007	Hauschild et al., 2015, 2016, and 2018 Tylko et al., 2015 Sullivan et al., 2014	Hauschild et al., 2016 Yoshida et al., 2011	
H33YO	Bilston et al., 2007, Charlton et al., 2004 Maltese et al., 2014 Wietholder et al., 2016 Manary et al., 2018 Manary et al., 2019 Maltese & Horn 2019 Mansfield et al., 2020 Sherwood et al., 2007	Ghati et al., 2009 Bilston et al., 2005 Charlton et al., 2004 Brelin-Fornari et al., 2014	Bilston et al., 2005	Mansfield et al., 2018
H36YO	Bilston et al., 2007, Bohman et al., 2018, Forman et al., 2008 Klinich et al., 2014 Maltese et al., 2014 Wietholder et al., 2016 Maltese & Horn 2019 Mansfield et al., 2020 Klinich et al., 2020	Huot et al., 2005	Huot et al., 2005	
P6/Q6/Q6S		Charlton et al., 2007 Tylko et al., 2015		
Q10	Bohman et al., 2020			
H310YO "10YO" PMHS	Klinich et al., 2014 Lopez Valdes et al., 2010 Wietholder et al., 2016 Klinich et al., 2020 Maltese & Horn, 2019			

Frontal Impact

Sixteen sled tests were conducted to explore the effect of tethering RFCRS (Manary et al., 2006). One model of convertible CRS was tested rear-facing in four tether conditions: untethered, tethered down to the floor, tethered down to the bottom of the test bench on which the CRS was installed, and tethered rearward to a point above the back of the test bench. Tests used the CRABI 12MO on the ECE R44.02 test bench in frontal and rear impacts. The highest ATD measures occurred during the primary impact of a frontal test, rather than on rebound. The lowest HIC, neck forces, and chest accelerations in both impact directions were observed with the rearward tether. The upper neck moment data did not show a clear trend relative to tethering geometry. ATD and CRS motions were best controlled in frontal impact by the rearward tethering geometry while the motions in rear impact were best controlled by tethering to the floor.

To develop an updated version of the FMVSS No. 213 test bench, Wietholter et al. (2016) performed two series of tests to check durability, repeatability, and CRS fleet performance. Frontal tests were performed using the CRABI 12MO, H33YO, H36YO, and H310YO using the FMVSS No. 213 pulse. The first series included 26 tests, each performed with two different ATDs positioned on the left and right sides of the bench. Variations in foam stiffness and securement method were tested with a range of CRS products. Upgrades were made to the bench design to improve durability and usability, and a second series of tests was performed in which the CRABI 12MO was tested in 7 RF infant seats and 1 RF convertible, the H33YO was tested in 3 RF convertible seats and 3 FF convertible seats, the H36YO was tested in 10 FFCRS and 8 boosters, and the H310YO was tested in 4 FFCRS and 3 boosters. Results showed good repeatability and durability with the latest design.

To provide validation data for modeling, a Q1.5 was tested in frontal impact using the ECE R129 bench and a crash pulse with a change in velocity of 50 km/h (He et al., 2018). The ATD was seated in a shield-style FFCRS.

The reproducibility and repeatability of the proposed replacement FMVSS No. 213 bench and procedure was evaluated by comparing results from testing at Calspan to those from the Vehicle Research and Test Center (VRTC) (Maltese & Horn, 2019). Frontal tests were performed using the CRABI 12MO, H33YO, H36YO, and H310YO using the FMVSS No. 213 pulse. Three tests each were performed on 13 different CRSs to assess repeatability. For 2 of these CRSs, 3 tests on each were also performed at VRTC to compare repeatability levels. Six additional tests were performed on 6 more CRS models. Results demonstrated acceptable levels of reproducibility across labs.

Sixteen tests were performed to explore methods for evaluating RFCRS using ATDs larger than the CRABI 12MO (Manary et al., 2018). The study evaluated five installation methods using the H33YO and the CRABI 18MO. Three child restraint system models were evaluated using the current FMVSS No. 213 test bench. None of the ATD conditions produced a systematic change in the dynamic response criteria evaluated by FMVSS No. 213, but some methods were easier to implement in the laboratory.

Fifty-two tests were conducted to examine the effects of misuse on dynamic performance (Manary et al., 2019). Three commercial convertible child restraint models were loaded with the H33YO and secured by either LATCH or seat belt on a modified FMVSS No. 213 bench. Tests were conducted in both forward-facing and rear-facing modes. Misuses included loose harness,

loose installation, incorrect installation angle, incorrect belt path, loose/no tether, and incorrect harness clip usage. In the RF condition, misrouting the LATCH belt or seat belt through the incorrect belt path was the only misuse that significantly affected outcomes of interest and was associated with high levels of undesirable CRS rotation. In FF tests, loose installation and tether misuse had large adverse effects on three of four key response variables. Use of the tether helped offset the adverse effects of loose installation or loose harness.

The performance of RFCRS and FFCRS, secured by rigid LATCH, flexible LATCH, or seat belt, were evaluated in frontal impacts sled testing in a vehicle sedan buck (Charlton et al., 2004). Seven tests were performed with 3 RFCRS models using the CRABI 6MO. Two FFCRS were evaluated in 6 tests using the H33YO. Crash severity was 71 km/h. Installation method did not have a strong effect for the FFCRS or RFCRS in frontal impacts.

Fourteen tests were conducted with the CRABI 12MO to investigate the effect of attachment method on dynamic response (Sherwood et al., 2004). Tests were performed on a bench seat from a minivan, with a pulse similar to the FMVSS No. 213 pulse. Two FFCRS secured by lower attachments and tether were evaluated in six tests. Three models of RFCRS were tested using six different attachment/support methods. The authors noted non-biofidelic neck loads and differences in head injury measures with attachment technique. A companion study evaluated the effect of interaction with different forward vehicle components (Sherwood et al., 2005). Tests were performed with the CRABI 12MO and the same pulse using three different RFCRS on a minivan bench seat. Test conditions included no forward structure, a vehicle seat, a rigid structure, and a rigid structure plus gap. Contact with the rigid structure, which simulates a RFCRS installed in the front row of a pickup, produced the worst injury measures.

An additional follow-on study (Sherwood & Crandall, 2007) explored the response differences in six RF and FFCRS using four different ATDs. Variations in installation using flexible and rigid LATCH systems, as well as support legs, were also evaluated. Thirty-one tests were performed using a 48 km/h, 24 g nominal pulse using a captain's chair from a minivan second row. The CRABI 12MO, Q1.5, H33YO, and Q3 were used. RFCRS produced better injury response measures than FFCRS across all ATDs and products. Among products, those secured with rigid LATCH and a support leg had the lowest injury measures.

Eight crashes involving children 3 to 8 years old (Bilston et al., 2007) were reconstructed through sled testing. Half the cases involved injury, while the other half did not. Six tests were performed with the H33YO, while the other 2 used the H36YO. All crash pulses had a sled acceleration of 19 g, with change in velocities ranging from 31 to 37 km/h. Seat, door, and seat belt components from the same vehicles involved in the crash were mounted to the sled. Two tests used a belt-positioning booster, while the rest used a lap/shoulder belt. Restraint misuse and out-of-position postures were simulated. Between 1 and 5 sled tests were used to investigate possible variables in each crash, for a total of 24 tests. For each crash, a test was run with the ATD placed in the recommended child restraint to provide comparison measures. Based on test results, the authors hypothesized that most of the injuries in the real cases resulted from poor position of the child relative to the adult seat belts. They also noted the inadequacies of the ATD measures to differentiate between minor and serious injuries, particularly to the cervical spine.

A study of the effects of seat belts with and without load limiters and pretensioners included twelve tests using the H36YO seated in a high-back Graco TurboBooster belt-positioning booster seat (Forman et al., 2008). Tests were run with change in velocities of 48 km/h and 29 km/h

using a sled buck based on a mid-sized sedan; three tests were performed in each condition. The lower level of the seat belt load limiter was reached in all tests with the H36YO. The advanced seat belt system reduced loading to the chest of the 6YO and generally reduced most injury measures.

Three frontal sled tests were performed with the Q3 to provide validation data for an MADYMO model (Johansson et al., 2009). The ATD was seated in an integrated booster seat, and tests were performed in a body-in-white of a station wagon. One test used the ECE R44 pulse and a seat belt with a pretensioner and load limiter. Two tests were performed with the NPACS pulse: one with a seat belt with a pretensioner and load limiter and one without either feature.

Thirty-six tests were performed to compare the response of three RFCRS when tested on the CMVSS 213 bench seat versus three different vehicle rear seats (Tylko et al., 2013). All tests were performed with the CRABI 12MO. Each CRS was tested with the base secured by the lower anchors of the LATCH system, with the based secured by a 3-point belt, and without the base secured by a 3-point belt. The 24-g, 48-km/h pulse required in CMVSS 213 was used in all tests. Tests on the vehicle seats showed greater forward excursions when secured with the 3-point belt compared to the lower anchors, while the tests performed on the test bench showed minimal differences in excursion between the two installation methods.

In a companion study 53 tests were performed to compare the response of three FFCRS when tested on the CMVSS 213 bench seat versus three different vehicle rear seats (Maltese et al., 2014). Two CRS were evaluated using the Hybrid III 6YO, while the third CRS was tested with the Hybrid III 3YO. Four attachment configurations were evaluated for each CRS/seat combination: LATCH, 3-point belt and tether, lower anchors only, and 3-point belt only. The 24-g, 48-km/h pulse required in CMVSS 213 was used in all tests. Performance differences between bench and vehicle seats were minimal when CRS were secured by lower anchors only, and slightly greater when secured by 3-point belt. Differences between bench and vehicle seat were largest when the tether was used, with CRS showing a rearward rotation on the bench that differed from the forward rotation exhibited across all three vehicle seats.

Thirteen tests were performed to determine the effect of cushion length and belt geometry on the kinematics of the H36YO and H310YO (Klinich et al., 2014). Cushion length of a vehicle seat was varied from production length of 450 mm to a shorter length of 350 mm. Lap belt geometry was set to rear, mid, and forward anchorage locations that span the range of lap belt angles found in vehicles. Six tests each were performed with the H36YO and H310YO. One additional test was performed using a booster seat with the H36YO. The ATDs were positioned using techniques to achieve realistic posture. Shortening the seat cushion improved kinematic outcomes, particularly for the 10YO. Lap belt geometry had a greater effect on kinematics with the longer cushion length, with mid or forward belt geometries producing better kinematics than the rearward belt geometry. The worst kinematics for both ATDs occurred with the long cushion length and rearward lap belt geometry. The improvements in kinematics from shorter cushion length or more forward belt geometry are smaller than those provided by a booster seat.

The effect of realistic posture on kinematics and injury response was investigated through seventeen sled tests with the Hybrid III 6YO (Bohman et al., 2018). Tests were performed using a mid-size vehicle body with a change in velocity of 64 km/h. The ATD was positioned in a high-back booster in all tests, and attached with a tether in 10 conditions. Postures included different levels of forward or lateral lean, and 8 of the tests were run at 15° relative to the

forward direction. The belt slipped off the shoulder in all of the 15° tests and 6 out of 9 of the 0-degree tests. The authors noted difficulty in achieving realistic postures because of the characteristics of the H36YO.

Twelve tests were performed to compare the response of P3 and P6 ATDs when using a high-back belt-positioning booster seat on two different vehicle seat types (Juste-Lorente et al., 2018). Half the tests were performed using the ECE R44 bench and a lap-shoulder belt with a nonlocking retractor. The other half of tests were performed on a vehicle seat using a production seat belt equipped with an emergency locking retractor. Kinematics and ATD metrics differed as a result of differences in cushion stiffness, seat pan geometry, and belt geometry.

Three sled tests were conducted with a 54-year-old post-mortem human subject whose anthropometry (body mass=27.2 kg, stature=147 cm) approximated that of the H310YO (Maheshwari et al., 2018). Tests were performed with the PMHS seated on a backless Graco TurboBooster, using either a standard seat belt system or one with a progressive load limiter and pretensioners. Two tests had a change in velocity of 49 km/h (one with each belt system), while the third test had a change in velocity of 29 km/h (advanced belt system). The advanced belt system improved kinematics and reduced injury likelihood, demonstrating benefits for smaller sized occupants.

Three tests were performed with the Q10 to provide validation data for the PIPER child model (Bohman et al., 2020). Three different boosters were evaluated, and none were secured with the ISOFIX attachments. The bench was rotated 14° relative to frontal. A production seat belt with load limiter and pretensioners was used. Analysis showed different belt loading behaviors with the three types of boosters.

The effect of cushion stiffness and cushion length on CRS kinematics were evaluated in 18 tests (Mansfield et al., 2020). The CRABI 12MO was used in tests of the RFCRS, the H33YO was used in tests with a FFCRS, and the H36YO was used in tests with a belt-positioning booster seat. All tests used the FMVSS No. 213 pulse. Three cushion stiffnesses and two cushion lengths were evaluated. Effect of cushion stiffness was small across all conditions. For the RFCRS response, shorter cushion length increased rotation but reduced other metrics, while cushion length had minimal effect on the FFCRS response. For the booster tests, shorter cushion length increased chest acceleration but did not affect other responses.

Klinich et al., (2020) conducted a combination of volunteer testing of belt fit and posture along with dynamic sled tests of booster seats to explore candidate booster performance metrics that may have the potential to identify less effective booster systems. Dynamic testing was performed using a surrogate seat belt retractor to provide a more realistic restraint system, used on the most recent preliminary design update for the FMVSS No. 213 seat assembly. Eleven booster products were evaluated, as well as the no-booster condition, with six tests performed using the H310YO and 33 tests run with the H36YO. Possible metrics associated with good ATD kinematics (no submarining or rollout) were the difference between knee and head excursion, maximum torso angle, as well as lumbar MomentZ and ForceY.

Side Impact

The performance of two FFCRS in side impact were evaluated in 11 tests with the Hybrid III 3YO and 13 tests with the CRABI 12MO (Bilston et al., 2005). The Australian/New Zealand child restraint test bench was rotated 90° relative to the frontal direction, and tests were run with

a nominal sled pulse of 32 km/h, 14 g. (As described in the Oblique section, additional tests were performed with a 45° orientation.) Two different harnessed FFCRS with different designs of side structure were evaluated. All tests used a top tether, while the main CRS attachment method was varied among 3-point belt, lap belt, rigid ISOFIX, and two styles of flexible attachments to lower anchors. The FFCRS were selected because of their different side structure designs, and some tests included different types of additional foam padding. Results demonstrate better performance of rigid ISOFIX attachments in side impact, as well as a potential benefit from larger side wings and additional padding. In addition, flexible lower attachments fastened to the sides of the CRS structure had better performance than those routed through the belt path while attaching to the lower anchorages.

The performance of 4 RFCRS and 4 FFCRS in side impact conditions, and how they vary with attachment method, was evaluated in 48 tests (Ghati et al., 2009). Rear-facing tests used the CRABI 12MO, while FFCRS tests used the Hybrid III 3YO. Tests were performed using the FMVSS No. 213 bench rotated 90° from the frontal direction. Tests were performed at three severities (with change in velocity of 24, 29, or 36 km/h), and the CRSs were secured with either seat belt or LATCH. None of the CRS designs nor attachment methods seemed to provide adequate response under side impact.

Five CRS models were evaluated in four 90° side impact test configurations using the CRABI 12MO positioned in the center position of a modified FMVSS No. 213 test bench (Hauschild et al., 2013). The four conditions were 35 km/h with no simulated door, and 35, 29, and 24 km/h with a simulated door. Five different models of RFCRS were tested when secured to the bench with the lower anchor attachment. The bench was modified to place lower anchors from a Ford Taurus in the center seating position. Tests showed potential for head injury from contact with the side door when the RFCRS is placed in a center seating location. Level of head containment varied with the features of the CRS.

NHTSA performed several series of side impact tests to develop specifications for a proposed side impact test procedure (Sullivan et al., 2014). Tests were performed with the 12MO CRABI and the Q3S. Preliminary tests series evaluated the effects of cushion stiffness, door panel foam stiffness, armrest presence, and sill height. Four vehicle crash tests were performed for comparison with the sled test results. In the final proposed configuration, the Q3S was used to evaluate 5 RFCRS models and 12 FFCRS; the CRABI 12MO was used to evaluate 12 RFCRS. Additional modifications were made to the test fixture. The Q3S was then used to compare response of 2 RFCRS and 2 FFCRS when secured by LATCH or seat belt, and the CRABI 12MO was used to evaluate the securement effect with three more RFCRS.

Researchers performed side impact tests to evaluate a deceleration-sled version of NHTSA's proposed side impact test fixture (Brelin-Fornari & Janca, 2014a, 2014b). The bench was oriented 80° relative to the forward direction, and includes a simulated door on the left side. Six tests on 2 RFCRS were performed with the CRABI 12MO, 6 left-side tests on 2 FFCRS were performed with the Q3S, and 6 right-side tests on 2 RFCRS were performed with the Q3S. A second series of tests was performed after modifying the fixture to address concerns identified in the first series. Six left-side tests were performed with the Q3S in 2 different FFCRS, while 2 tests were performed with the CRABI 12MO in a RFCRS. Additional control parameters were adjusted, followed by a third series of tests: 5 with the CRABI 12MO in two RFCRS, 3 left-side with the Q3S in two CRS, and 4 right-side with the CRS in two CRS.

The performance of RFCRS and FFCRS, secured by ISOFIX, flexible LATCH, or seat belt, were evaluated in side through sled testing in a vehicle sedan buck (Charlton et al., 2004). One FFCRS was tested in nearside, while the second was tested in farside conditions, all using the P3 ATD. For the RFCRS, all tests were farside except one, and run with the CRABI 12MO. Results demonstrate better performance with rigid ISOFIX attachments.

In a follow-up study Charlton et al. (2007) used the same fixture to study the effect of securement and adjacent occupant interaction. A crash severity of 30 km/h was used. An RFCRS was in the center position with the 6MO CRABI, the P1.5 was in a FFCRS in the farside position, and the P6 was in a belt-positioning booster in the near side position. One test used seat belts to attach the CRS, while the second test used ISOFIX (including the belt-positioning booster). Another test was performed with the booster attached with ISOFIX and no adjacent occupant. Injury measures for the booster occupant were worse with an adjacent occupant. Injury measures were better with the ISOFIX for the RFCRS and FFCRS, but not for the booster occupant.

Huot et al. (2005) evaluated belt-positioning boosters in a lateral (90° from frontal) position. Seven tests were run with the H36YO. One test was run without a booster, 2 with a booster with smaller side wings, and 4 with a booster with larger side wings. They used the same pulse and bench as Bilston et al., (2005), which was the Australian/New Zealand test bench with a fixed simulated side door. They evaluated different supplemental methods of attaching the booster: with and without tether; no attachment, rigid, and two flexible lower attachment designs. They found that larger side wings are needed to adequately protect the head in side impact, although attaching the booster with a rigid ISOFIX connector provided some benefit.

Eight tests were performed with the Q3S in a FFCRS secured with LATCH, with and without the side wing structures (Hauschild et al., 2015). Two different vehicle seats with different head restraint designs were used. The seats were mounted 70° relative to the forward direction. A nominal pulse of 31 km/h, 21 g was used. The side wings did not provide adequate containment of the ATD's head, and the design of the vehicle's head restraint made a difference in the benefit provided by the tether.

Four tests were performed with the Q3S to evaluate the effect of tether use on a FFCRS in lateral impact (Hauschild et al., 2016). (Additional tests were performed at 60° as reported in the oblique impact section.) The fixture used a 2013-2014 SUV rear seat, rotated 80° relative to the forward direction to the near-side, and included a simulated left-side interior door. A FFCRS was secured with flexible lower attachments in the center position. Tests were performed with and without a tether. The nominal pulse (35 km/h/24-g) was based on that proposed in the FMVSS No. 213 Side Impact NPRM. Potential for injurious head contact with the interior door was reduced with tether use.

Fifteen test were performed with the Q3S to evaluate CRS attachment method in lateral impact (Hauschild et al., 2018). The fixture used a 2013-2014 SUV rear seat, rotated 80° relative to the forward direction. A FFCRS was modified to allow attachment using rigid lower anchors, a LATCH belt through the belt path, or flexible LATCH attachments fastened on each side. Tests were performed with and without a tether. The nominal pulse (35 km/h, 24 g) was based on that proposed in the FMVSS No. 213 Side Impact NPRM. Tests performed with the LATCH belt through the belt path performed worse than the two other conditions.

Child ATDs were tested in 44 vehicle side impacts (four different test conditions) and 9 sled impact tests to evaluate potential interactions among occupants (Tylko et al., 2015). The main occupant of interest was a Q6 or Q6S seated in a farside second-row position, while seated in a low or high-back booster. The nearside position was occupied by an H310YO, a 5th percentile WorldSID, a SIDIIs, a Q3S in a RFCRS or FFCRS, or a CRABI 12MO in a RFCRS. Head contact occurred most frequently when the nearside position was occupied by the Q3S in a FFCRS. Results showed that belt pretensioners reduced risk of head contact for the farside occupant. In addition, the best farside protection for the H36YO was achieved with a high-back booster secured with LATCH, with the ATD secured by a seat belt with a pretensioner.

Oblique Impact

Four studies have examined pediatric ATD response in oblique impacts. One study (Bilston et al., 2005) included 9 tests with the Hybrid III 3YO and 10 tests with the CRABI 12MO, performed on a laboratory bench seat conforming to Australian/New Zealand standards for CRS testing that was oriented at 45° relative to the forward direction. (Additional tests were performed with the bench oriented at 90°.) Two different harnessed FFCRS with different designs of side structure were evaluated. Nominal sled pulse was 32 km/h, 14 g. CRS attachment methods were 3-point belt, lap belt, rigid ISOFIX, and two styles of flexible attachments to lower anchors. All tests used the top tether. Some tests also added additional foam padding to the CRS. Tests with the rigid ISOFIX attachments had better performance than other attachment methods; flexible attachments fastened to the side of the CRS structure had better performance than those routed through the belt path. Padding and deeper side wings also offered greater head protection.

A companion study evaluated belt-positioning boosters in the 45° oblique condition (Huot et al., 2005). Seven tests were run with the H36YO. One test was run without a booster, 2 with a booster with smaller side wings, and 4 with a booster with larger side wings. They used the same pulse and bench as Bilston et al., (2005). They evaluated different supplemental methods of attaching the booster: with and without tether; no attachment, rigid, and two flexible attachment designs. They found a benefit from attaching the booster with rigid ISOFIX attachments, but indicated that larger side wings would be needed to provide adequate head protection.

The third study evaluated the performance of a FFCRS with and without a tether in oblique impacts, with the seat rotated 60° from frontal (Hauschild et al., 2016). (Additional tests were performed at 80° as reported in the side impact section.) Five tests were performed with the Q3S ATD in a FFCRS secured with flexible lower attachments. The CRS was positioned in the center position of a 2013-2014 SUV rear seat; tests were performed with and without a tether. The nominal pulse was 35 km/h, 24 g. A simulated left-side interior door was also included. Using the tether reduced the likelihood or severity of head impact with the side door.

The fourth study evaluated the kinematics of the Q3S in a FFCRS first in a vehicle crash, and then examined through a series of sled tests (Yoshida et al., 2011). A Q3S was seated in a FFCRS in the second row left position of a small sedan, with 75 mm of slack in the harness to represent a common misuse. The vehicle was struck in the left front door by an SUV, at an angle of 45° and speed of 50 km/h. The ATD's head struck the window. For the sled tests intended to duplicate kinematics of the vehicle crash, an ECE R44 bench was used, mounted 45° relative to the forward direction. A door from the same model vehicle as the target car was mounted, and additional plate was located near the front of the door to simulate the B-pillar intrusion. The sled conditions showed good agreement with the ATD measures and kinematics from the crash. Four

additional tests were conducted to examine the effect of slack and chest clip use, and 2 more tests were run with the seat oriented 60° from frontal. These 6 sled tests were also repeated with the P3 ATD. They found that P3 results were generally higher than those of the Q3S, and that use of a chest clip retained the harness on the ATDs' shoulders.

Rear Impact

We identified only four studies that examined the performance of child restraints in rear impact; none of them evaluated belt-positioning boosters. One study (Manary et al., 2006) examined the effects of different tethering methods on a rear-facing child restraint in front and rear impacts, in comparison to a forward-facing child restraint. Sixteen tests were performed using the CRABI 12MO and a single convertible CRS model on the ECE bench. A 48-km/h, 24-g pulse was used for the frontal tests (similar to FMVSS No. 213), while a 25-km/h, 15-g pulse was used for the rear tests. Results indicate a potential benefit, in both front and rear impacts, of tethering RFCRS to a point above the vehicle seatback.

Thirty-six tests were conducted to explore the effect of securing RFCRS with lower anchors or seat belt during rear impacts (Williams et al., 2015). Three different RFCRS were tested. They found higher HIC15 values when lower anchors were used to secure the CRS compared to a 3-point belt. In a companion study, the response of 4 RFCRS in rear impact, with and without tethers attached down to the floor, was evaluated in 24 tests using the CRABI 6MO (O'Donel, 2017). Four different convertible CRS models were tested using a rear seat from a Toyota Camry using a 48-km/h, 24-g pulse. Tethering from the top of CRS increased HIC measures in tests with three products.

Another study examining CRS performance in rear impact (Mansfield et al., 2018) explored the effect of attachment method and CRS features on performance. Eight tests were performed with the CRABI 12MO and 4 tests were performed with the Hybrid III 3YO on a rear seat from a recent model-year sedan. Four CRSs were evaluated: two rear-facing only (Evenflo Embrace and Maxi Cosi Mico AP/Mico Max 30) and two convertibles (Diono Radian and Safety 1st Continuum). A nominal 28-km/h, 18-g pulse was used. Minimal changes in ATD response were observed with handle position up/down, testing with the 12MO or 3YO, and using lower anchors or seat belt as securement. Larger differences were observed in tests run with and without Swedish tether,⁶ with and without anti-rebound bar, and with and without the base of the RF only CRS.

Summary of Child ATD Testing

- The majority of child ATD tests have been performed in frontal impacts.
- More ATD tests have been conducted using different vehicle seats than standardized test benches, and the exact vehicle make/model/model year is not provided in the literature, making reproduction of conditions via modeling a challenge.
- No tests have been performed in rear impact using belt-positioning boosters; the four different test series studying rear impact response have focused on RFCRSs.
- Several studies have compared kinematics of CRSs when tested on a bench seat and on vehicle seat, which may provide insights as we model CRS performance on vehicle seats after validating from test data collected on a bench seat.

⁶ A Swedish-style tether is an upper tether that attaches near the floor of a rear-facing CRS.

- Many tests have compared the differences in responses when CRSs are secured by different types of flexible lower attachments, rigid lower attachments, the seat belt, and various tether routings. The main method of attachment has a greater effect in side and oblique responses compared to frontal crashes, with rigid lower attachments providing the best kinematics; the tether offers the most benefit in frontal impacts but could potentially help in side/oblique crashes as well. Attachment effects can vary if testing is conducted on a test bench or vehicle seat.
- In frontal impacts, differences in metrics resulting from main attachment method are small compared to misuse effects.

Child Injury Measures and IARVs

Table 5 shows the injury criteria and maximum allowable values required in FMVSS No. 213, while Table 6 shows a set of injury measures and IARVs compiled based on injury biomechanics literature (Mertz et al., 2003, 2016). Because of the lack of cadaver tests for pediatric subjects, all H3 child ATD IARVs heavily rely on scaled adult data. Instead of using scaled values for each size of ATD, FMVSS No. 213 uses the same criteria for each size of ATD for head and chest injury measures. FMVSS No. 213 also includes evaluations of head and knee excursions, which is appropriate because the majority of the head injuries for children are due to a direct head contact. Monitoring the ATD kinematics and the potential for occupant-to-interior contacts in various impact conditions associated with ADS-equipped vehicles would be most relevant.

Table 5. FMVSS No. 213 Injury Criteria

ATD	HIC36	ChestG (g)	Head Excursion With Tether	Head Excursion No Tether	Knee Excursion	RFCS Rotation
12 MO CRABI	1000	60	720 mm	813 mm	915 mm	70 deg
H33YO	1000	60	720 mm	813 mm	915 mm	70 deg
H36YO	1000	60	720 mm	813 mm	915 mm	NA
H310YO	1000	60	720 mm	813 mm	915 mm	NA

Table 6. H3 Child ATD IARVs

ATD	HIC15	Nij	ChestG (g)	ChestD (mm)
12 MO CRABI	390	1.0	50	30
H33YO	570	1.0	55	34
H36YO	700	1.0	60	40
H310YO	700	1.0	60	46

Summary of the Literature Review

- Based on this literature review, the size and shape of automated vehicles may be highly variable. Consequently, a range of vehicle sizes may be required for a study on future ADS-equipped vehicles.
- In addition to conventional seating orientations, consistent trends have shown in the literature that future vehicles with high-level ADS may include unconventional seating orientations, like face-to-face configurations with or without angled seats.

- For a simulation study focusing on unconventional seating associated with ADS-equipped vehicles, it is reasonable to consider a diverse set of impact scenarios including frontal, side, oblique, and rear impacts.
- The majority of previous child ATD testing and modeling studies have been performed in frontal impacts, and there is a critical need for physical tests in side, rear, and oblique impact conditions with varied sizes of pediatric ATDs. It is also necessary to validate the child ATD, CRS, seat, and other restraint system models under side, rear, and oblique impact conditions.
- Due to the lack of pediatric cadaver tests, researchers may not fully understand child injury tolerances. Thus, the current IARVs heavily rely on scaled adult data. Therefore, future studies on child passenger protection should not only consider the injury measures, but also occupant excursions and potential injurious contacts.

Simulation Conditions

Following the literature review, a simulation plan was finalized to identify the specific details of modeling conditions that may represent relevant future crash scenarios associated with ADS-equipped vehicles. Specific CRS models were selected based on availability of validation tests and current product availability. Additional sled tests were conducted to provide additional data for validating each ATD/CRS combination in frontal, oblique, side, and rear impacts. Existing computational models were updated and additional models were created. All the models were validated against the new sled tests.

Vehicle Models

The literature review showed that the size and shape of ADS-equipped vehicles might vary widely. While future AVs may differ in geometry compared to current vehicle configurations, many AVs are being developed based on current platforms. Therefore, performing the study with current vehicle geometries is a reasonable first step. To simulate a range of potential occupant spaces, we selected a small sedan model and a minivan model for simulations. For the sedan, we chose a Ford Fiesta because the model has been used in two previous NHTSA-funded projects, including rear-seat occupant protection (Hu et al., 2017) and restraint performance in oblique impacts (Hu et al., 2019). For the minivan, we used a Dodge Grand Caravan model that was available in NHTSA database, and has been used in a NHTSA-funded project on wheelchair transportation safety (Klinich et al., 2021). Figure 15 shows a comparison of the Caravan and Fiesta interior geometries relative to the forward-facing vehicle seats. The Caravan is longer and wider than the Fiesta, which provides larger space for each of the occupants.

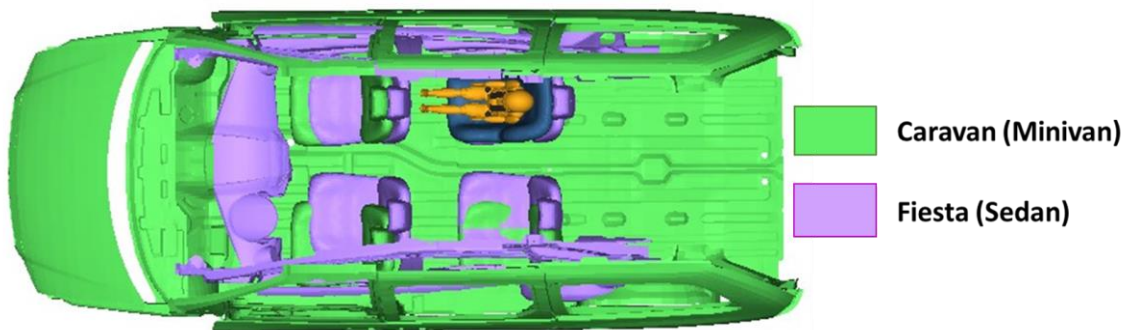


Figure 15. Comparison of Dodge Grand Caravan and Ford Fiesta interiors relative to the forward-facing vehicle seats

Seating Arrangements and Occupant Seating Locations

The seating configurations considered in this project are shown in Figure 16, including 1) Baseline: two front seats, two rear seats, all facing forward, 2) Carriage: two rear seats facing forward, two front seats facing rearward, and 3) Campfire: four seats all angled towards center. The Carriage and Campfire configurations are the two most popular unconventional seating configurations for future highly automated vehicles based on survey studies reviewed in the literature. For the campfire configuration, we used an angle of 15° seat rotation in both vehicles selected.

Five seating locations were simulated for each combination of ATD and CRS as also shown in Figure 16: (1) forward-facing in first row, (2) forward-facing in second row, (3) rear-facing in

first row, (4) angled forward-facing in second row, and (5) angled rear-facing in first row. The first two seating locations represent conventional seating, while the next three seating locations represent unconventional seating for ADS-equipped vehicles. We selected all occupants to be on the right side of the vehicles because these locations will result in farside and farside oblique impacts in 9 to 11 o'clock impacts. Because nearside safety depends more on vehicle side structural characteristics than restraint systems, this study focused on farside impacts where the CRS plays a greater role in providing protection. The simulations used seat belts integrated with the vehicle seats, with the shoulder belt anchor on the right side of forward-facing seats. When rotated to a rear-facing orientation, this placed the shoulder belt on the inboard side of the seat.

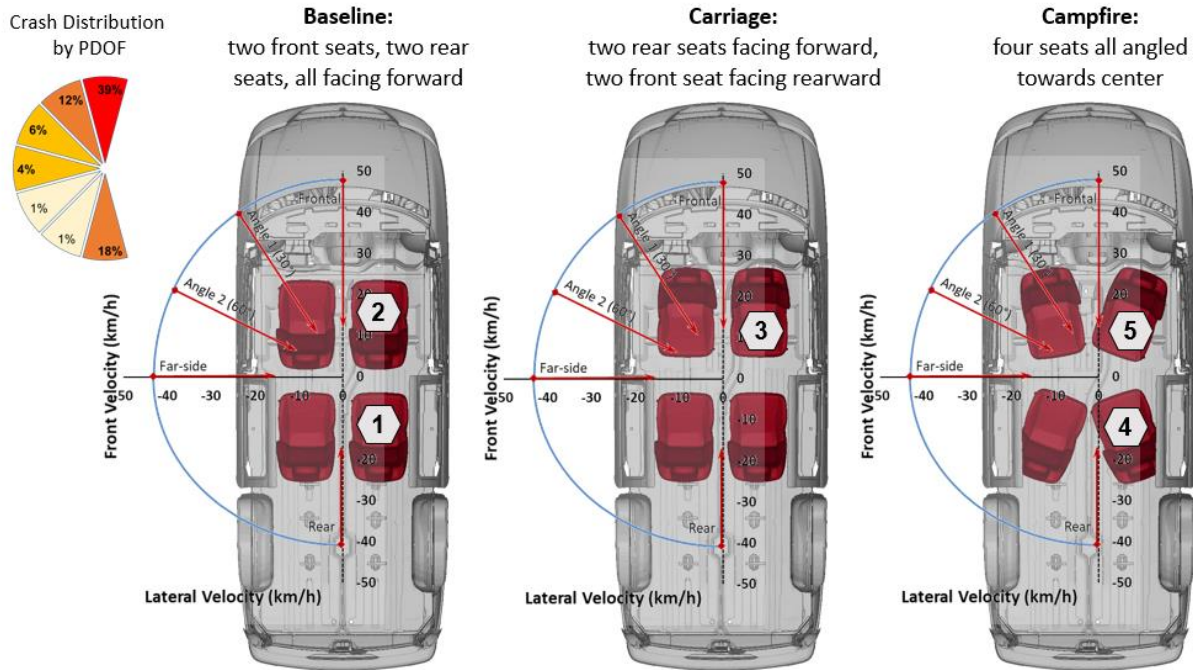


Figure 16. Proposed crash scenarios, seating configurations, and seating locations

Crash Configurations and Severities

Based on the literature review, we planned simulations in five impact directions (6 o'clock-rear, 9 o'clock-side, 10 o'clock, 11 o'clock, and 12 o'clock-frontal) as shown in Figure 16, based on the crash distribution data shown in Figure 4. For the simulations, we chose to model a ~98th percentile delta V for each direction based results shown in Table 2, because the 98th percentile delta V for frontal crashes is consistent with FMVSS No. 213 test severities. For the other crash directions, 98th percentile corresponds to 43.2 (90% of 48) km/h for side impact and 40.8 (85% of 48) km/h for rear impact. The simulated delta V from the PDOF of 9 o'clock through 10 and 11 o'clock to 12 o'clock are shown in Figure 16, in which an ellipse equation was fit using a semi-major axis of 48 km/h and semi-minor axis of 43.2 km/h between 9 and 12 o'clock. While future highly automated vehicles may be involved in lower severity crashes than conventional vehicles, the potential for high severity crashes remains with a mixed fleet, and occupant protection systems will need to work in more severe crashes for the foreseeable future, so selecting 98th percentile severity crashes is appropriate for this study.

To determine the pulse shape for the non-frontal directions, we reviewed the side impact acceleration profiles from five vehicles, scaled them to have a delta V of 43.2 km/h, and overlaid them with the average FMVSS No. 213 frontal corridor, scaled to have a delta V of 43.2 km/h. As shown in Figure 17, the scaled FMVSS No. 213 frontal corridor provides a good approximation of the shape of the scaled vehicle side impact accelerations. As a result, a scaled version of the FMVSS No. 213 corridors was also used for the oblique and rear impacts with different target delta Vs corresponding to the impact directions, where crash pulse data are not available.

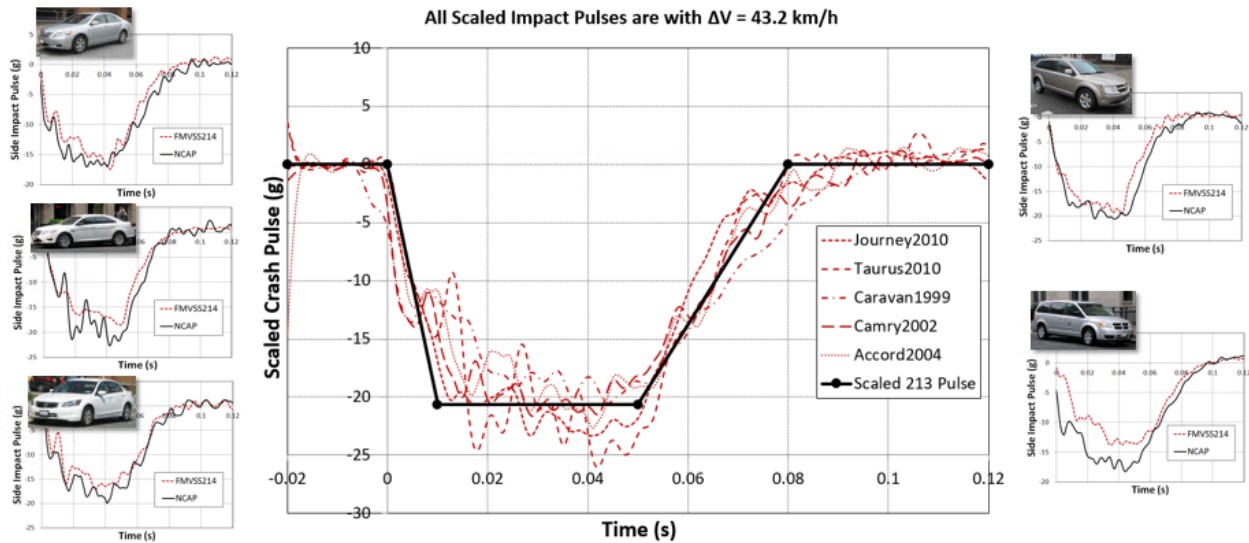


Figure 17. Scaled FMVSS No. 213 frontal pulse and NCAP side impact pulses (All pulses were scaled to the side impact target delta V of 43.2 km/h.)

ATD, CRS, and Vehicle Seat Models

In this study we used MADYMO models for all simulations. Models of the CRABI 12MO in a rear-facing infant seat and an H33YO ATD in a forward-facing convertible CRS were first selected to represent occupants using harnessed child restraints. However, best practice recommendations since 2011 from NHTSA and the AAP recommend staying rear-facing as long as possible, so we also considered the H33YO ATD in a rear-facing convertible in this study. Because RFCRS designed to accommodate larger children are necessarily bigger, it would be more challenging to design alternative seating configurations that accommodate a larger convertible CRS used rear-facing than a rear-facing only CRS. Therefore, a total of three ATD/harnessed CRS conditions were simulated in this study, including CRABI 12MO in a RFCRS, H33YO ATD in a RFCRS, and H33YO ATD in a FFCRS.

For the rear-facing infant seat, we selected Graco SnugRide 30, because (1) an MADYMO model of this seat is already available at UMTRI and has been validated against sled tests with the 12MO CRABI in frontal crashes (Hu, Wu, Klinich, et al., 2013), and (2) a version of the Graco SnugRide 30 is still available on the market for additional sled tests. For the convertible CRS, we chose to use the Evenflo SureRide XL, because 32 frontal sled tests were available for model validation (Manary et al., 2019), and a version of this product is still available for additional sled tests.

In terms of CRS installation methods, Manary et al. (2019) found that securing rear-facing or forward-facing convertibles using the seat belt or the lower anchorage attachments did not have a significant effect on performance measures in forward-facing impacts. However, this may differ in angled, side, or rear impacts. Tether use reduces ATD head excursions in frontal crashes. Past research has shown that rigid LATCH anchorage hardware could provide a benefit for side impacts (Hauschild et al., 2018; Kapoor et al., 2011). However, given that there are few CRS models equipped with rigid LATCH attachments being sold in the United States, we performed simulations using flexible LATCH attachments. Therefore, in summary, we explored three CRS installation methods (LATCH versus seat belt with tether versus seat belt without tether) for the FF convertible seat.

To represent children restrained by the vehicle belt, we used the UMTRI parametric MADYMO child model to represent the H36YO and H310YO ATDs. A backless belt-positioning booster seat was selected for simulations with H36YO, because it would be a worse-case scenario compared to a high-back booster that has some structure to prevent lateral movement. In addition, in a shared services model most commonly expected for initial deployment of highly automated vehicles, a backless booster would often be preferred because of its more convenient size. Simulations were also conducted with the H310YO directly seated on the vehicle seat without a booster. The belt-positioning booster seat selected for the study was a Graco TurboBooster, because the project to develop optimized restraint systems for the rear seat (Hu et al., 2017) validated the performance of an H36YO in a Graco Turbo backless booster in the rear seat of a Ford Fiesta model.

The vehicle seat used in this study is a captain's chair with integrated belt restraints. For unconventional seating arrangements, a seat-integrated belt seems to be the only type of seat/restraint system combination that would be feasible. While other seat/restraint options are available for the baseline condition, results would be more directly comparable if we use the same seat and restraint for all conditions. We have developed and validated the captain's chair MADYMO model through our previous studies (Hu, Wu, Reed, et al., 2013; Wu et al., 2012). In that model, the geometry of seat cushion and back was based on scan data of a captain's chair and two cylinders were used to simulate the seat supporting structure. The characteristics of the seat cushion and supporting structure were tuned based on frontal impact sled tests with H36YO and H310YO ATDs.

Validation Testing

Sled Test Matrix

Table 7 shows the matrix of validation tests. The objective was to provide tests in frontal, 40° oblique, 80° oblique, and rear impact conditions using the CRABI 12MO, H33YO, H36YO, and H310YO ATDs. Because of budgetary constraints, one oblique test condition of 40° was selected for validation tests, although the simulations would be performed with oblique angles of 30 and 60°. Following current best practice recommendations, tests were performed with a rear-facing CRS (RFCRS) with the CRABI 12MO, a convertible CRS both RF and FF with the 3YO, a belt-positioning booster seat with the H36YO, and a lap-shoulder belt with the H310YO.

In the first column of the matrix, the first two numeric digits of the test ID indicate the year the test was performed. Fifteen tests were performed in 2021, two in 2014, one in 2015, and one in 2018. Appendix B describes the differences between the test benches used in each of these tests. The two tests from 2014 were part of a larger study on CRS misuse. Test NT2102 was performed to compare to NT1419, to identify potential differences in response resulting from the changes made between the 2014 and 2018/2020 test benches. If responses are comparable, this would indicate findings from the 2014 misuse tests could also be used for validation testing.

Table 7. Sled Test Matrix

Test No	ATD	Bench	CRS	Orientation	Securement	Tether
NT1419	H33YO	Frontal, 2014 213	SureRide	FF	3PB	Yes
NT1447	H33YO	Frontal, 2014 213	SureRide	RF	3PB	Yes
NT1515	H36YO	Frontal, 2015 213	Backless TurboBooster	FF	3PB w SR	No
NT1845	H310YO	Frontal, 2018/20 213	None	FF	3PB w SR	No
NT2101	CRABI 12MO	Frontal, 2018/20 213	Snugride30	RF	3PB	No
NT2102	H33YO	Frontal, 2018/20 213	SureRide	FF	3PB	Yes
NT2103	H33YO	Oblique 40°	SureRide	FF	3PB	Yes
NT2104	H33YO	Oblique 40°	SureRide	RF	3PB	No
NT2105	CRABI 12MO	Oblique 40°	Snugride30	RF	3PB	No
NT2106	CRABI 12MO	Oblique 80°	Snugride30	RF	3PB	No
NT2107	H33YO	Oblique 80°	SureRide	RF	3PB	No
NT2108	H33YO	Oblique 80°	SureRide	FF	3PB	Yes
NT2109	H33YO	Vehicle seat 180°	SureRide	RF	3PB	No
NT2110	H33YO	Vehicle seat 180°	SureRide	FF	3PB	Yes
NT2111	CRABI 12MO	Vehicle seat 180°	Snugride30	RF	3PB	No
NT2112	H36YO	Vehicle seat 180°	Backless TurboBooster	FF	3PB w SR	No
NT2113	H310YO	Vehicle seat 180°	None	FF	3PB w SR	No
NT2114	H310YO	Oblique 40°	None	FF	3PB w SR	No
NT2115	H310YO	Oblique 80°	None	FF	3PB w SR	No
NT2116	H36YO	Oblique 80°	Backless TurboBooster	FF	3PB w SR	No
NT2117	H36YO	Oblique 40°	Backless TurboBooster	FF	3PB w SR	No

Because the number of recent tests of CRS in non-frontal conditions are limited, tests were also performed under oblique and lateral test conditions. The test bench was rotated 40° for oblique conditions, and 80° for lateral conditions. The lateral conditions matches the angle in the proposed FMVSS No. 213 side impact test procedure (Docket No. NHTSA-2014-0012), selected because most side impact crashes also have a frontal component.

Previous test data using CRSs in rear impact conditions were also limited. Because the 2020 FMVSS No. 213 bench does not have a realistic vehicle head restraint or seatback contour, rear impact tests were performed using a reinforced 2008 Dodge Caravan vehicle seat. This seat fixture was previously used in a past UMTRI study (Klinich et al., 2011), so a validated frontal impact model was already available, as were the vehicle seats themselves. For the current study, the seat was mounted rear-facing on the sled buck as shown in Figure 18. In addition, the belt geometry was adjusted so it more closely matched the geometry on the FMVSS No. 213 bench.



Figure 18. Illustration of vehicle seat mounted rear-facing on FMVSS No. 213 bench

In this study, all of the harnessed restraints were installed on the bench using the lap-shoulder belt with fixed anchors. Tests performed with the SnugRide 30 used the base, the top harness slots, and the handle in the mid position. The tests run with the Evenflo SureRide used the harness slots two down from the top location in all tests; the upright setting was used in the forward-facing tests and the reclined setting in the rear-facing tests. The tether was used in the forward-facing test with the SureRide.

For the tests with the H36YO and H310YO, a sliding latch plate was used on the belts, and the surrogate seat belt retractor developed in a prior UMTRI study (Manary et al., 2018) was also used. The surrogate retractor was configured to allow for ~50 mm of webbing payout to be similar to OEM retractor payouts. The tests with the H36YO were run with the armrests of the Graco TurboBooster in the lowest position.

Sled Pulses

A limitation of the UMTRI sled is that it cannot produce an FMVSS No. 213 pulse that is completely within the corridor, as shown in Figure 19. To address questions regarding potential significance, simulations were performed using the H310YO model seated on a vehicle seat, with the pulse set to the UMTRI sled pulse, a sled pulse that matches the UMTRI pulse for the first 60 ms but is compliant afterwards, and a linear representation of the average FMVSS No.

213 corridor. Differences in kinematics, injury measures, and excursions from the pulse differences were negligible compared to standard test-to-test variation. In addition, the differences in response between these two pulses were smaller than the differences between a fully-compliant pulse and the linear representation of the average FMVSS No. 213 corridor pulse that would be used in simulations. As a result, the UMTRI pulse was considered reasonable to use for this research study.

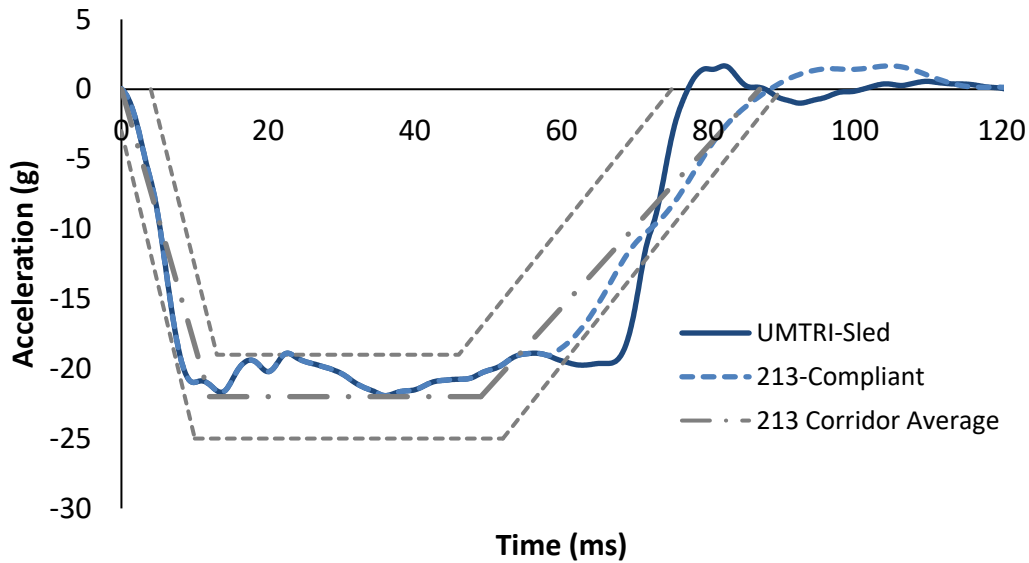


Figure 19. Comparison of UMTRI sled approximation of FMVSS No. 213 pulse, a completely compliant pulse, the FMVSS No. 213 corridor, and an average of the FMVSS No. 213 corridor

Data Collection

All ATDs were calibrated prior to the test series and were equipped with triaxial head and chest accelerometers and upper neck load cells. In addition, all ATDs were equipped to measure fore-aft chest displacement, except for the CRABI 12MO where it is not available. Lap and shoulder belt loads were measured in all tests. To facilitate consistent analysis of kinematics as we ran tests with the bench oriented in multiple conditions, six camera views were recorded as shown in Figure 20. CRS, head and knee kinematics were measured using TEMA 3D motion analysis software. Several targets on the ATD's head were tracked and transformed to represent the actual Head CG, so excursion traces and maximums reported are relative to the CG initial position in the X, Y and Z plane relative to the seat fixture local coordinate system (not the sled global coordinate system). For tests with the H36YO and H310YO, a silicone lap shield was used to prevent the lap belt from dropping into the gap at the front of the ATD pelvis and engaging the ATD in a non-biofidelic manner.



Figure 20. Example screen shots of six camera views used in study: rear, rear oblique, lateral, front oblique, front, and overhead

Results

Appendix C contains overlay plots of key ATD outputs. Full results and videos will be available from the NHTSA CRASH database (www.nhtsa.gov/research-data/databases-and-software).

Frontal Impacts

Table 8 contains a summary of key injury measures and excursions for the frontal validation tests. As expected, all tests met existing FMVSS No. 213 requirements. Photos of the peak excursions are included in as part of the model validation results in Figure 23A through Figure 27A. When reviewing the resultant signals in Appendix C, all of the forward-facing tests with the H33YO have a secondary peak head acceleration late in the event caused by rebound head contact with the upper seatback structure of the bench, although it is reduced with the newer version of the bench.

Table 8. Frontal Injury Reference Measures

TestID	HIC36	Chest 3ms Clip (g)	Peak Chest Deflect (deg)	Res. Upper Neck F (N)	Res. Upper Neck M (Nm)	N_{ij}	Peak Forw Head Excur (mm)	Peak Rear Head Excur (mm)	Peak Lateral Head Excur (mm)
NT2101 12R	764	47	--	1254	11	1.37 N_{te}	232	-17	3
NT2102 3F	499	46	--	2682	28	1.98 N_{te}	601	0	87
NT1419 3F	481	42	--	--	--	--	571*	--	--
NT1447 3R	490	45	--	--	--	--	581*	--	--
NT1515 6	724	54	--	2160	36	0.95 N_{te}	560*	--	--
NT1845 10	787	49	--	3755	48	1.82 N_{te}	501*	--	--

* Excursion measurements from past tests are relative to the sled global coordinate system with the origin at the sled Z-point.

The bench design was changed as described in Appendix B between test NT1419 and NT2102. The peak HIC 36 and chest acceleration measures are fairly close, and Figure 21 shows a comparison at the time of peak excursion, with maximum excursion differing by 30 mm. The inclusion of the shoulder belt in the later test as part of the securement may have affected kinematics slightly.



Figure 21. Comparison of peak head excursion from tests NT1419 (left) and NT2102 (right)

Oblique Impacts

Results for the 40° oblique impacts are shown in Table 9. Photos of the time of peak excursion are included in Figure 23B through Figure 27B. The peak resultant neck force of the H33YO was about three times higher in the forward-facing condition compared to the rear-facing test. The test with the H36YO showed substantially lower head and chest accelerations, as well as neck loads, compared to the H310YO tests, because the shoulder belt slipped off the shoulder of the H36YO, but was caught between the neck and clavicle for the H310YO. This also caused differences in how the shoulder belt loaded the thorax relative to the location of the chest displacement instrumentation. For the H310YO tests, the signals show peaks from chin-to-chest contact around 90 ms and with the side of the bench structure at 150 ms.

Table 9. Oblique Injury Reference Measures

TestID	HIC36	Chest 3ms Clip (g)	Peak Chest Deflect (deg)	Res. Upper Neck F (N)	Res. Upper Neck M (Nm)	N_{ij}	Peak Forw Head Excur (mm)	Peak Rear Head Excur (mm)	Peak Lateral Head Excur (mm)
NT2105 12R	503	33	--	980	13	1.18 N_{te}	183	-188	301
NT2104 3R	375	42	--	860	16	0.86 N_{te}	166	0	418
NT2103 3F	502	41	--	2491	27	1.75 N_{te}	565	0	347
NT2117 6	118	10	40.6	1305	29	0.50 N_{te}	292	0	529
NT2114 10	664	49	5.6	2278	51	1.11 N_{te}	215	-117	487

Side Impacts

Injury measures from the five tests run at 80° to represent a typical side impact scenario are shown in Table 10. Images of the peak excursion are shown as part of the model validation results in Figure 23C through Figure 27C. In all cases, the CRS and ATDs rotated about the X-axis of the bench as well as about the Z-axis. The H33YO in the FFCRS had the least amount of lateral movement among these tests. While the model validation section shows the time of peak lateral head excursion on the overhead camera, Figure 22 shows that for all three ATD/CRS

conditions, the CRS/ATD continued to rotate off the bench seat. The RFCRS with the 3YO rotated to a level below the bench seat. The H36YO continued to rotate off the side of the bench seat, and the head struck the rigid structure of the seatback. The H310YO also rotated off the bench seat, but its head does not appear to make the same contact as the H36YO. Also visible in these photos is the difference in shoulder belt loading between the H36YO and H310YO. As in the oblique tests, the shoulder belt slipped off the shoulder of the H36YO but was trapped on the clavicle of the H310YO. The excessive motion of the H310YO in the lateral tests led to both shoulder blocks fracturing, and one shoulder joint stop broke off.

Table 10. Side Impact Validation Test Injury Measures

TestID	HIC36	Chest 3ms Clip (g)	Peak Chest Deflect (deg)	Res. Upper Neck F (N)	Res. Upper Neck M (Nm)	N_{ij}	Peak Forw Head Excur (mm)	Peak Rear Head Excur (mm)	Peak Lateral Head Excur (mm)
NT2106 12R	461	40	--	1475	21	2.14 N_{te}	35	-136	616 ^φ
NT2107 3R	478	32	7.5	1087	24	1.12 N_{te}	45	-164	753 ^φ
NT2108 3F	846	48	17.5	1828	43	1.40 N_{te}	81	0	451
NT2116 6	1267	49	6.5	3259	90	0.96 N_{te}	41	-143	534
NT2115 10	359	13	21.9	2339	38	1.19 N_{te}	65	-15	680

^φExcursion tracked before targets were obscured, so may not be maximum.

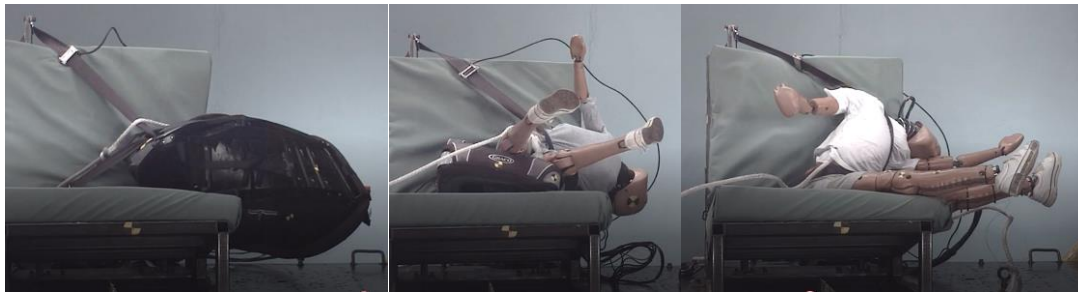


Figure 22. Extreme rotation of RF H33YO, H36YO, and H310YO during lateral tests

Rear Impacts

Injury measures for the five tests performed on a rear-facing vehicle seat are shown in Table 11. Photos from the time of peak rearward excursion are shown in the model validation section in Figure 23D through Figure 27D. For the two tests run with RFCRS, the ATD's head did not contact the vehicle seatback or head restraint. Review of the signals in Appendix C shows that the 12MO CRABI, H36YO, H310YO have chest acceleration peaks above 60 g, including some spikes over 100 g. Given that we do not have any documented field cases of severe chest injury to children in rear impacts, we suspect that these signals are artifacts of the ATDs or the vehicle seat. When comparing the head position of the 6YO and 10YO at peak rear excursion, the H36YO appears to be extending further rearward, although both are positioned at a similar height relative to the seat's head restraint. The interaction of the two larger ATDs with the seatback led to very high resultant neck moments.

Table 11. Rear Impact Validation Test Injury Measures

TestID/ ATD/ Orient	HIC36	Chest 3ms Clip (g)	Peak Chest Deflect (deg)	Res. Upper Neck F (N)	Res. Upper Neck M (Nm)	N_{ij}	Peak Forw Head Excur (mm)	Peak Rear Head Excur (mm)	Peak Lateral Head Excur (mm)
NT2111 12R	131	71	--	1172	7	1.03 N_{ce}	0	-435	32
NT2109 3R	184	45	20	1531	15	1.08 N_{te}	0	-413	7
NT2110 3F	282	41	15	1036	15	0.42 N_{te}	133	-93	27
NT2112 6	325	70	8	2272	59	1.01 N_{te}	243	-117	15
NT2113 10	352	79	10	2103	94	0.83 N_{tf}	189	-143	15

Model Validation

Each of the sled tests conducted in this study was used to validate the MADYMO models. All MADYMO models of the ATDs, CRSs, seat, and seat belt were developed previously, except that the model for the Evenflo SureRide XL convertible seat was newly developed and shared at https://deepblue.lib.umich.edu/data/concern/data_sets/5d86p059s. The ATD and CRS kinematics and ATD injury measures were compared between the tests and simulations. CORrelation and Analysis (CORA) scores were used to quantitatively evaluate the time histories of ATD head excursions. The contact characteristics between the ATD and CRS and between the CRS and seat were adjusted consistently across different crash conditions to achieve the overall best match.

Kinematics Validation

Figure 23 through Figure 27 show examples of each simulation compared to the validation test at the time of peak excursion for the five ATD/restraint combinations being considered in this study. In each of these figures, A shows frontal impact, B oblique, C lateral, and D rear impact. In general, the model-predicted ATD/CRS kinematics compared well against test results.

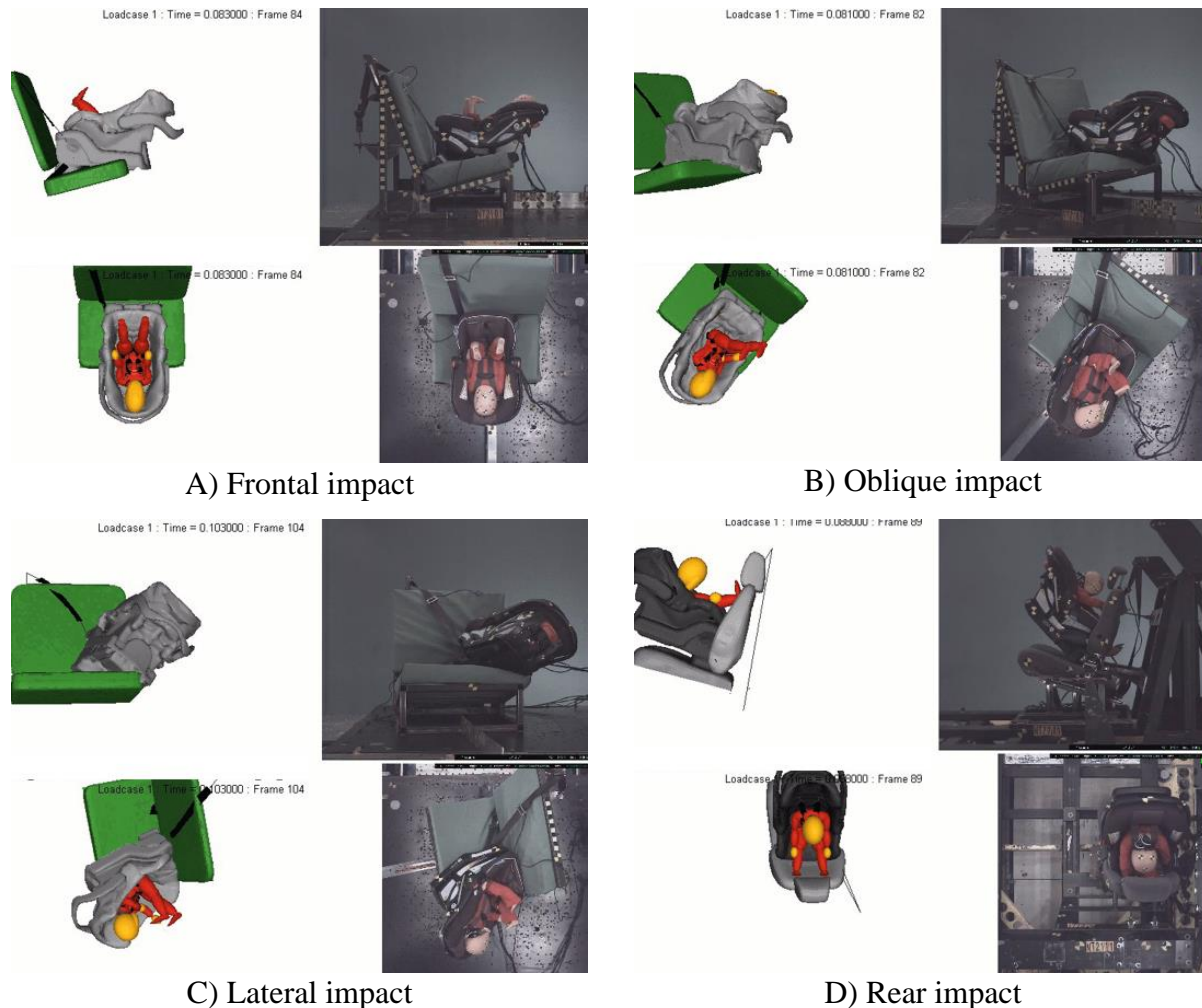
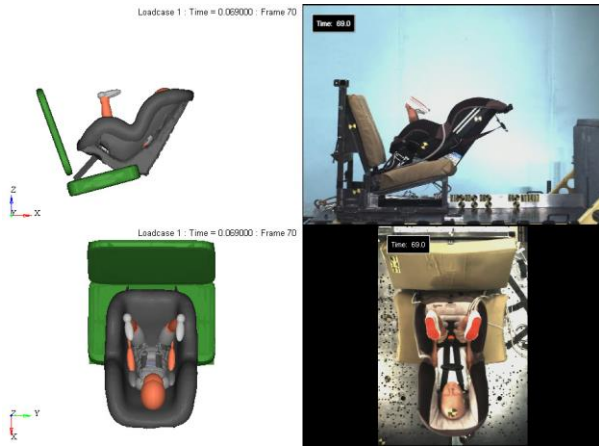


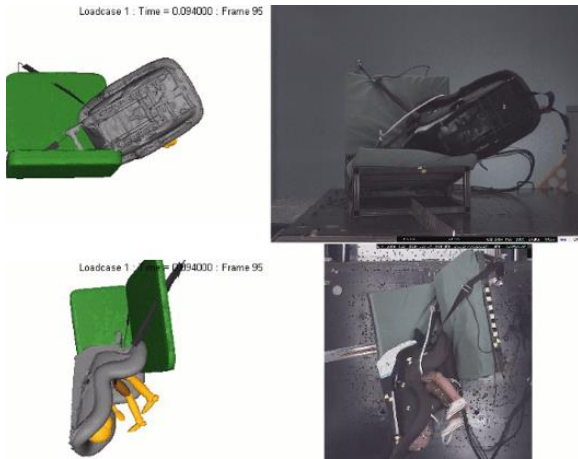
Figure 23. Comparison of model and test for CRABI 12MO in infant seat at time of peak excursion in various impact conditions



A) Frontal impact



B) Oblique impact

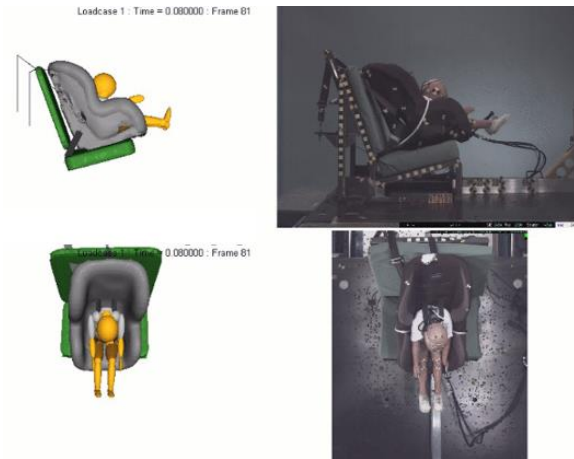


C) Lateral impact

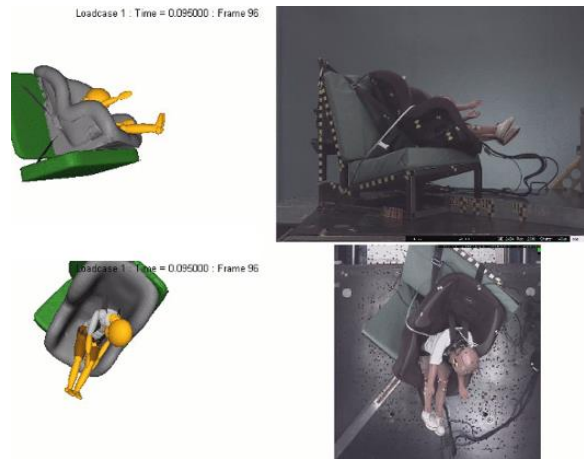


D) Rear impact

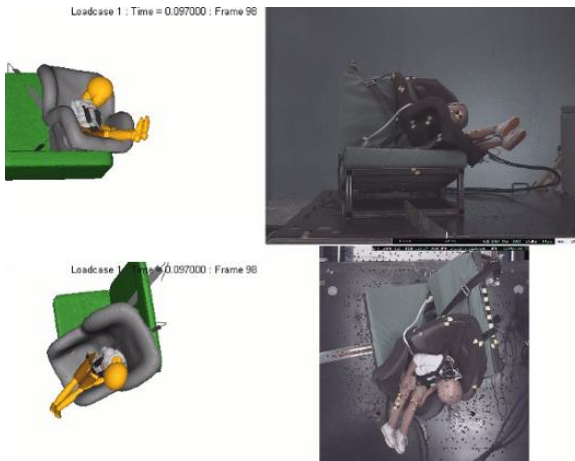
Figure 24. Comparison of model and test for H33YO in rear-facing convertible at time of peak excursion in frontal impact



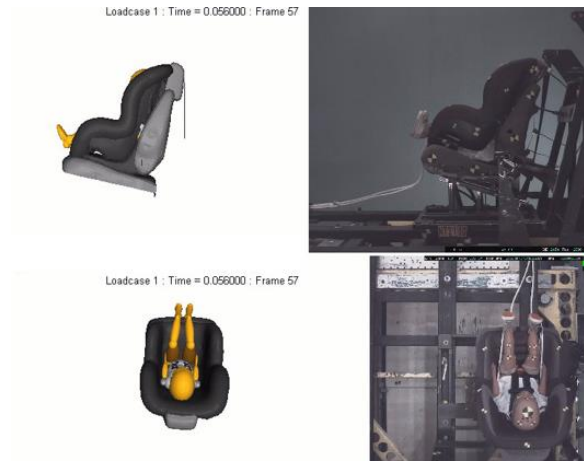
A) Frontal impact



B) Oblique impact

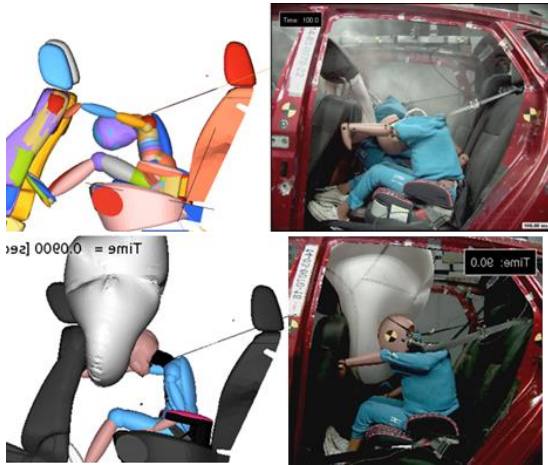


C) Lateral impact

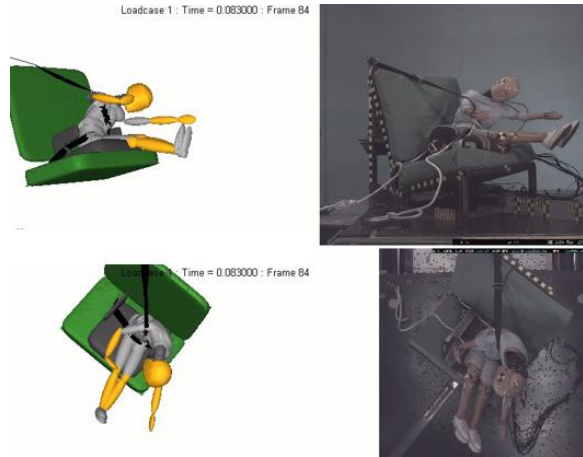


D) Rear impact

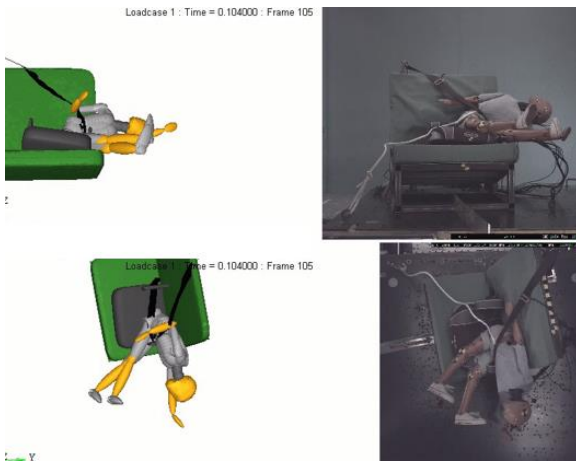
Figure 25. Comparison of model and test for H33YO in forward-facing convertible at time of peak excursion in frontal impact



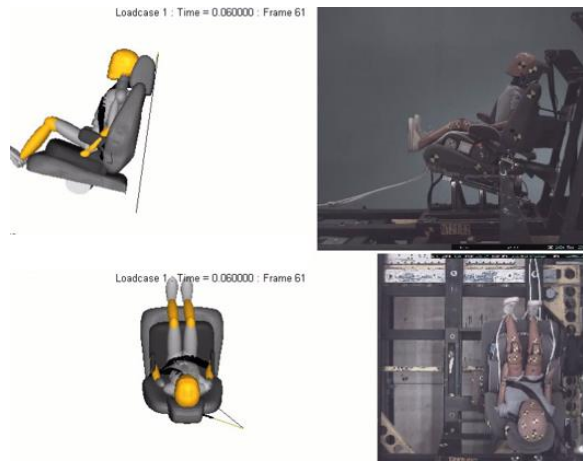
A) Frontal impact (previous study)



B) Oblique impact

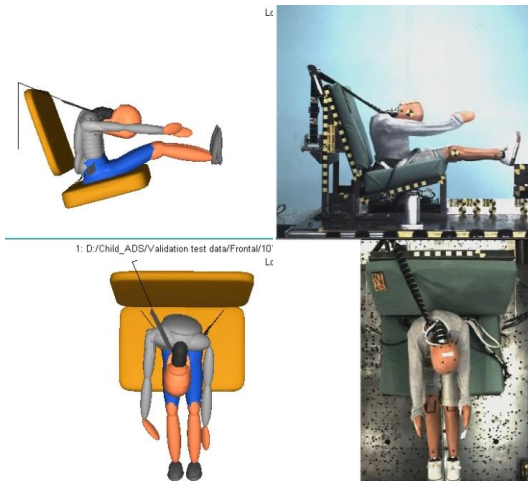


C) Lateral impact

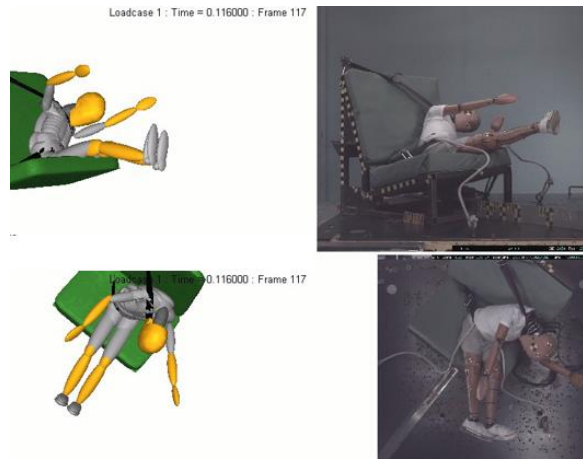


D) Rear impact

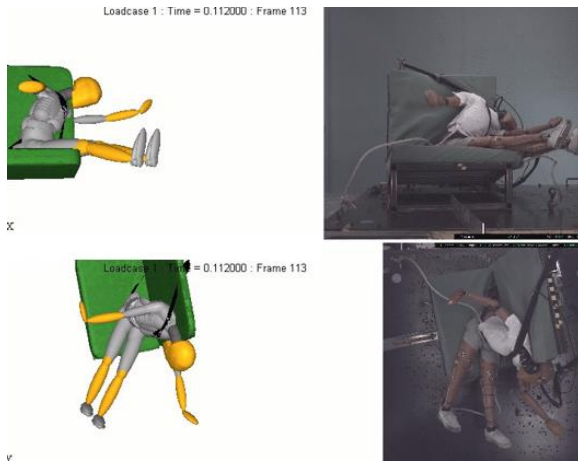
Figure 26. Comparison of model and test for H36YO in backless booster in various impact conditions



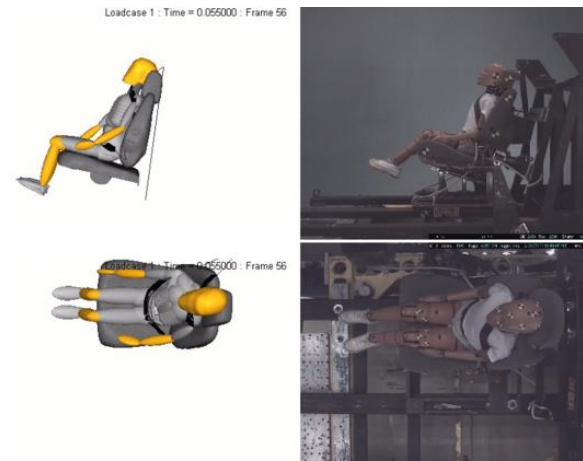
A) Frontal impact



B) Oblique impact



C) Lateral impact



D) Rear impact

Figure 27. Comparison of model and test for H310YO in frontal impact conditions

CORA Scores for ATD Head Excursion Time Histories

To further quantify the model validity in terms of the ATD kinematics, CORA scores were calculated for the time histories of head X (horizontal), Y (lateral), Z (vertical), and resultant excursions as shown in Table 12. CORA scores for excursions with peaks less than 100 mm were neglected, as they do not provide meaningful results. In general, the simulations produced good CORA scores (>0.80) in all loading conditions, and the head excursions along the impact directions (resultant excursion) typically have higher CORA scores. The CORA scores in rear impacts have slightly lower CORA scores, because the head excursions are typically small in those conditions.

Table 12. CORA Scores for Head Excursions*

ATD	CRS	Impact	Bench	X	Y	Z	Resultant
CRABI 12MO	RF	Frontal 0°	New 213	0.774	Negl	0.807	0.800
CRABI 12MO	RF	Oblique 40°	New 213	0.802	0.793	0.608	0.900
CRABI 12MO	RF	Side 80°	New 213	0.816	0.942	0.636	0.935
CRABI 12MO	RF	Rear 180°	Vehicle Seat	0.826	Negl	Negl	0.828
H33YO	RF	Oblique 40°	New 213	0.859	0.800	0.549	0.865
H33YO	RF	Side 80°	New 213	0.757	0.905	0.587	0.933
H33YO	RF	Rear 180°	Vehicle Seat	0.701	Negl	Negl	0.720
H33YO	FF	Frontal 0°	New 213	0.936	Negl	0.555	0.905
H33YO	FF	Oblique 40°	New 213	0.893	0.943	0.768	0.952
H33YO	FF	Side 80°	New 213	Negl	0.903	0.648	0.902
H33YO	FF	Rear 180°	Vehicle Seat	Negl	Negl	Negl	Negl
H36YO	Booster	Oblique 40°	New 213	Negl	0.998	0.437	0.993
H36YO	Booster	Side 80°	New 213	0.992	0.974	0.813	0.986
H36YO	Booster	Rear 180°	Vehicle Seat	0.466	Negl	Negl	0.547
H310YO	3PB	Oblique 40°	New 213	0.961	0.699	0.783	0.837
H310YO	3PB	Side 80°	New 213	0.979	0.967	0.869	0.910
H310YO	3PB	Rear 180°	Vehicle Seat	0.796	Negl	Negl	0.794

*Excursions with peaks <100 mm were considered negligible and CORA scores not calculated.

ATD Injury Measure Validation

Table 13 shows the comparison of HIC 36 and chest acceleration between the tests and simulations. The simulation results compared reasonably well against the test results. The model predicted chest accelerations more accurately than the HIC 36 due to the nonlinear nature of HIC 36. However, the HIC 36 values are generally below the FMVSS No. 213 criteria, except for the H310YO in side impact, in which the ATD's head contacted the seat frame behind the seat back. Because such contact is not likely to occur in real vehicle crashes, we did not simulate the head contact to the seat frame. As a result, the simulation under-estimated the HIC36 for H310YO in the side impact condition. In rear impact condition, both the simulations and the sled tests yielded chest accelerations that may be over the injury criterion, although the results may not be comparable to real-world crashes due to the rigidized seat back used in the sled tests.

Table 13. Comparison of HIC 36 and Chest Acceleration Between Tests and Simulations

ATD	CRS	Impact	Bench	HIC 36* Test	HIC 36* Sim	ChestG (g)* Test	ChestG (g)* Sim
CRABI 12MO	RF	Frontal 0°	New 213	764	374	47.4	53.5
CRABI 12MO	RF	Oblique 40°	New 213	503	430	33.1	43.1
CRABI 12MO	RF	Side 80°	New 213	461	304	40.1	35.1
CRABI 12MO	RF	Rear 180°	Vehicle Seat	131	137	70.7	43.7
H33YO	RF	Oblique 40°	New 213	375	310	41.6	47.7
H33YO	RF	Side 80°	New 213	478	354	32.1	30.3
H33YO	RF	Rear 180°	Vehicle Seat	184	289	44.5	49.3
H33YO	FF	Frontal 0°	New 213	499	281	45.7	38.3
H33YO	FF	Oblique 40°	New 213	502	318	40.6	36.4
H33YO	FF	Side 80°	New 213	846	306	48.2	49.7
H33YO	FF	Rear 180°	Vehicle Seat	282	638	40.5	63.5
H36YO	Booster	Oblique 40°	New 213	118	402	9.8	30.1
H36YO	Booster	Side 80°	New 213	359	440	13.1	45.5
H36YO	Booster	Rear 180°	Vehicle Seat	325	414	69.9	82.8
H310YO	3PB	Oblique 40°	New 213	664	655	49.0	44.2
H310YO	3PB	Side 80°	New 213	1269**	776	49.0	49.2
H310YO	3PB	Rear 180°	Vehicle Seat	352	377	79.1	79.0

* Injury measures over IARVs in FMVSS No. 213 criteria are highlighted in red.

** High HIC value due to contact to the 213 seat frame.

Simulations of ATDs in Harnessed CRS

Simulation Matrix

As shown in Table 14, we designed three parametric studies using three ATD/CRS combinations for ATDs in harnessed CRS. All three parametric studies used the five crash scenarios and five seating location/orientation conditions shown in Figure 16 along with two vehicle models. Two CRS installation methods were applied to a CRABI 12MO in a RF infant seat and H33YO in a RF convertible, while three CRS installation methods were applied to an H33YO in a FF convertible. Three sets of a full factorial design of experiments resulted in a total of 350 simulations. Each parametric study was set up using MADYMO linked to modeFRONTIER (ESTECO), a general-purpose design of experiment and optimization software, which has been used in many previous UMTRI studies.

Table 14. Simulation Matrix for Harnessed Occupants

Study #	ATD/CRS	CRS Installation	Crash Scenarios	Seating Arrangement	Vehicles	# of Sim
1	12MO CRABI/ RF Infant Seat	1-Lower anchorage 2-Seat belt	1-front 2-side 3-rear 4-oblique frontal 5-oblique side See Figure 16	2 Conventional 3 Unconventional See Figure 16	1-Sedan 2-Minivan	100
2	H33YO ATD/ RF Convertible	1-Lower anchorage 2-Seat belt	1-front 2-side 3-rear 4-oblique frontal 5-oblique side See Figure 16	2 Conventional 3 Unconventional See Figure 16	1-Sedan 2-Minivan	100
3	H33YO ATD/ FF Convertible	1-LATCH 2-Seat belt No- tether 3-Seat belt & Tether	1-front 2-side 3-rear 4-oblique frontal 5-oblique side See Figure 16	2 Conventional 3 Unconventional See Figure 16	1-Sedan 2-Minivan	150
Total #	3	3	5	5	2	350

Injury Measures and Contact Definition

The output variables included 3D head and knee excursions of the ATDs, CRS rotation, ATD head and chest accelerations, H33YO ATD neck force/moment, and chest deflection. The output variables ensure a comprehensive view of ATD/CRS kinematics and ATD-based injury risks. We understand that the H33YO ATD does not have the capability to measure chest lateral deflection, such as Q3s. However, based on a field study by (Kuppa & Saunders, 2005), head injury accounted for nearly 80 percent of AIS 3+ injuries for 0- to 5-year-old children in motor vehicle crashes. Therefore, we focused on potential safety concerns related to head impact in data analysis. In addition, no nearside impact were simulated, so the chest deflections were mainly caused by belt loading and body inertia loads to the CRS, both of which were monitored in the simulations.

The ATD-to-vehicle-interior contacts were defined using a contact characteristic with a very low stiffness (1 N/m), which does not necessarily reflect the true contact force, but can effectively

detect potential ATD-to-vehicle-interior contacts. Because vehicle interior stiffness may vary significantly from vehicle to vehicle, defining a single contact characteristic likely does not represent the variations seen in vehicle interiors that could affect injury potential. Given that most pediatric head injuries result from direct contact, monitoring the potential for head contact using the current contact definition is suitable for identifying the potential safety hazard from contact.

Data Analysis

When presenting results, trends are most apparent when they are plotted according to “effective crash angle,” which is defined as the relative angle between the impact direction and occupant seat orientation. A combination of two different impact directions and two different vehicle seat orientations can result in the same effective crash angle. For example, a forward-facing seat in a frontal crash and a rear-facing seat in a rear crash both have an effective crash angle of 0 degrees. The conditions resulting each effective crash angle are summarized in Table 15.

Table 15. Effective Crash Angle for Each Combination of Impact and Vehicle Seat Orientation

Impact angle	Baseline 1: forward, row 2	Baseline 2: forward, row 1	Carriage 3: rearward, row 1	Campfire 4: angled, row 2	Campfire 5: angled, row 1
0°	0°	0°	180°	15°	165°
30°	30°	30°	150°	45°	135°
60°	60°	60°	120°	75°	105°
90°	90°	90°	90°	105°	75°
180°	180°	180°	0°	165°	15°

Note: The seating location numbers are corresponding to those shown in Figure 16.

To analyze the factor effects on ATD injury measures and CRS kinematics, student T-tests and one-way analysis of variance (ANOVA) were conducted to calculate the statistical significance of the results. A p-value less than 0.05 was considered as statistically significant in this study.

Simulation Results

CRABI 12MO in RFCRS

Figure 28 shows the HIC 15, chest acceleration, and Nij of the CRABI 12MO in RFCRS, as well as the CRS rotation angles relative to the effective crash angle. ATD excursion results are not reported here, because ATD-to-vehicle interior contacts were simulated and monitored, which are better indicators for safety hazards. The red line represents the ATD IARV (0) or FMVSS No. 213 (0) criteria. Among the 100 simulations, 20 simulations have HIC 15 over the 390 head IARV, 31 simulations have chest accelerations over the 50 g chest IARV, 8 simulations have Nij over 1.0 IARV, 4 simulations have CRS rotation over the 70 deg FMVSS No. 213 criteria, and 4 simulations predicted ATD-to-vehicle contacts. All simulations with higher ATD injury measures are in an effective crash angle between 90° to 180°, in which the RFCRS has larger rotation resulting contacts between the ATD head/torso and CRS/harness. The ATD-to-vehicle interior contacts only occurred in side/oblique impact and involved minor leg/foot impacts, which are not considered a significant injury concern.

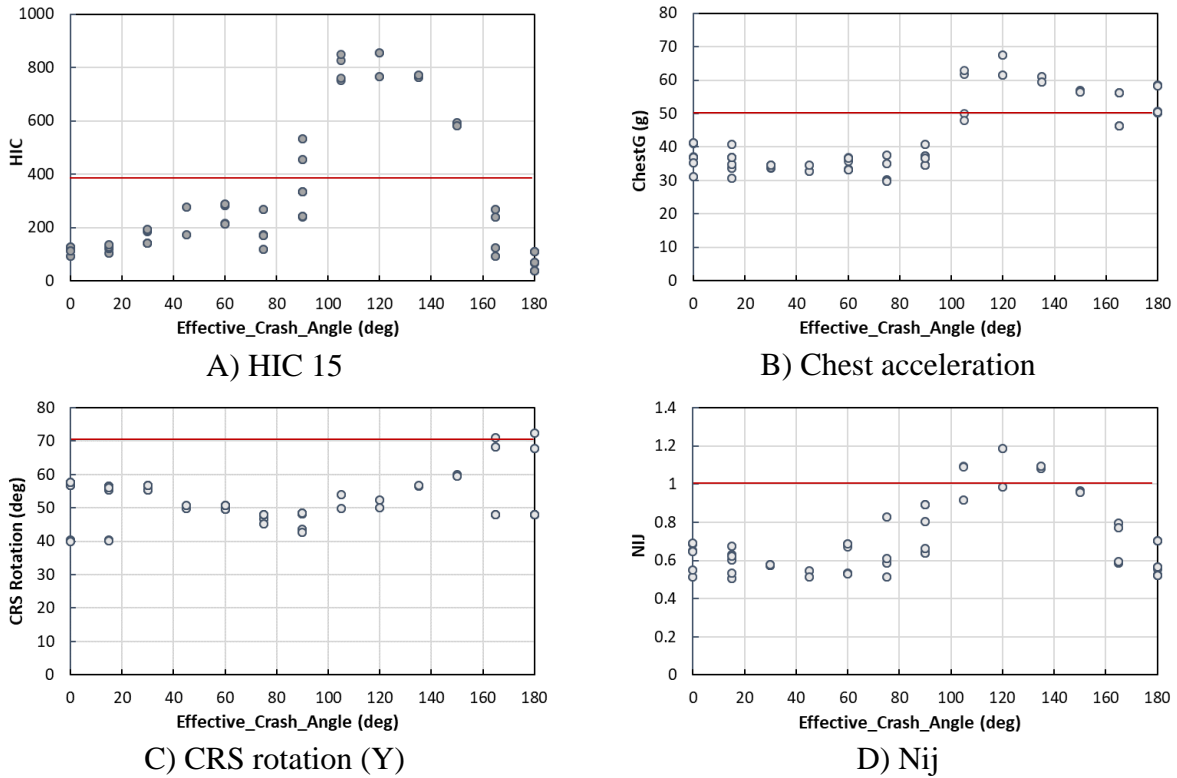


Figure 28. Model-predicted CRS/injury measures for CRABI 12MO in RFCRS by effective crash angle

Figure 29, Figure 30, and Figure 31 show the factor effects on ATD HIC 15, chest accelerations, and CRS rotations, respectively. Since the pediatric cervical spine injury risk is low in field crash data and Nij tends to over-estimate pediatric cervical spine injury risks, Nij was not further used for factor effect analysis. Impact direction is the most dominating factor affecting the ATD injury measures and CRS rotations ($p \leq 0.01$). Unconventional seating in vehicles with ADS (seating configurations 3 to 5 in Figure 16) sustained significantly higher HIC 15 and chest accelerations ($p = 0.00$) than those with the conventional seating (seating configurations 1 and 2 in Figure 16). CRS installation method (LATCH versus seat belt) and vehicle space (sedan versus minivan) have minimal impact on ATD HIC 15, chest acceleration, and CRS rotation ($p > 0.50$). The vehicle space is insignificant mainly due to ATD-to-vehicle-interior contact definition as described earlier. The four simulations, where ATD contacted the vehicle interior, are all in the sedan model, suggesting that smaller vehicles tend to have higher risk of ATD to vehicle interior contact.

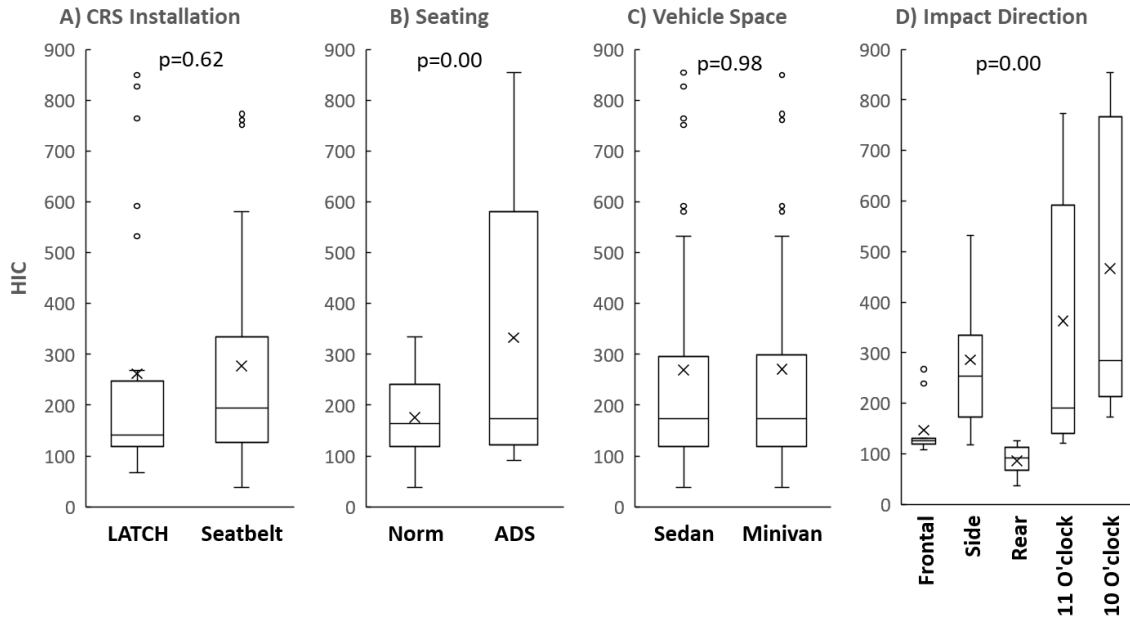


Figure 29. Factor effects on HIC of CRABI 12MO in RFCRS

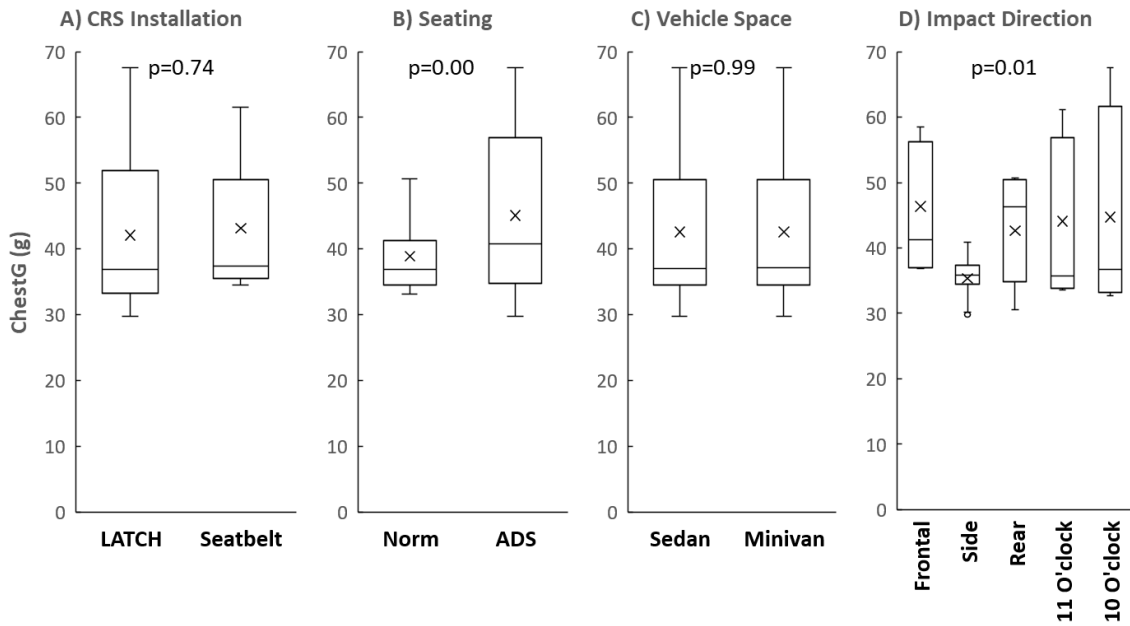


Figure 30. Factor effects on chest acceleration for CRABI 12MO in RFCRS

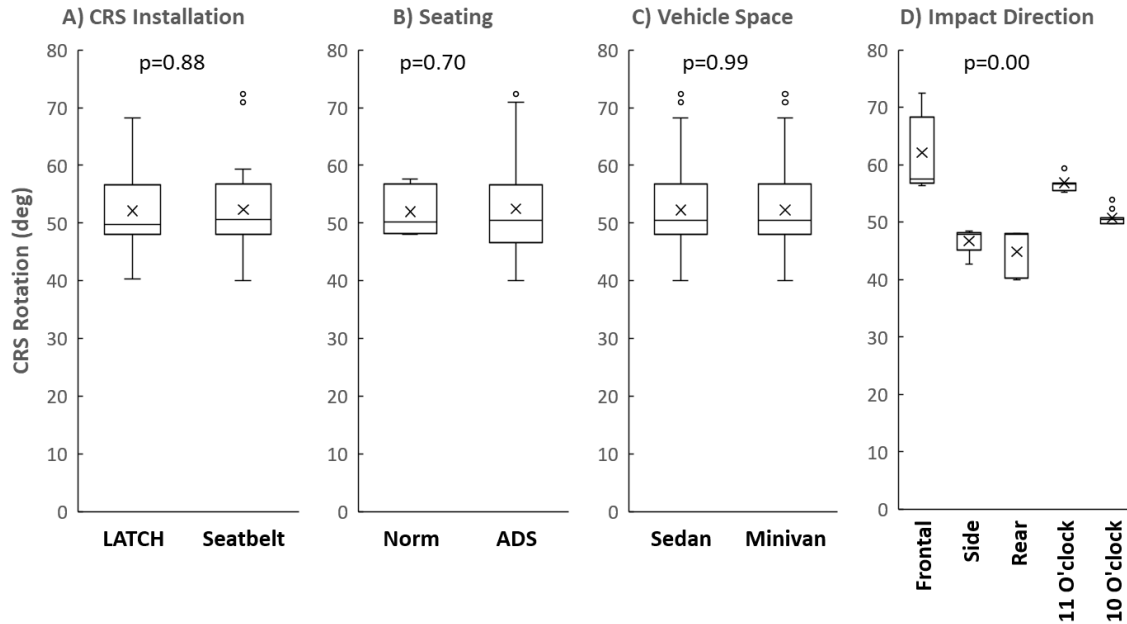


Figure 31. Factor effects on CRS rotation for CRABI 12MO in RFCRS

H33YO in RFCRS

Figure 32 shows the HIC 15, chest acceleration, chest deflection, and Nij of the H33YO ATD in RFCRS relative to the effective crash angle. The red line represents the IARV. Among the 100 simulations, 10 simulations have HIC 15 over the 570 head IARV, 34 simulations have chest accelerations over the 55 g chest IARV, 35 simulations have Nij over 1.0 IARV, and 9 simulations predicted ATD to vehicle contacts. None of the simulations has a chest deflection value over the IARV. All simulations with higher ATD injury measures are in effective crash angles between 60° to 180°, in which the RFCRS has larger rotation resulting in contacts between the ATD head/torso and CRS/harness. The ATD-to-vehicle interior contacts were minor leg/foot impacts that occurred in oblique impact in the sedan model, which does not pose a significant injury concern.

Figure 33, Figure 34, Figure 35 show the factor effects on H33YO ATD HIC 15, chest accelerations, and chest deflection in the RFCRS, respectively. Similar to the CRABI 12MO results, impact direction is the most dominant factor affecting the ATD injury measures ($p \leq 0.01$). Unconventional seating in vehicles with ADS (seating configurations 3 to 5 in Figure 16) sustained significantly higher HIC 15 and chest deflection ($p=0.00$) than those with the conventional seating (seating configurations 1 and 2 in Figure 16). The CRS installation method (LATCH versus seat belt) and vehicle space (sedan versus minivan) have minimal impact on ATD HIC 15, chest acceleration, and chest deflection ($p > 0.70$). The vehicle space factor is insignificant for injury measures, mainly due to ATD-to-vehicle-interior contact definition being very soft as described earlier. The nine simulations, where the ATD contacted the vehicle interior, are all in the sedan model, once again suggesting that smaller vehicles tend to have higher risk of ATD to vehicle interior contact.

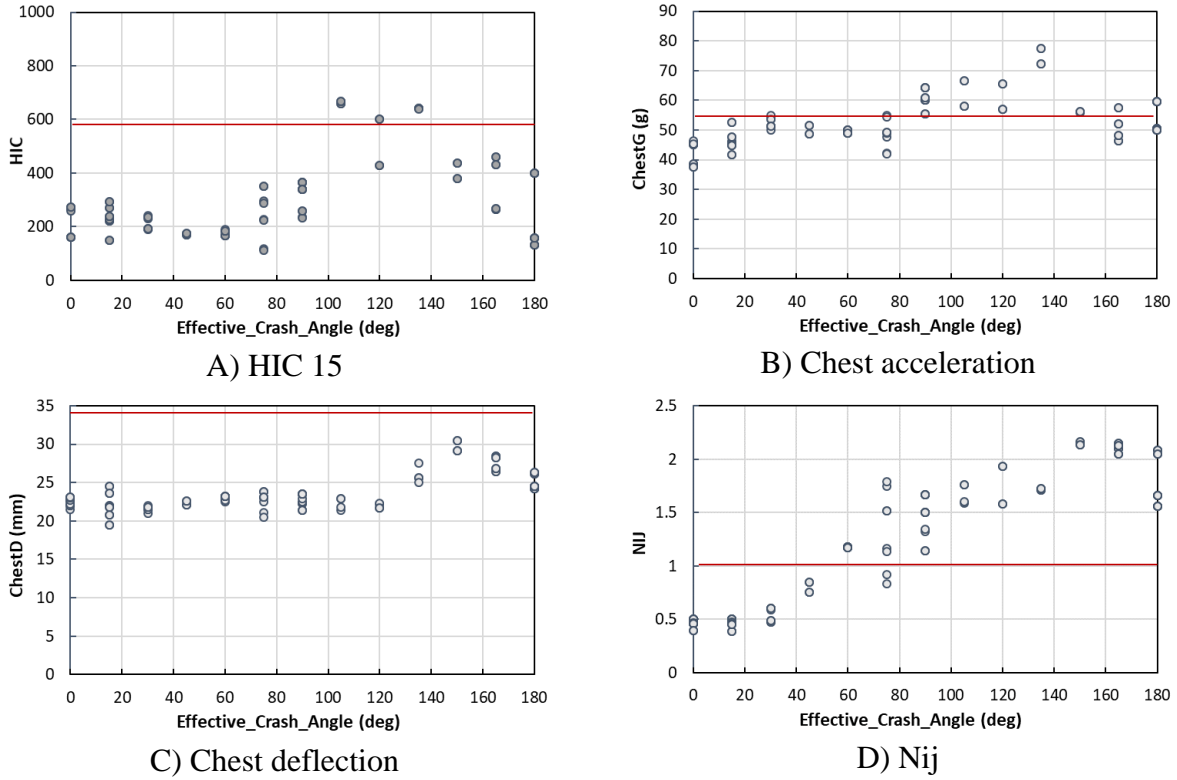


Figure 32. Model-predicted injury measures for H33YO in RFCRS at various impact directions

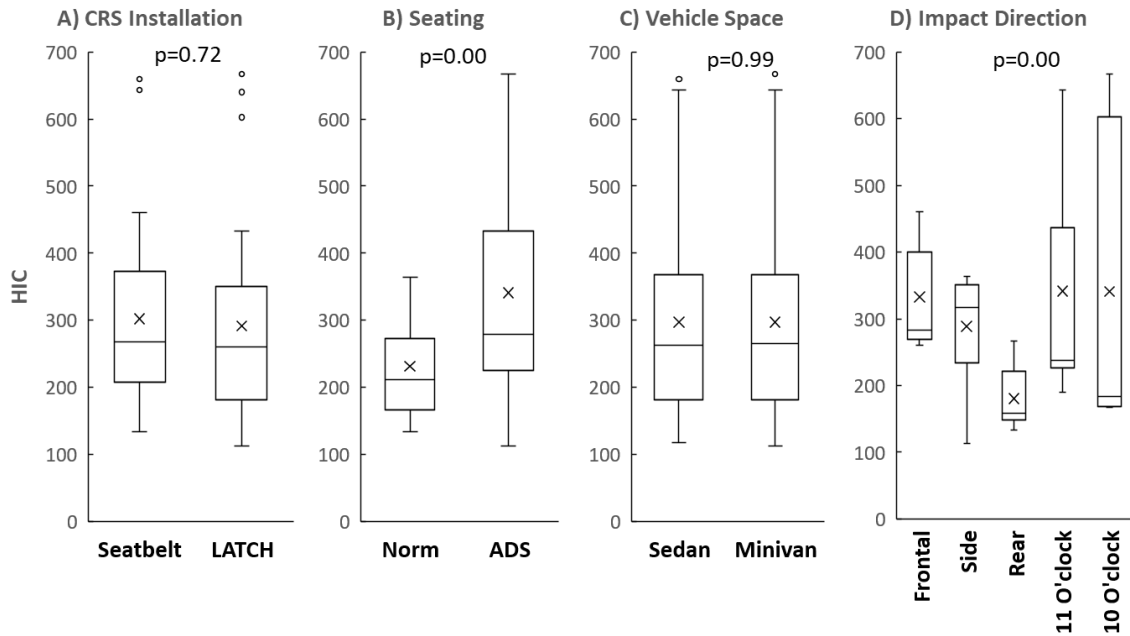


Figure 33. Factor effects on HIC15 for H33YO in RFCRS

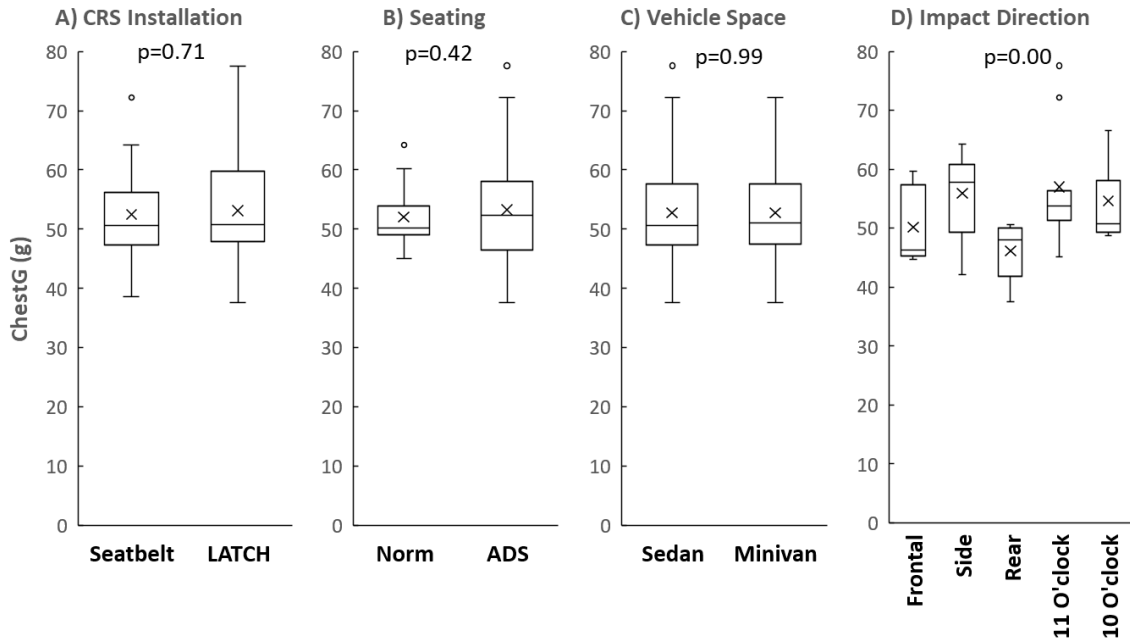


Figure 34. Factor effects on chest acceleration for H33YO in RFCRS

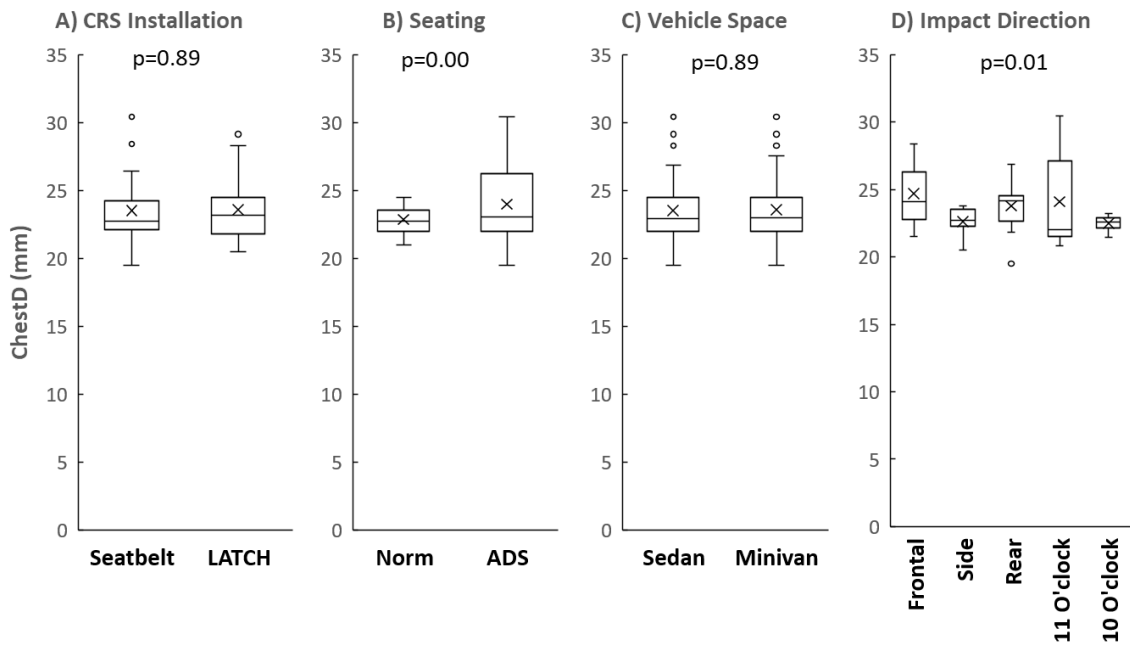


Figure 35. Factor effects on chest deflection for H33YO in RFCRS

H33YO in FFCRS

Figure 36 shows the HIC 15, chest acceleration, chest deflection, and Nij of the H33YO ATD in FFCRS relative to the effective crash angle. The red line represents the ATD IARV. Among the 150 simulations, 12 simulations have HIC 15 over the 570 head IARV, 63 simulations have chest accelerations over the 55 g chest IARV, 65 simulations have Nij over 1.0 IARV, and 22 simulations predicted ATD-to-vehicle contacts. None of the simulations has a chest deflection value over the IARV. Compared with the results from the H33YO ATD in RFCRS, the FFCRS are associated with slightly higher injury measures. Simulations with higher HIC 15 are associated with an effective crash angle between 60° to 90°, in which the RFCRS has larger lateral rotations resulting in contacts between the ATD head and CRS. Simulations with higher chest accelerations are associated with an effective crash angle between 60° and 180°, while simulations with higher Nij are across the full range of effective crash angles. The ATD-to-vehicle interior contacts were minor leg/foot impacts in all impact directions, which does not pose significant injury concerns.

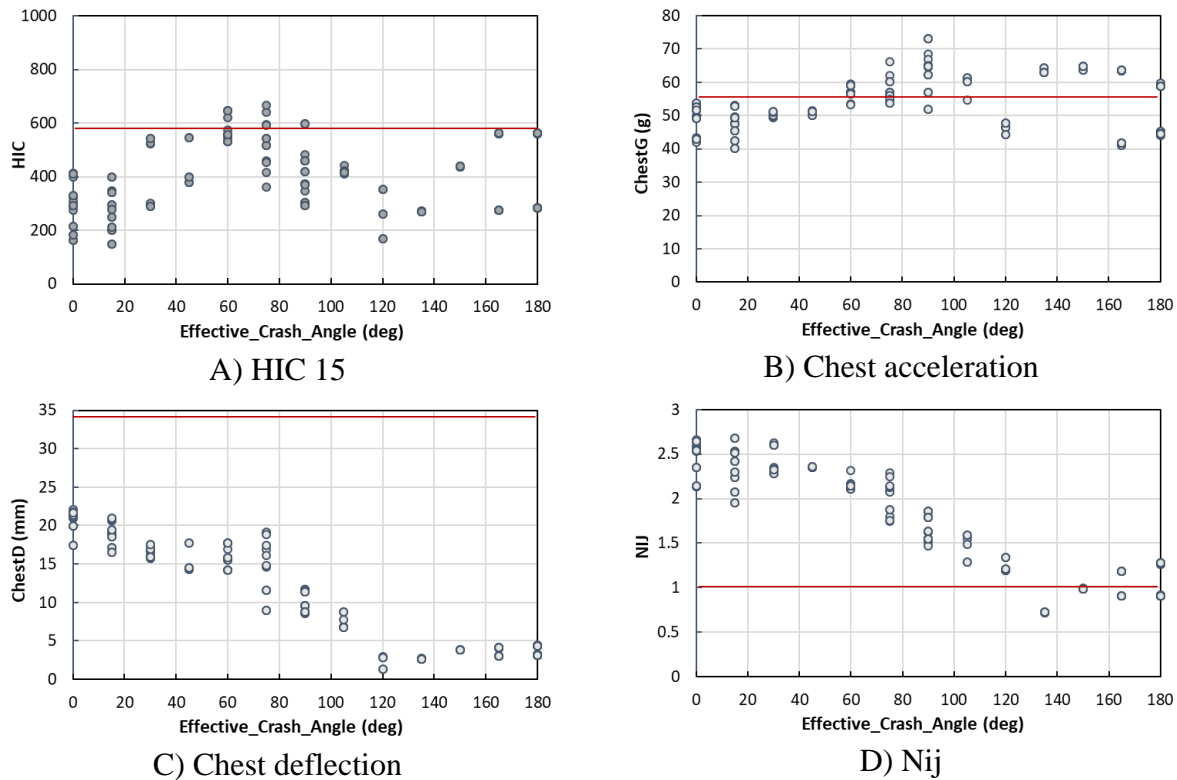


Figure 36. Model-predicted injury measures for H33YO in FFCRS at various impact directions

Figure 37, Figure 38, and Figure 39 show the factor effects on H33YO ATD HIC 15, chest accelerations, and chest deflection in the FFCRS, respectively. Impact direction is still the most dominating factor affecting the ATD injury measures, although it is only marginally significant in chest deflection. Unconventional seating in vehicles with ADS (seating configurations 3 to 5 in Figure 16) sustained significantly higher chest deflection ($p=0.02$) than those with the conventional seating (seating configurations 1 and 2 in Figure 16). CRS installation method (LATCH versus belt versus belt+tether) and vehicle space (sedan versus minivan) are not statistically significant on ATD HIC 15, chest acceleration, and chest deflection ($p>0.05$). The

vehicle space is insignificant mainly due to ATD-to-vehicle-interior contact definition being very soft as described earlier. The 22 simulations, where ATD contacted the vehicle interior, are all in the sedan model, once again suggesting that smaller vehicles tend to have higher risk of ATD to vehicle interior contact.

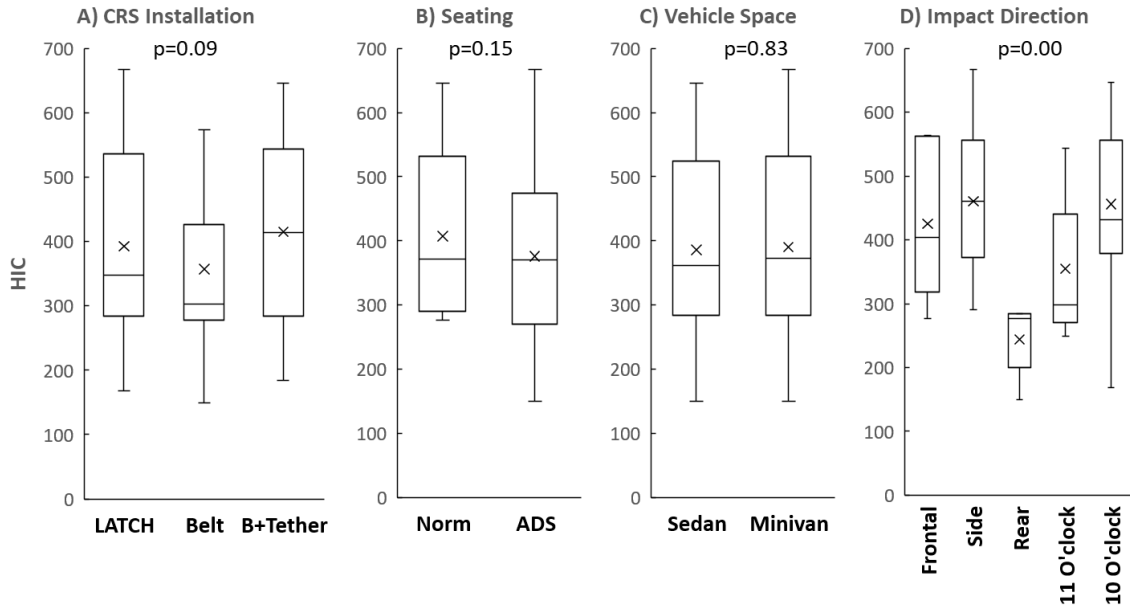


Figure 37. Factor effects on HIC15 for H33YO in FFCRS

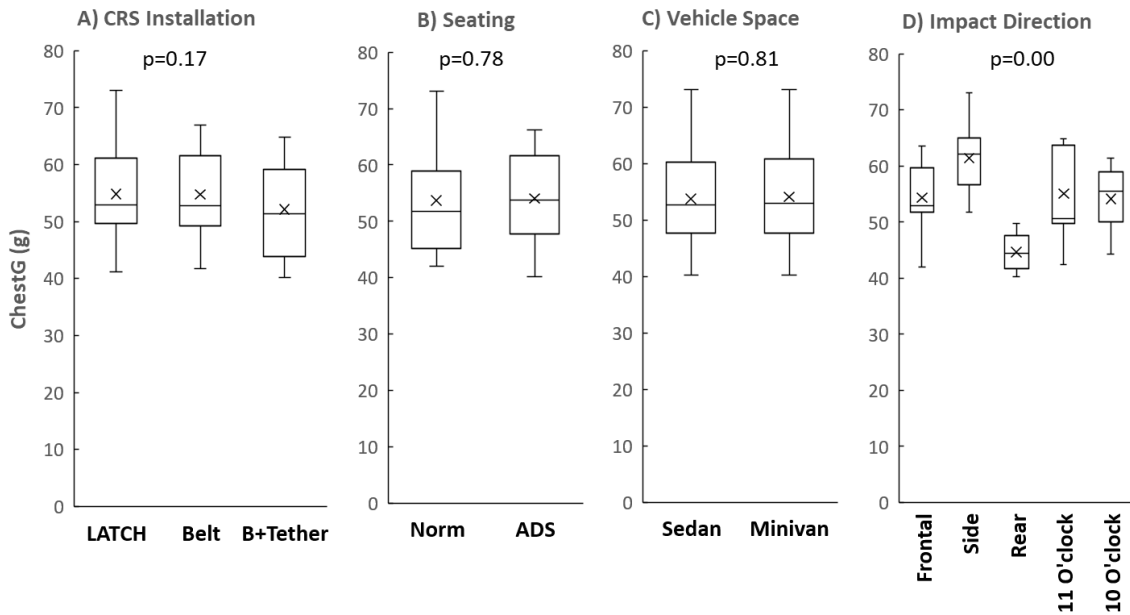


Figure 38. Factor effects on chest acceleration for H33YO in FFCRS

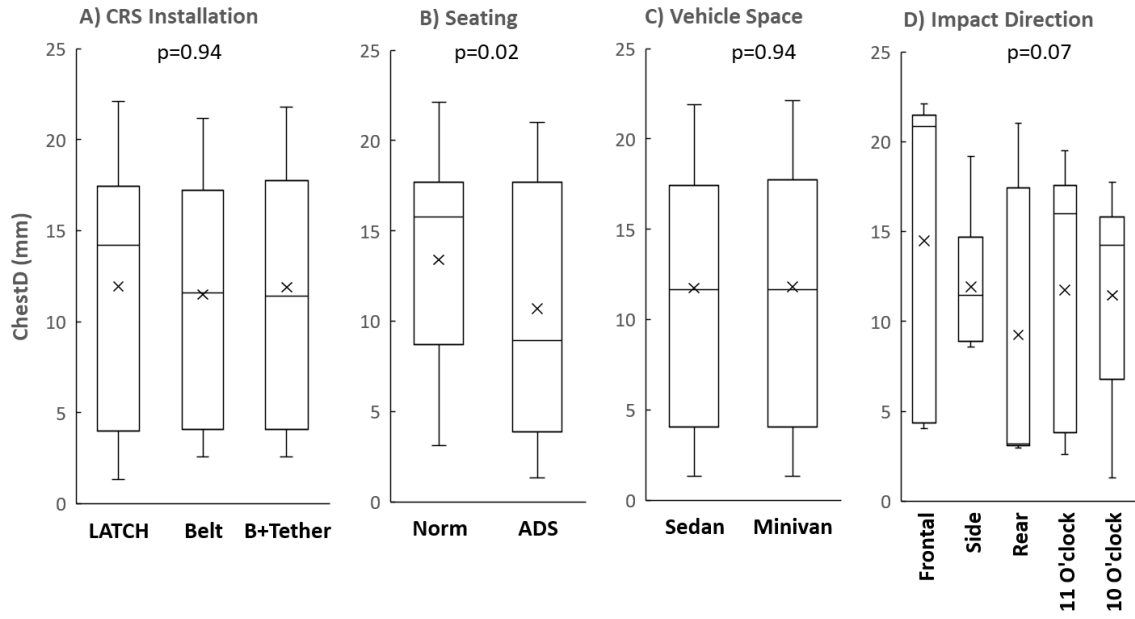


Figure 39. Factor effects on chest deflection for H33YO in FFCRS

Simulations of Vehicle Belt-Restrained ATDs

Simulation Methods

The parametric study and data analysis for vehicle belt-restrained occupants are similar to those for harnessed CRS occupants, with only minor differences. Although the seat belt provides the restraint for children using belt-positioning boosters, some researchers have hypothesized that attaching the booster using lower anchorage attachments would allow the child and booster to remain in better position relative to the seat belt in a crash (Charlton et al., 2007). Therefore, we explored this issue in the parametric runs. As shown in Table 16, two full factorial experiments resulted in a total of 200 simulations.

Table 16. Simulation Matrix for Belted Occupants

Study #	ATD/CRS	Booster Installation	Crash Scenarios	Seating Arrangement	Vehicles	# of Sim
1	H36YO ATD/ Booster	1-anchor attachment 2-free from vehicle seat	1-front 2-side 3-rear 4-oblique frontal 5-oblique side See Figure 16	2 Conventional 3 Unconventional See Figure 16	1-Sedan 2-Minivan	100
2	H310YO ATD/ Booster & No- booster	Free from vehicle seat	1-front 2-side 3-rear 4-oblique frontal 5-oblique side See Figure 16	2 Conventional 3 Unconventional See Figure 16	1-Sedan 2-Minivan	100
Total #	3	2	5	5	2	200

The simulation setup, contact definition, injury measures, and statistical analysis for the belt-restrained ATDs are the same as those with CRS harness-restrained ATDs.

Simulation Results

H36YO in Booster

Figure 40 shows the HIC 15, chest acceleration, chest deflection, and Nij of the H36YO ATD in a backless booster relative to the effective crash angle. The red line represents the ATD IARV. Among the 100 simulations, 44 simulations have chest accelerations over the 60 g chest IARV, 8 simulations have Nij over 1.0 IARV, and 69 simulations predicted ATD-to-vehicle contacts. None of the simulations had an HIC 15 or chest deflection value over the IARV. Simulations with higher chest accelerations are associated with an effective crash angle between 75° and 180°, while simulations with higher Nij are all associated with a 90° effective crash angle.

Figure 40, Figure 42, and Figure 43 show the factor effects on H36YO HIC 15, chest accelerations, and chest deflection in a booster, respectively. Impact direction dominates all three injury measures (p=0.00). Interestingly, unconventional seating in vehicles with ADS (seating configurations 3 to 5 in Figure 16) sustained significantly higher chest deflection (p=0.00) but significantly lower HIC 15 (p=0.00) than those with the conventional seating (seating configurations 1 and 2 in Figure 16). Booster installation method (attached versus free) and

vehicle space (sedan versus minivan) are not statistically significant on ATD HIC 15, chest acceleration, and chest deflection ($p > 0.10$).

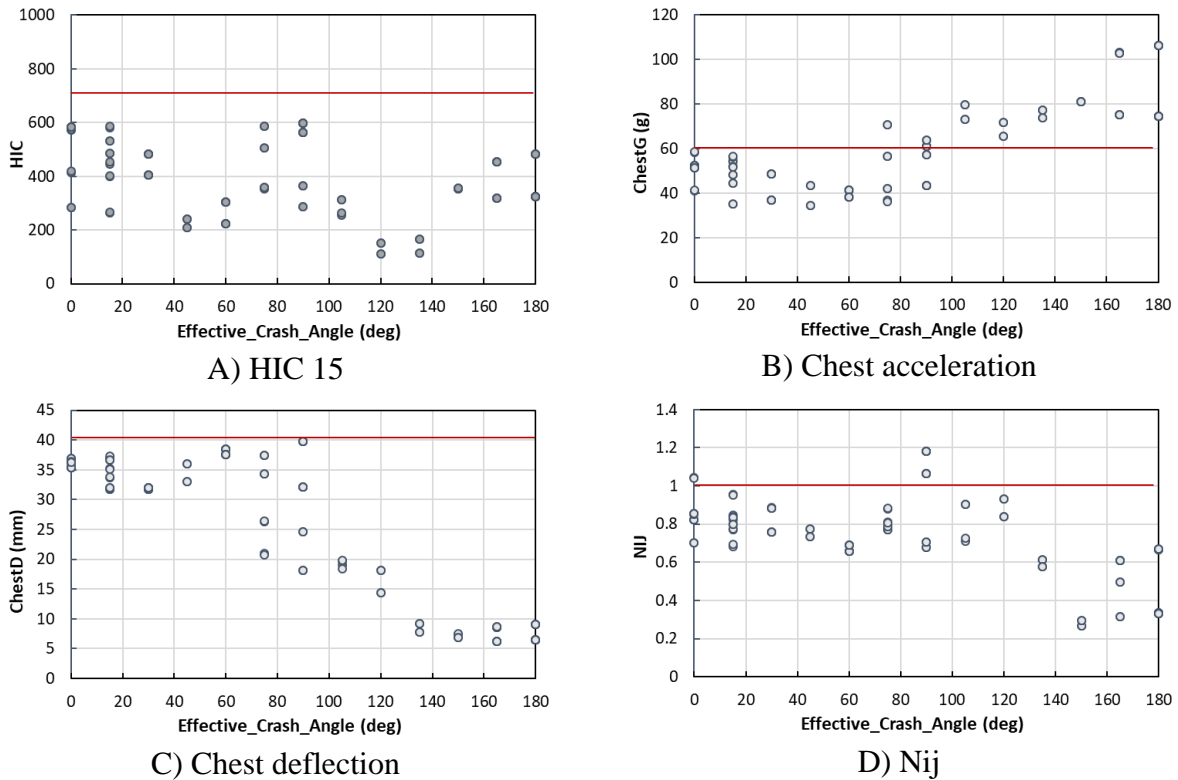


Figure 40. Model-predicted injury measures for H36YO in booster at various impact directions

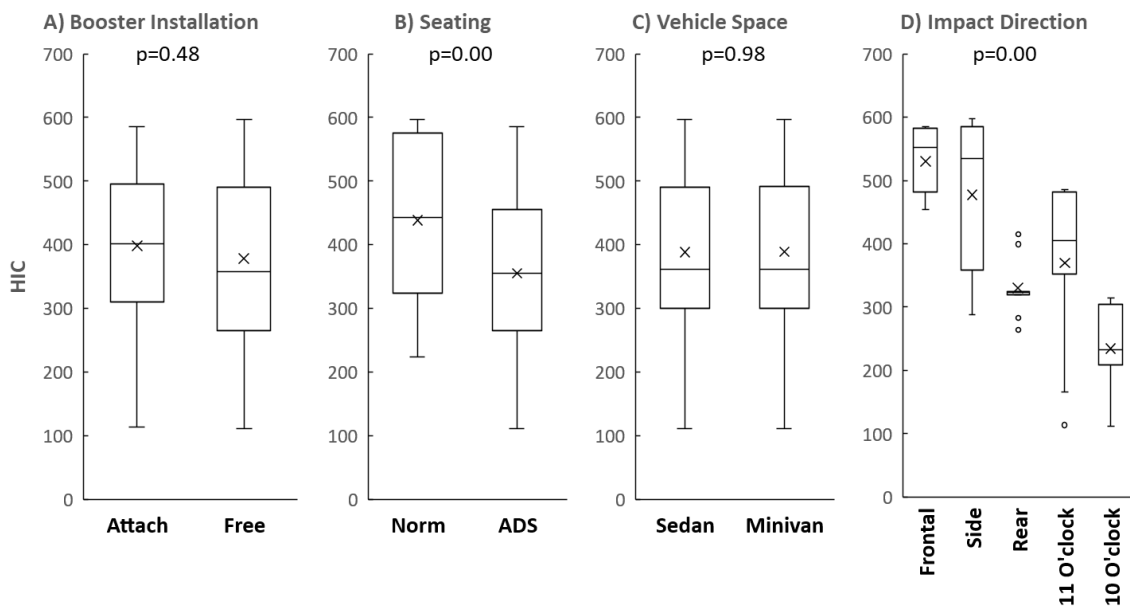


Figure 41. actor effects on HIC15 for H36YO in booster

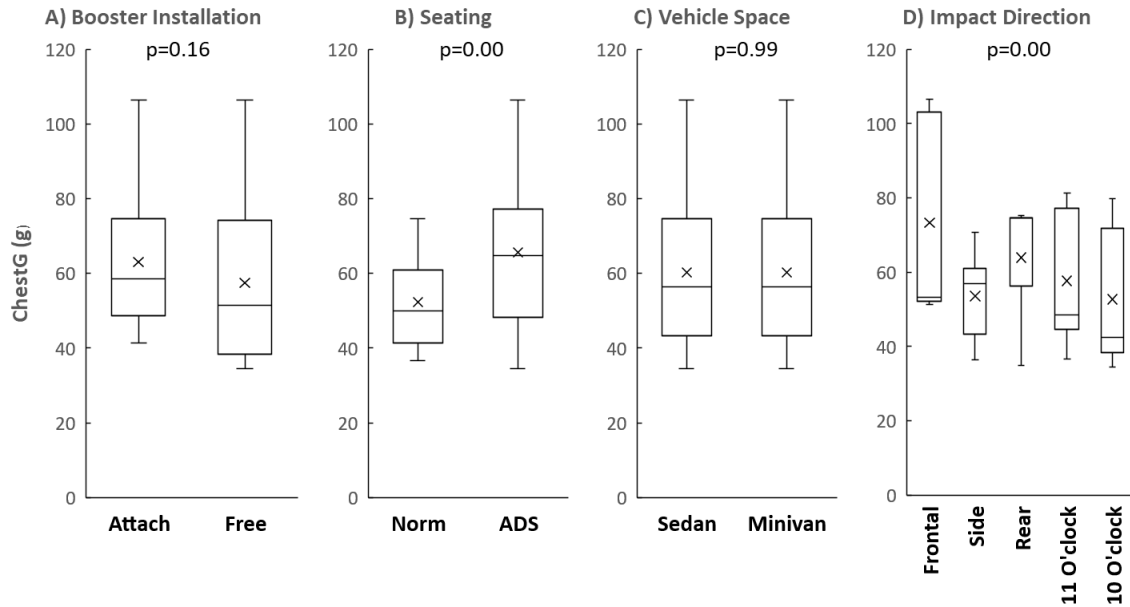


Figure 42. Factor effects on chest acceleration for H36YO in booster

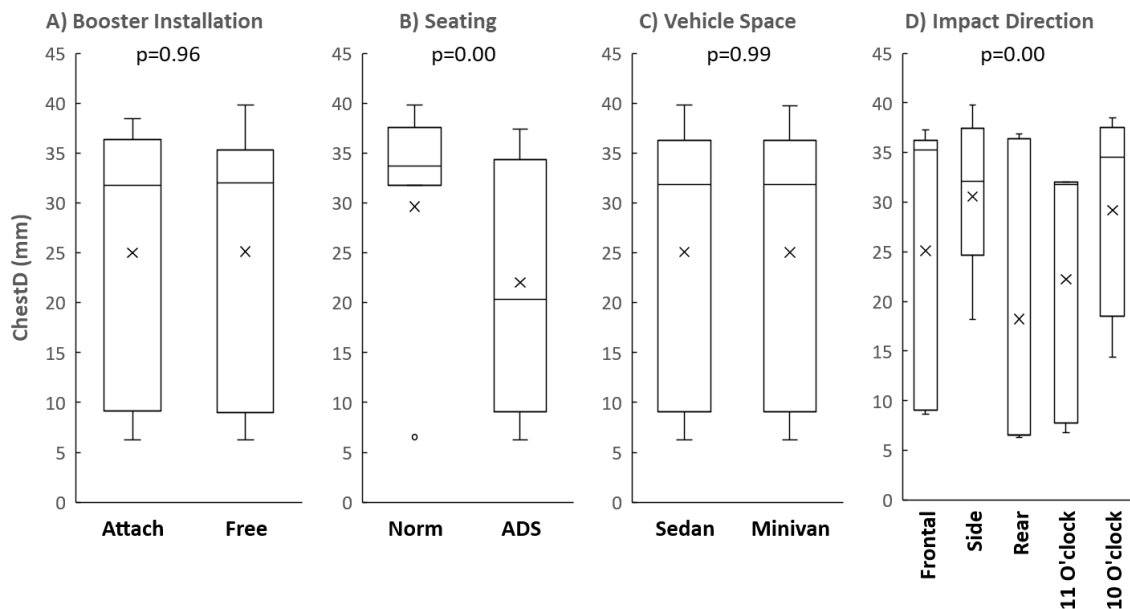


Figure 43. Factor effects on chest deflection for H36YO in booster

Figure 44 shows the factor effects on H36YO-to-vehicle-interior contacts. Vehicle space (sedan versus minivan) and impact direction are statistically significant ($p=0.00$), while booster installation (attached versus free) and seating arrangement (conventional versus unconventional) are not significant. More specifically, sedan and side/side oblique (11 o'clock) impacts are associated with higher chance to have ATD-to-vehicle-interior contact.

Figure 45 further illustrates the nature of H36YO-to-vehicle-interior contacts, separated by body contact regions. In particular, contacts to the extremities occurred in almost all impact directions, which are not major injury concerns. However, contacts to the ATD head and torso could be

much more severe than the extremity contacts, and they occurred with an effective crash angle between 60° and 105° . The exemplar contact cases shown in Figure 45 suggested that, in a side or side oblique impact, H36YO ATD could contact the seat next to it. Such contact could occur in both conventional and unconventional seating arrangements. In addition, the H36YO ATD's head could contact the instrument panel behind the seat in an unconventional seating orientation.

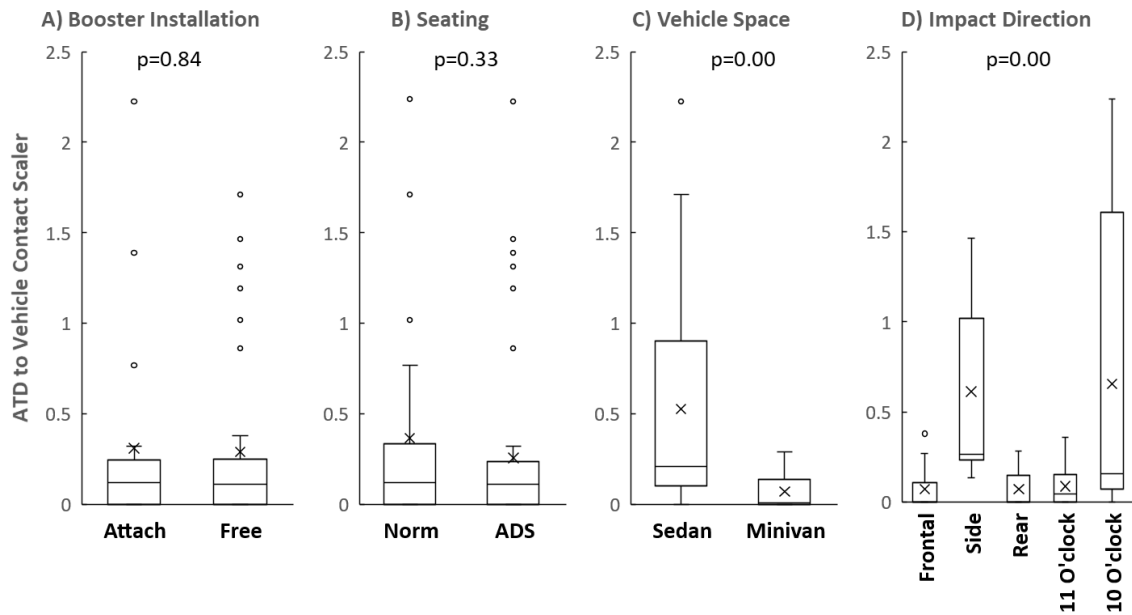


Figure 44. Factor effects on ATD to vehicle contact scaler for H36YO in booster

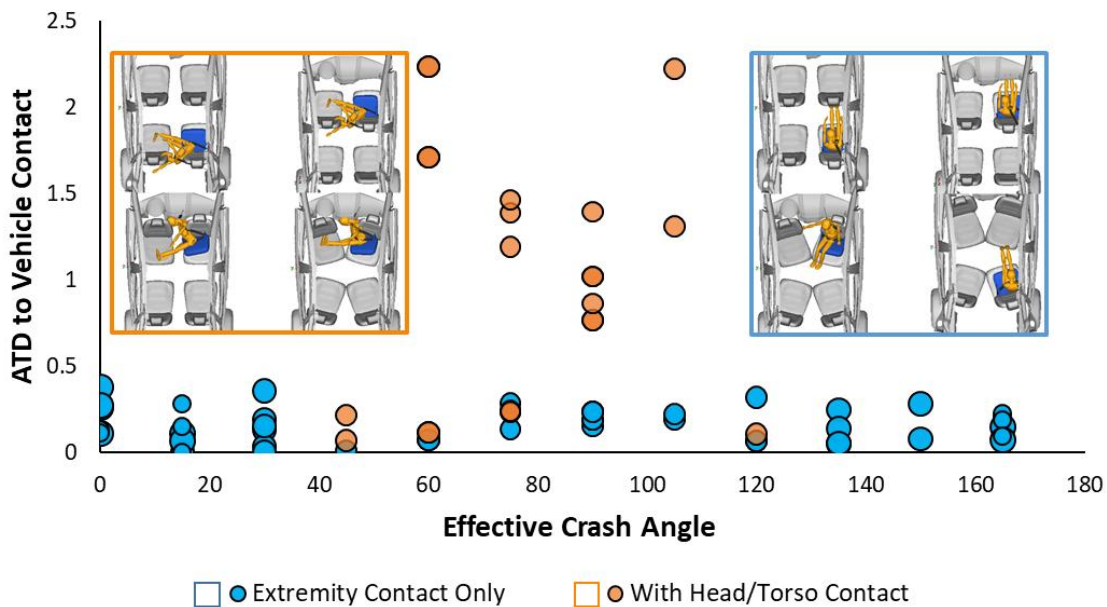


Figure 45. ATD to vehicle contact distribution and exemplar contact cases for H36YO in booster

H310YO With and Without Booster

Figure 46 shows the HIC 15, chest acceleration, chest deflection, and Nij of the H310YO with and without a booster relative to the effective crash angle. The red line represents the ATD IARV. Among the 100 simulations, 6 simulations have HIC 15 over 700 head IARV, 30 simulations have chest accelerations over the 60 g chest IARV, 8 simulations have chest deflection over 46 mm chest IARV, 12 simulations have Nij over 1.0 IARV, and 81 simulations predicted ATD to vehicle contacts. Simulations with higher HIC 15 and chest accelerations are associated with an effective crash angle between 120° and 180°, while simulations with higher Nij are associated with an effective crash angle between 75° and 150°. Conversely, simulations with higher chest deflections are associated with an effective crash angle between 30° and 60°.

Figure 47, Figure 48, and Figure 49 show the factor effects on H310YO HIC 15, chest accelerations, and chest deflection, respectively. Impact direction is still the most dominating factor affecting all three injury measures ($p \leq 0.01$). Unconventional seating in vehicles with ADS (seating configurations 3 to 5 in Figure 16) sustained significantly higher chest deflection ($p = 0.02$) than those with the conventional seating (seating configurations 1 and 2 in Figure 16). The presence of a booster (yes versus no) and vehicle space (sedan versus minivan) are not statistically significant factors affecting ATD injury measures.

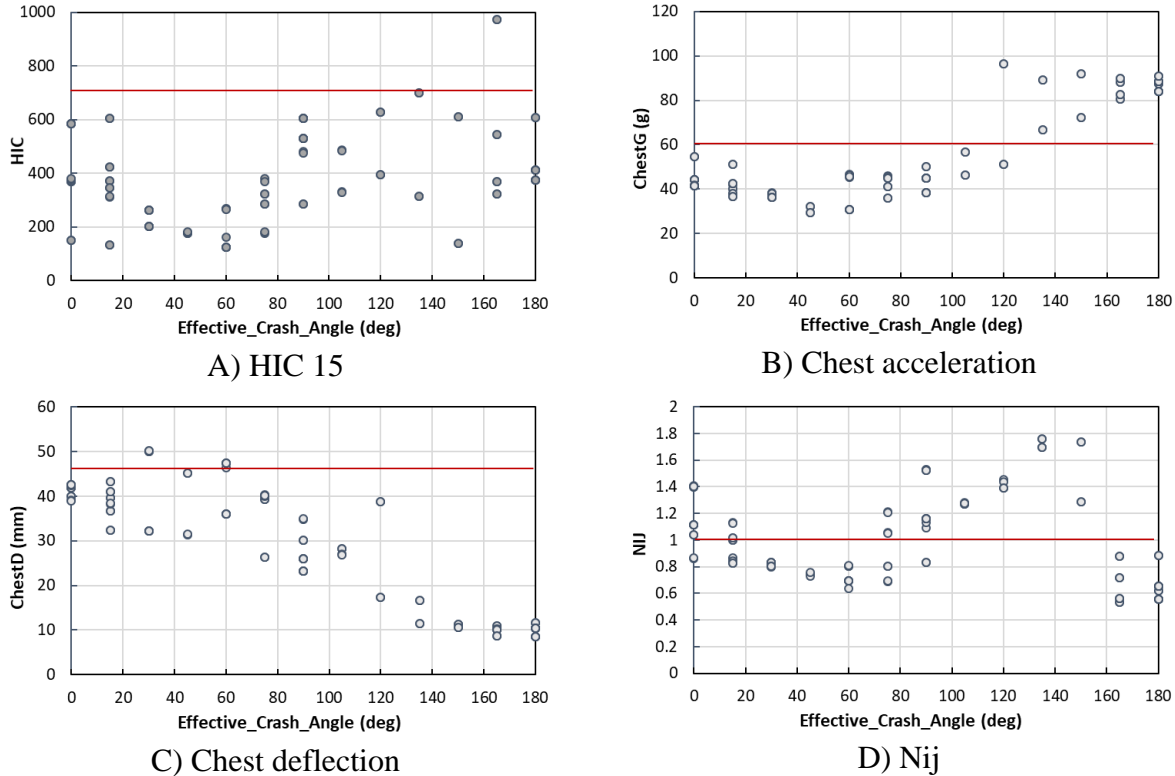


Figure 46. Model-predicted injury measures for H310YO at various impact directions

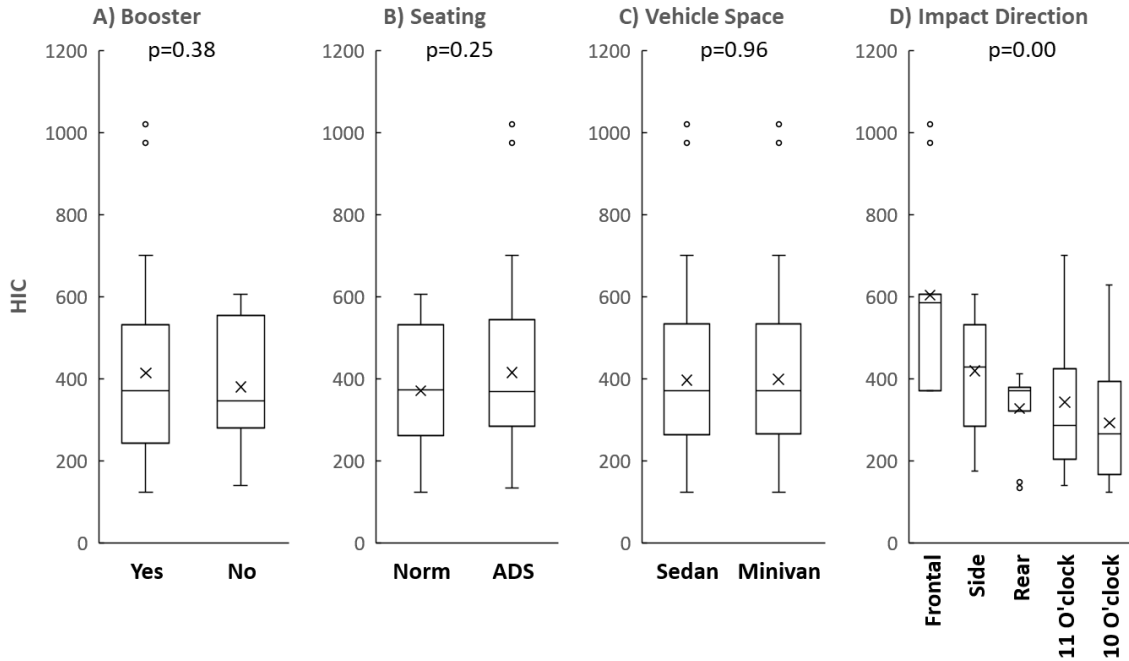


Figure 47. Factor effects on HIC15 for H310YO

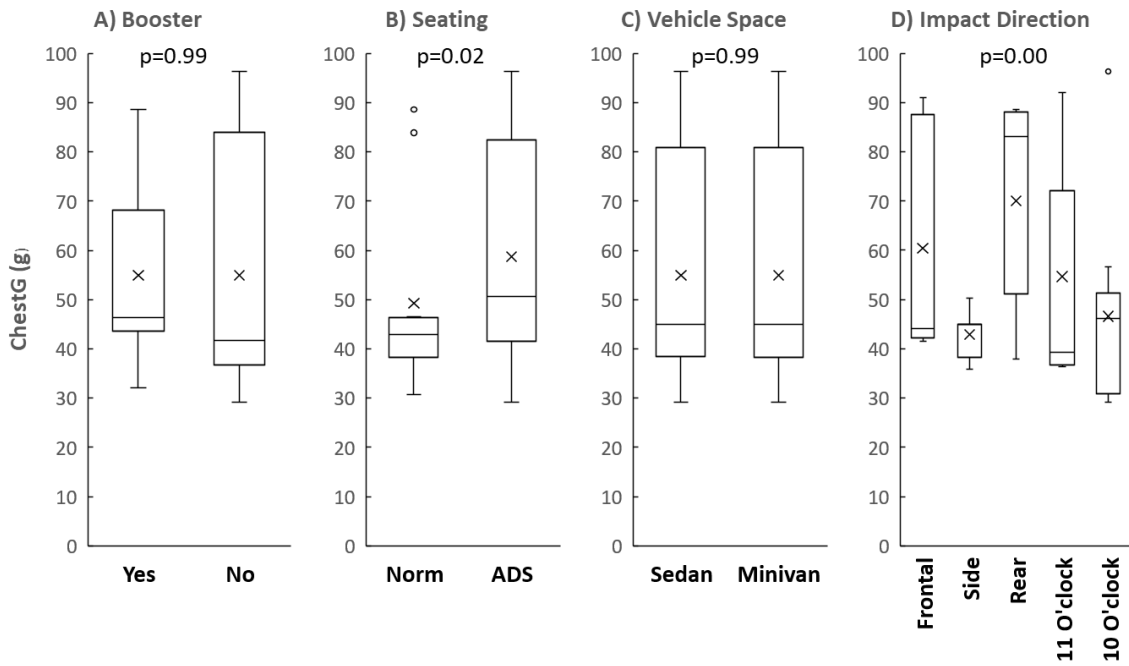


Figure 48. Factor effects on chest acceleration for H310YO

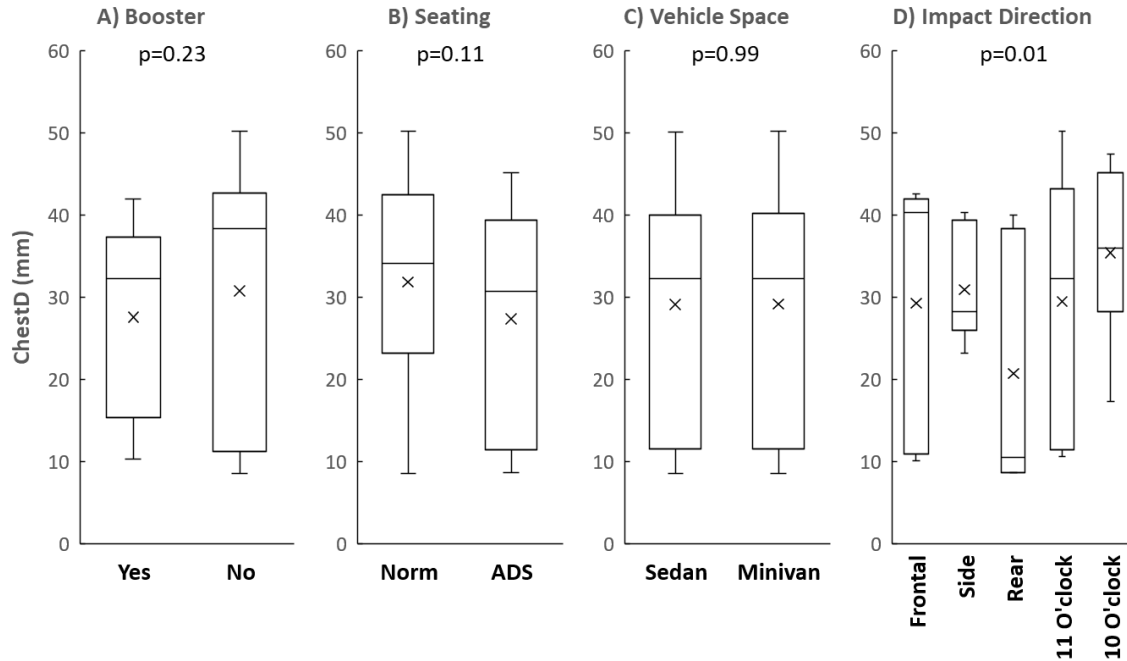


Figure 49. Factor effects on chest deflection for H310YO

Figure 50 shows the factor effects on H310YO-to-vehicle-interior contacts. Similar to the results from the H36YO, vehicle space (sedan versus minivan) and impact direction are statistically significant ($p=0.00$), while the presence of booster (yes versus no) and seating arrangement (conventional versus unconventional) are not significant. More specifically, sedan and side impact are associated with higher chance to have ATD to vehicle interior contact(s).

Figure 51 further illustrates the nature of H310YO-to-vehicle-interior contacts separated by body contact regions. Contacts to the extremities occurred in almost all impact directions, which are not a major injury concern. However, contacts to the ATD head and torso could be much more severe than the extremity contacts, and they occurred with an effective crash angle between 75° and 90° . The exemplar contact cases shown in Figure 51 suggested that, in a side impact, H310YO could contact the seat next to it. Such contact could occur in both conventional and unconventional seating arrangements. In addition, the H310YO ATD's head could contact the instrument panel behind the seat in an unconventional seating orientation.

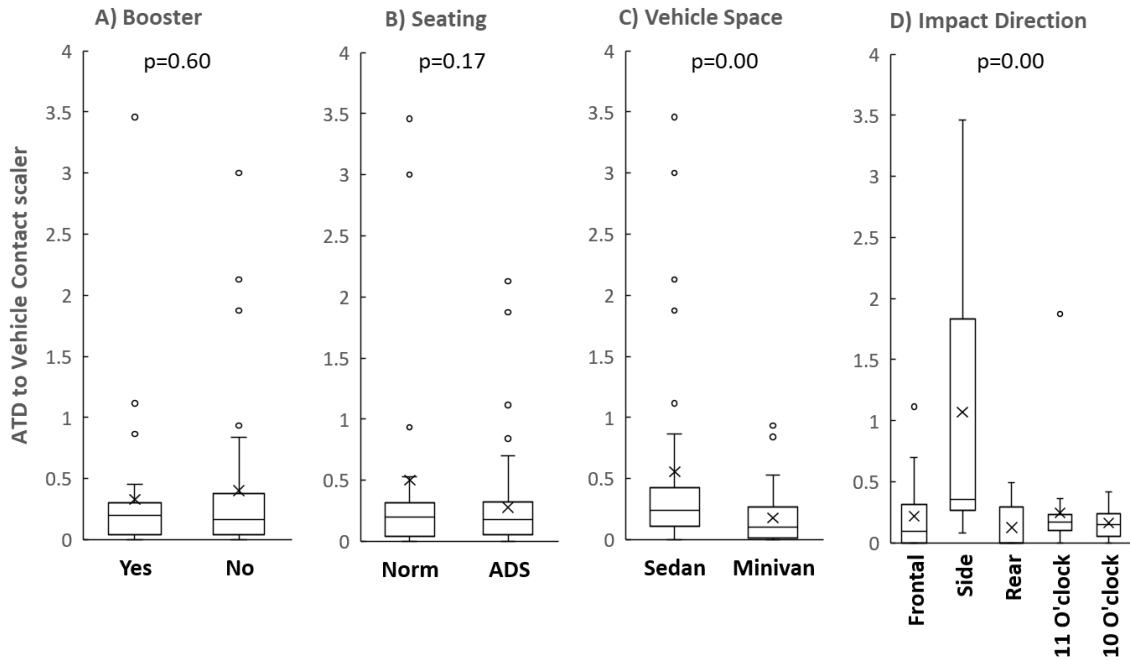


Figure 50. Factor effects on ATD to vehicle contact scaler for H310YO

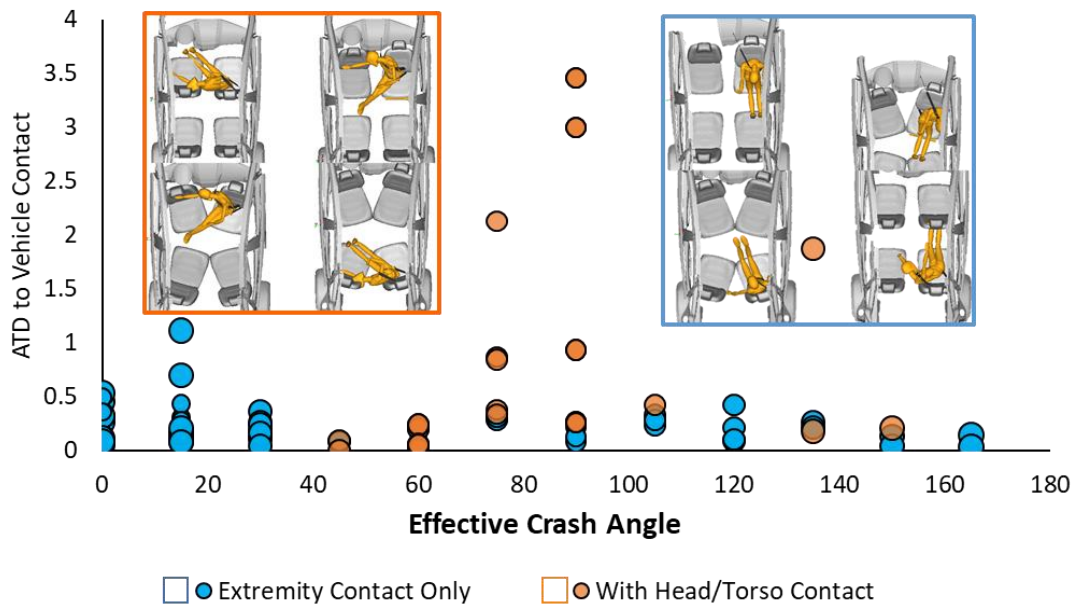


Figure 51. ATD to vehicle contact distribution and exemplar contact cases for H310YO

Discussion

Safety Concerns

Head Contacts for Older Children in Farside Impacts

This study demonstrated the potential of injurious head contact for older children restrained by a 3-point belt, with or without a booster, under conditions that would be described as farside or farside oblique impacts. These concerns exist for conventional seating (i.e., forward-facing) as well as unconventional seating (i.e., rear-facing or angled). Similar head contact potential in farside loading also exists for adults. In the past, because serious injuries from frontal, nearside, and rollover crashes have outweighed the risk of serious injuries from farside impacts, farside impact induced head injuries have not been a priority for countermeasure development. In addition, while side impact ATDs exist, they have been designed to assess injury risk from direct loading, and their ability to detect injury risk and provide appropriate kinematics under the inertial loading seen in farside impacts has not been systematically evaluated for either adult or pediatric ATDs. In the future, the potential for farside head contact in AVs may receive higher priority if side impacts may make up a higher proportion of AV crashes, which may happen because frontal and rollover crashes are easier to prevent (Klinich et al., 2016). The current study identifies a potential for head injury under farside-impact-like loading that is similar between conventional and unconventional seating arrangements. Potential side-facing seats in AVs could further increase the proportion of farside-impact-like loading conditions in future crashes, although such seating arrangement was not evaluated in this study.

The 3-point seat belt used for H36YO and H310YO ATDs aimed to mimic seat-integrated seat belts, as this is the only feasible design for unconventional seating. Consequently, a rear-facing or angled rear-facing seating orientation results in an inboard shoulder D-ring location. Thus, this approach modeled not only a change in seat orientation, but also variations in belt configuration. Future research that considers seat orientation and belt configuration separately would be beneficial. In theory, an inboard shoulder D-ring will reduce head/torso lateral excursions in a farside impact compared with an outboard shoulder D-ring location. However, our results show that an inboard D-ring cannot prevent head contact to the vehicle interior in farside or farside oblique impacts. It is possible that moving the shoulder D-ring closer to the occupant shoulder may further reduce the head lateral excursions and potentially avoid head contacts. However, in this study, all seat belt anchorage locations are consistent with the belt geometry used in the validation sled tests, and variations in belt anchorage locations were not considered.

Injury Concerns for Children Restrained by Harnessed CRS

Our simulation results show impact scenarios with higher head, neck, and chest injury measures, which are over the IARV. However, the IARVs used in our analysis are more stringent than the current FMVSS No. 213 criteria, and the ATDs used in this study were designed for frontal crashes. Therefore, we should interpret these results with caution. Specifically, we believe that head injury should still be the main focus, because field data have shown that majority of injuries to children using harnessed CRS result from direct head contact. In this study, higher HIC values for ATDS in harnessed CRS are almost always in farside or farside oblique impacts. In such impact directions, the CRS tends to rotate laterally, causing relatively high inertia forces between the ATD and CRS. Since there is no significant head contact to surfaces outside the CRS in these

simulations, the true head injury risks may not be significant and the CRS seems to be capable of keeping the head within the CRS as intended.

Given that we are unaware of any field data showing serious chest injury to rear-facing children in any crash direction, and head injuries are also the predominant concern for harnessed forward-facing children, we do not have confidence that the high chest accelerations for harness-restrained children are a true reflection of higher risk of chest injuries.

Cervical spine injuries for children using harnessed CRS are also rare in the field (Fuchs et al., 1989; Huelke et al., 1992) while our simulations predicted a significant portion of simulations with the H33YO ATDs sustaining high Nij. Due to the limitations of the pediatric ATDs and the potential of over-estimating pediatric cervical spine injury risks using Nij (Sherwood et al., 2005), we believed that the true risk of cervical spine injuries in the simulated crash conditions is low. In addition, Nij is not currently measured in FMVSS No. 213 testing because measures are not consistent with field experience. Therefore, Nij was not further used for factor sensitivity analyses.

Some of the potentially concerning contacts involved a RFCRS in a rear-facing vehicle seat under frontal-oblique loading, where the rotation of the ATD in the CRS led to contact with the center of the instrument panel. Because the design of future AVs is uncertain, our simulations used a vehicle interior representative of a current vehicle. However, if a future AV has a front row of rear-facing vehicle seats, it is unclear whether the adjacent structure would resemble a current instrument panel. The other point to consider is that there have been very few cases of serious injury in rear impacts to children secured in rear-facing CRS. While our simulations demonstrate the potential for injury under these conditions to occur, decades of field data do not.

Rear and Rear-Oblique Impacts

Our simulation results show that, based on the effective crash angle, rear and rear-oblique impacts are associated with higher HIC values for ATDs in RFCRS and higher chest accelerations for almost all ATD/CRS combinations simulated in this study. It should be mentioned that the seat back frame was rigidized in the validation tests, so our models simulated near rigid seat back frame. Although it is not clear what stiffness values will be used in future seats in AVs, the current seat model may over-predict the chest accelerations and the chest injury risks in rear or rear-oblique impacts. However, it is reasonable to believe that future vehicles using unconventional seating orientations need to consider a proper seat back stiffness and energy absorbing technologies to deal with potential high-speed rear and rear-oblique impacts.

Conventional Seating Versus Unconventional Seating

The comparison between conventional seating (seating configurations 1 and 2 in Figure 16) and unconventional seating is interesting. Unconventional seating is associated with significantly higher HIC 15 for the CRABI 12MO and H33YO ATD in RFCRS and significantly higher chest accelerations in CRABI 12MO, H36YO, and H310YO ATDs than conventional seating. However, unconventional seating is also associated with significantly lower HIC 15 in the H36YO and significantly lower chest deflection in H36YO and H310YO ATDs. In terms of potential injurious contacts, there is no significant difference between conventional and unconventional seating arrangements. In this study, we considered two forward-facing seats for conventional seating, and two rear/angled-rear-facing seats and a single angled-forward-facing seat for unconventional seating. In the five impact directions, four of them are between 9 and 12

o'clock. Consequently, unconventional seating has been involved in a higher percentage of simulated oblique rear impacts than conventional seating. As impact direction is the most dominating factor affecting ATD injury measures, we believe that the difference in impact direction distribution between the conventional and unconventional seating may be the main contributor in their differences in injury measures. In this study, we selected the impact directions without weighting, so the injury metrics may be over-weighted or under-weighted relative to expected real-world crash scenario sampling.

Potential Countermeasures

Belt-Restrained Older Children in Farside/Oblique Impacts

One of the major safety concerns found in this study is that belt-restrained older children, represented by the H36YO and H310YO ATDs, sustained significant risks of contacting the seat next to them or the instrument panel behind them in farside or farside oblique impacts. Such impact conditions have not yet been covered by any regulated or consumer information crash tests. In theory, proper energy-absorbing padding and middle interaction air bag could potentially reduce the head and torso contact energy and in turn reduce the occupant injury risks. To address concerns about farside kinematics for occupants seated in wheelchairs, researchers at ZF and UMTRI designed a new Center Airbag To Contain Humans (CATCH) that can effectively limit occupant lateral excursions in farside impacts (Klinich et al., 2021). Variations on air bag designs like this could benefit other occupants, including older children in the simulated crash conditions in this study.

Children Using Harnessed CRS in Farside/Oblique Impacts

Based on the nature of ATD contacts, we do not think there are major safety concerns for children using harnessed restraints in all simulated conditions, but the CRSs may rotate laterally in farside or oblique impacts. Such motion may increase the inertia loading between ATD and CRS, and could also potentially lead to CRS to vehicle contacts, which might be more injurious. Based on the literature, rigid CRS attachment has shown the potential to reduce CRS movements during crashes, which could be beneficial in farside and oblique impacts (Charlton et al., 2004, Bilston et al., 2005, Huot et al., 2005, Charlton et al., 2007, Hauschild et al., 2018). In this study, we only simulated CRS installations using LATCH and seat belt, and rigid attachment was not considered due to the low availability in the U.S. market. In addition, additional energy-absorbing features in the CRS may be necessary for further reducing ATD head and torso inertia-induced contact forces.

Limitations

In this study, we monitored ATD excursions as well as injury measures based on scaled adult IARV. The criteria used in this study are more rigorous than those used in FMVSS No. 213 tests. Many of the conditions that fail the IARV(s) would still meet FMVSS No. 213 criteria. Given that FMVSS No. 213 criteria have led to development of child restraint systems with an excellent record of preventing pediatric injury and death from motor-vehicle crashes, conditions that exceed the biomechanical criteria should be viewed with caution as to whether they truly represent a harmful condition.

Of particular concern is the Nij. This injury criterion was developed in the early 1990s to evaluate risk of first-generation deploying air bags. It is not included among FMVSS No. 213 criteria, because it would predict a high risk of cervical spine injury under FMVSS No. 213 test conditions that we do not see in the field. The Nij may not appropriately reflect the risk of cervical spine injury to children because the bending characteristics of the ATD spine sections are not realistic for children; the thoracic spine is a rigid box and all motion from head to lumbar is through the cervical spine. We include Nij for reference to allow comparison of neck loading across conditions, but do not think that conditions exceeding the limits are cause for alarm given the problems with using these criteria with pediatric ATDs.

Some other conditions where excessive injury measures are questionable include the high chest accelerations for the 12MO in rear-facing CRS in conditions that resemble a rear impact. In a review of the literature (and 30+ years of experience of several team members as international experts in child passenger safety), we cannot identify any cases of thoracic injury to a child properly secured in a rear-facing child restraint, either in a rear impact or from rebound after a frontal impact.

This is the first study that estimated risk of injury for children in boosters in a rear impact condition, either through sled tests or through simulations. Like the adult midsize male H3 ATDs, the H33YO and H36YO were designed for severe frontal impact conditions and may not be biofidelic under rear impacts. The BioRID was designed specifically to allow more realistic assessment of rear impact injury potential; its spine includes flexible thoracic vertebrae which differ from the rigid spine box used in frontal adult and child H3 ATDs. Some of the rear impact simulations with the H33YO and H36YO suggested high chest measures that we view with skepticism given the limitations of the ATD spine structure.

Oblique and farside tests were performed with ATDs designed for frontal impacts, because side impact versions of the ATDs (and corresponding models) are not available to represent all four child ages of interest. In addition, very few previous tests of child ATDs have been performed in oblique impacts, and the suitability of using frontal impact ATDs in oblique conditions was of interest.

Oblique and farside performance of the CRABI 12MO and H33YO were reasonable, as the ATD was restrained by a properly snug harness. The initial validation testing with the H36YO and H310YO under oblique and lateral conditions identified some challenges in using these frontal ATDs under non-frontal conditions. Because the belt-positioning booster does not actually restrain the ATD, there was some initial shifting of the ATD on our rebound sled on the initial approach down the track. This was resolved with masking tape to preposition the ATD without affecting kinematics. Of more concern was the fracture of shoulder components of the ATD in the farside test conditions. This damage suggests that these ATDs may not be suitable for non-frontal evaluation of booster seats.

Summary

This study used computer models to study how unconventional seating positions and orientations and those that could be relevant for in ADS-equipped vehicles may affect occupant response metrics for children restrained by harnessed CRS or the vehicle belt, with or without booster.

- We first conducted a literature review to frame a simulation plan, including selections of surrogate ADS-equipped vehicles, potential seating arrangements, impact scenarios, ATD models, and CRS models that are relevant to the selected ATD occupant models.
- Due to the lack of impact tests with child ATD and CRS in farside, oblique, and rear impacts, we conducted 16 sled tests with CRS harness-restrained ATDs and vehicle belt-restrained ATDs seated in conventional and unconventional vehicle seat orientations in frontal, farside, oblique, and rear impact conditions, and use the sled tests to validate a set of computational models.
- A total of 350 MADYMO simulations were conducted with CRABI 12MO in RFCRS, H33YO ATD in both RFCRS and FFCRS across a range of conventional and unconventional seating locations and orientations under five impact directions and various CRS installation methods. We did not find major safety concerns in all simulations based on the nature of ATD contacts, although some injury measures are over IAR. We found that the CRS may rotate laterally in farside and oblique impacts, which could result in higher HIC and chest acceleration due to inertia loading to the CRS, and there is a risk that the larger lateral rotation of the CRS may lead to a contact between CRS and vehicle interior.
- A total of 200 MADYMO simulations were conducted with H36YO in a backless booster and H310YO with and without a booster across a range of conventional and unconventional seating locations and orientations under five impact directions. The major safety concern is that both ATDs have the potential to contact the seat next to them or the instrument panel behind them in a farside or oblique impact.
- Based on all the simulation results, unconventional seating does not necessarily create additional safety concerns beyond what we know with the conventional seating. However, due to the orientation of the unconventional seats, they may involve in higher percentage of oblique and rear-oblique impacts than the conventional seats, which should be considered in future design process.
- This study also demonstrated the challenges of using pediatric ATDs in a wide range of crash conditions. This is especially true when using H36YO and H310YO in farside, oblique and rear impacts. The ATD biofidelity, injury measures and the associated IARVs need to be carefully considered when interpreting the results.
- This is the first study using different child ATDs and CRSs to investigate child occupant responses in a wide range of impact directions and seating orientations. Results from the sled tests and simulations provide a better understanding of child occupant responses in those crash conditions, but identified several limitations of using frontal ATDs in other crash directions.

References

- Andersson, M., Pipkorn, B., & Lövsund, P. (2012a). Evaluation of the head kinematics of the q3 model and a modified q3 model by means of crash reconstruction. *Traffic Injury Prevention, 13*(6), 600–611. <https://doi.org/10.1080/15389588.2012.676223>
- Andersson, M., Pipkorn, B., & Lövsund, P. (2012b). Parameter study for child injury mitigation in near-side impacts through FE simulations. *Traffic Injury Prevention, 13*(2), 182–192. <https://doi.org/10.1080/15389588.2011.637411>
- Arbogast, K. B., & Maltese, M. R. (2015). Pediatric biomechanics. In N. Yoganandan, A. M. Nahum, & J. W. Melvin (eds.), *Accidental Injury: Biomechanics and Prevention*, 3rd edition. https://doi.org/10.1007/978-1-4939-1732-7_22
- Belwadi, A., Sarfare, S., Tushak, S., Maheshwari, J., & Menon, S. (2019). Responses of the scaled pediatric human body model in the rear- and forward-facing child seats in simulated frontal motor vehicle crashes. *Traffic Injury Prevention, 20*(sup2), S143–S144. <https://doi.org/10.1080/15389588.2019.1661684>
- Bilston, L. E., Brown, J., & Kelly, P. (2005). Improved protection for children in forward-facing restraints during side impacts. *Traffic Injury Prevention, 6*(2), 135–146. <https://doi.org/10.1080/15389580590931608>
- Bilston, L. E., Yuen, M., & Brown, J. (2007). Reconstruction of crashes involving injured child occupants: The risk of serious injuries associated with sub-optimal restraint use may be reduced by better controlling occupant kinematics. *Traffic Injury Prevention, 8*(1), 47–61. <https://doi.org/10.1080/15389580600990352>
- Bohman, K., Arbogast, K. B., Loeb, H., Charlton, J. L., Koppel, S., & Cross, S. L. (2018). Frontal and oblique crash tests of HIII 6-year-old child ATD using real-world, observed child passenger postures. *Traffic Injury Prevention, 19*, S125–S130. <https://doi.org/10.1080/15389588.2017.1385781>
- Bohman, K., Östh, J., Jakobsson, L., Stockman, I., Wimmerstedt, M., & Wallin, H. (2020). Booster cushion design effects on child occupant kinematics and loading assessed using the PIPER 6-year-old HBM and the Q10 ATD in frontal impacts. *Traffic Injury Prevention, 21*(sup1), S25–S30. <https://doi.org/10.1080/15389588.2020.1795148>
- Brelín-Fornari, J., & Janca, S. (2014a, April). *Development of NHTSA's side impact test procedure for child restraint systems using a deceleration sled: Part 1* (Vol. 1). (Report No. DOT HS 811 994). National Highway Traffic Safety Administration. https://digitalcommons.kettering.edu/cgi/viewcontent.cgi?article=1000&context=mechanical_grants
- Brelín-Fornari, J., & Janca, S. (2014b, May). *Development of NHTSA's side impact test procedure for child restraint systems using a deceleration sled: Part 2*. (Report No. DOT HS 811 995). National Highway Traffic Safety Administration. www.nhtsa.gov/sites/nhtsa.gov/files/811995-sideimpcttest-chrestraintdecelsled_pt2.pdf
- Brolin, K., Stockman, I., Andersson, M., Bohman, K., Gras, L. L., & Jakobsson, L. (2015). Safety of children in cars: A review of biomechanical aspects and human body models. *IATSS Research, 38*(2), 92–102. <https://doi.org/10.1016/j.iatssr.2014.09.001>

- Charlton, J. L., Fildes, B., Taranto, D., Laemmle, R., Smith, S., & Clark, A. (2007). Performance of booster seats in side impacts: effect of adjacent passengers and ISOfix attachment. *Annals of Advances in Automotive Medicine*, 51, 155–167. www.ncbi.nlm.nih.gov/pubmed/18184490
- Charlton, J. L., Fildes, B., Laemmle, R., Smith, S., & Douglas, F. (2004). A preliminary evaluation of child restraints and anchorage systems for an Australian car. *Association for the Advancement of Automotive Medicine*, 73–86.
- Charlton, J. L., Fildes, B., Taranto, D., Laemmle, R., Smith, S., Clark, A., & Holden, G. M. (2007). Performance of booster seats in side impacts: Effect of adjacent passengers and ISOfix attachment. *Association for the Advancement of Automotive Medicine*, 155–167.
- Cruz-Jaramillo, I. L., Torres-San-Miguel, C. R., Cortes Vásquez, O., & Martínez-Sáez, L. (2018). Numerical low-back booster analysis on a 6-year-old infant during a frontal crash test. *Applied Bionics and Biomechanics*, 2018. <https://doi.org/10.1155/2018/2359262>
- Deo, A. (2005). A reverse engineering approach for development and validation of a belt positioning booster child seat. Master's thesis, Wichita State University.
- Forman, J., Michaelson, J., Kent, R., Kuppa, S., & Bostrom, O. (2008, October). Occupant restraint in the rear seat: ATD responses to standard and pre-tensioning, force-limiting belt restraints. *Annals of Advances in Automotive Medicine 52nd Annual Scientific Conference*, 52, 141–153.
- Fuchs, S., Barthel, M., Flannery, A., & Christoffel, K. (1989). Cervical spine fractures sustained by young children in forward-facing car seats. *Pediatrics*, 84, 348–354.
- Ghati, Y., Menon, R. A., Milone, M., Lankarani, H., & Oliveres, G. (2009, October). Performance evaluation of child safety seats in far-side lateral sled tests at varying speeds. *Annals of Advances in Automotive Medicine - 53rd Annual Scientific Conference*, 53, 221–235.
- Hauschild, H W, Humm, J. R., Pintar, F. A., Yoganandan, N., Kaufman, B., Maltese, M. R., & Arbogast, K. B. (2018). The influence of child restraint lower attachment method on protection offered by forward facing child restraint systems in oblique loading conditions. *Traffic Injury Prevention*, 19(sup1), S139–S145. <https://doi.org/10.1080/15389588.2017.1369532>
- Hauschild, H W., Humm, J. R., Pintar, F. A., Yoganandan, N., Kaufman, B., Kim, J., Maltese, M. R., & Arbogast, K. B. (2016). Protection of children in forward-facing child restraint systems during oblique side impact sled tests: Intrusion and tether effects. *Traffic Injury Prevention*, 17(S1), 156–162. <https://doi.org/10.1080/15389588.2016.1194982>
- Hauschild, H W., Humm, J. R., Pintar, F. A., Yoganandan, N., Kaufman, B., Maltese, M. R., & Arbogast, K. B. (2015). The influence of enhanced side impact protection on kinematics and injury measures of far- or center-seated children in forward-facing child restraints. *Traffic Injury Prevention*, 16, S9–S15. <https://doi.org/10.1080/15389588.2015.1064116>

- Hauschild, H W., Humm, J. R., Pintar, F. A., Yoganandan, N., Kaufman, B., Maltese, M. R., & Arbogast, K. B. (2018). The influence of child restraint lower attachment method on protection offered by forward facing child restraint systems in oblique loading conditions. *Traffic Injury Prevention, 19*, S139–S145. <https://doi.org/10.1080/15389588.2017.1369532>
- Hauschild, H W., Humm, J. R., & Yoganandan, N. (2013). Injury potential at center rear seating positions in rear-facing child restraint systems in side impacts. *Annals of Advances in Automotive Medicine, 57*, 281–295.
- He, J., Zhang, X., & Xu, C. (2018). Comparison of Q-series child dummy and human model restrained in shield CRS in frontal impact. *International Journal of Crashworthiness, 23*(5), 486–496. <https://doi.org/10.1080/13588265.2017.1345591>
- Hu, J., Fischer, K., Schroeder, A., Boyle, K., Adler, A., & Reed, M. (2019). Development of oblique restraint countermeasures. (Report No. DOT HS 812 814). National Highway Traffic Safety Administration. <https://rosap.nhtl.bts.gov/view/dot/44143>
- Hu, J., & Jayakar, H. R. R. (2014). Improving child safety seat performance through finite element simulations. *ASME International Mechanical Engineering Congress and Exposition, Proceedings (IMECE), 12*. <https://doi.org/10.1115/IMECE2014-38471>
- Hu, J., Klinich, K. D., Reed, M. P., Ebert-Hamilton, S. M., & Rupp, J. D. (2014). Characterizing child head motions relative to vehicle rear seat compartment in motor vehicle crashes. (Report No. DOT HS 812 105). National Highway Traffic Safety Administration. www.nhtsa.gov/sites/nhtsa.gov/files/documents/812105_characterizingchildheadmotions.pdf
- Hu, J., Klinich, K. D., Reed, M. P., Kokkolaras, M., & Rupp, J. D. (2012). Development and validation of a modified Hybrid-III six-year-old dummy model for simulating submarining in motor-vehicle crashes. *Medical Engineering and Physics, 34*(5), 541–551. <https://doi.org/10.1016/j.medengphy.2011.08.013>
- Hu, J., Manary, M. A., Klinich, K. D., & Reed, M. P. (2015). Evaluation of ISO CRS envelopes relative to u.s. vehicles and child restraint systems. *Traffic Injury Prevention, 16*(8). <https://doi.org/10.1080/15389588.2015.1014550>
- Hu, J., Reed, M. P., Rupp, J. D., Fischer, K., Lange, P., & Adler, A. (2017). Optimizing seat belt and airbag designs for rear seat occupant protection in frontal crashes. *Stapp Car Crash Journal*. <https://doi.org/10.4271/2017-22-0004>
- Hu, J., Wu, J., Klinich, K. D., Reed, M. P., Rupp, J. D., & Cao, L. (2013). Optimizing the rear seat environment for older children, adults, and infants. *Traffic Injury Prevention, 14*(SUPPL1). <https://doi.org/10.1080/15389588.2013.796043>
- Hu, J., Wu, J., Reed, M. P., Klinich, K. D., & Cao, L. (2013). Rear seat restraint system optimization for older children in frontal crashes. *Traffic Injury Prevention, 14*(6). <https://doi.org/10.1080/15389588.2012.743123>
- Huelke, D., Mackay, G., Morris, A., & Bradford, M. (1992, February 24-28). *Car crashes and non-head impact cervical spine injuries in infants and children* (SAE Paper 920562). [Society of Automotive Engineers] International Congress & Exposition Detroit, MI.

- Hulme, K. F., Patra, A., Vusirikala, N., Galganski, R. A., & Hatziprokopiou, I. (2004, March 8-11). *A virtual prototyping toolkit for assessment of child restraint system (CRS) safety* (SAE Technical Paper 2004-01-0484). SAE 2004 World Congress & Exhibition, Detroit, MI. <https://doi.org/10.4271/2004-01-0484>
- Huot, M., Brown, J., Kelly, P., & Bilston, L. E. (2005). Effectiveness of high back belt positioning booster seats in side impacts. *Traffic Injury Prevention*, 6(2), 147–155. <https://doi.org/10.1080/15389580590931626>
- Ibrahim, M. S., Siregar, R. A., Adom, A. H., Khan, S. F., & Zakaria, H. (2009, October 11-13). *Development of numerical child dummy model and the analysis of head impact criterion*. International Conference on Applications and Design in Mechanical Engineering, Penang, Malaysia.
- Ive, H. P., Sirkin, D., Miller, D., Li, J., & Ju, W. (2015, September 1-3). “Don’t make me turn this seat around!”: Driver and passenger activities and positions in autonomous cars. AutomotiveUI '15: 7th International Conference on Automotive User Interfaces and Interactive Vehicular Applications, Nottingham, United Kingdom. <https://doi.org/10.1145/2809730.2809752>
- Jóhannsdóttir, S. K. (2019). *Evaluation of head and neck injuries during misuses of child restraint systems evaluation of head and neck injuries during misuses of child restraint systems simulations of car accidents performed with the PIPER child model*. KTH [Kungliga Tekniska högskolan] Royal Institute of Technology.
- Johansson, M., Pipkorn, B., & Lövsund, P. (2009). Child safety in vehicles: validation of a mathematical model and development of restraint system design guidelines for 3-year-olds through mathematical simulations. *Traffic Injury Prevention*, 10(5), 467–478. <https://doi.org/10.1080/15389580903149243>
- Jorlöv, S., Bohman, K., & Larsson, A. (2017, September 13-15). *Seating positions and activities in highly automated cars – A qualitative study of future automated driving scenarios* (Paper No. IRC-17-11). International Research Council on the Biomechanics of Injury, Antwerp, Belgium.
- Juste-Lorente, O., Maza, M., Lorente, A. I., & Lopez-Valdes, F. J. (2018). Differences in the kinematics of booster-seated pediatric occupants using two different car seats. *Traffic Injury Prevention*, 19(1), 18–22. <https://doi.org/10.1080/15389588.2017.1334119>
- Kapoor, T., Altenhof, W., Snowdon, A., Howard, A., Rasico, J., Zhu, F., & Baggio, D. (2011). A numerical investigation into the effect of CRS misuse on the injury potential of children in frontal and side impact crashes. *Accident Analysis and Prevention*, 43(4), 1438–1450. <https://doi.org/10.1016/j.aap.2011.02.022>
- Kapoor, T., Altenhof, W., Tot, M., Zhang, W., Howard, A., Rasico, J., Zhu, F., & Mizuno, K. (2008). Load limiting behavior in CRS tether anchors as a method to mitigate head and neck injuries sustained by children in frontal crash. *Traffic Injury Prevention*, 9(3), 243–255. <https://doi.org/10.1080/15389580801975210>
- Kapoor, T., Altenhof, W., Wang, Q., & Howard, A. (2006). Injury potential of a three-year-old Hybrid III dummy in forward and rearward facing positions under CMVSS 208 testing

- conditions. *Accident Analysis and Prevention*, 38(4), 786–800.
<https://doi.org/10.1016/j.aap.2006.02.005>
- Klinich, K. D., Boyle, K. J., Malik, L., Manary, M. A., Eby, B. J., & Hu, J. (2018, September). *Development of Fit Envelopes to Promote Compatibility Among Vehicles and Child* (Report No. DOT HS 812 610.). National Highway Traffic Safety Administration.
<https://rosap.nhtsa.gov/view/dot/38823>
- Klinich, K. D., Flannagan, C. A. C., Hu, J., & Reed, M. P. (2016, September 14-16). *Potential safety effects of low-mass vehicles with comprehensive crash avoidance technology*. 2016 International Research Council on the Biomechanics of Injury, Malaga, Spain, 755–764.
- Klinich, K. D., Jones, M. H., Manary, M. A., Ebert, S. H., Boyle, K. J., Malik, L., Orton, N. R., & Reed, M. P. (2020). Investigation of potential design and performance criteria for booster seats through volunteer and dynamic testing (Report No. DOT HS 812 919). National Highway Traffic Safety Administration. <https://rosap.nhtsa.gov/view/dot/49119>
- Klinich, K. D., Reed, M. P., Ebert, S. M., & Rupp, J. D. (2014). Kinematics of pediatric crash dummies seated on vehicle seats with realistic belt geometry. *Traffic Injury Prevention*, 15(8), 866–874. <https://doi.org/10.1080/15389588.2014.890720>
- Koppel, S., Jiménez-Octavio, J., Bohman, K., Logan, D., Raphael, W., Quintana Jimenez, L., & Lopez Valdes, F. (2019). Seating configuration and position preferences in fully automated vehicles. *Traffic Injury Prevention*, 20(sup 2), S103–S109.
<https://doi.org/10.1080/15389588.2019.1625336>
- Kuppa, S., & Saunders, J. (2005, June 6-9). *Rear seat occupant protection in frontal crashes*. 19th International Technical Conference on the Enhanced Safety of Vehicles, Washington, DC.
- Lopez-Valdes, F. J., Bohman, K., Jimenez-Octavio, J., Logan, D., Raphael, W., Quintana, L., Suarez Del Fueyo, R., & Koppel, S. (2020). Understanding users' characteristics in the selection of vehicle seating configurations and positions in fully automated vehicles. *Traffic Injury Prevention*, 21(sup1), S19–S24.
<https://doi.org/10.1080/15389588.2020.1810245>
www.tandfonline.com/doi/abs/10.1080/15389588.2020.1810245?journalCode=gcpi20
- Maheshwari, J., Duong, N., Sarfare, S., & Belwadi, A. (2018). Evaluating the response of the PIPER scalable human body model across child restraining seats in simulated frontal crashes. *Traffic Injury Prevention*, 19(sup2), S140–S142.
<https://doi.org/10.1080/15389588.2018.1532204>
- Maltese, M. R., & Horn, W. (2019). *Repeatability and reproducibility of the updated FMVSS No. 213 frontal standard seat assembly*. Docket No. NHTSA-2020-0093-0011. National Highway Traffic Safety Administration.
- Maltese, M. R., Tylko, S., Belwadi, A., Locey, C., & Arbogast, K. B. (2014). Comparative performance of forward-facing child restraint systems on the C/FMVSS 213 bench and vehicle seats. *Traffic Injury Prevention*, 15, S103–S110.
<https://doi.org/10.1080/15389588.2014.935358>

- Manary, M. A., Flannagan, C. A. C., Reed, M. P., Orton, N. R., & Klinich, K. D. (2019). Effects of child restraint misuse on dynamic performance. *Traffic Injury Prevention, 20*(8), 860–865. <https://doi.org/10.1080/15389588.2019.1665177>
- Manary, M. A., Klinich, K. D., & Orton, N. R. (2018, March). Assessment of ATD Selection and Use for Dynamic Testing of Rear-Facing Child Restraint Systems for Larger Infants and Toddlers (Report No. DOT HS 812 469). National Highway Traffic Safety Administration. www.nhtsa.gov/sites/nhtsa.gov/files/documents/812469_assess-atd-selection-and-use-testing-rear-facing-child-restraint-systems-larger-infants-and-toddlers.pdf
- Manary, M. A., Reed, M. P., Klinich, K. D., Ritchie, N. L., & Schneider, L. W. (2006, October 16-18). *The effects of tethering rear-facing child restraint systems on ATD responses*. 5th Annual Association for the Advancement of Automotive Medicine, Chicago, IL, 397–410.
- Mansfield, J., Kang, Y. S., & Bolte, J. (2018). *Rear-facing child restraint systems in rear impact sled tests* (SAE Technical Paper 2018-01-1325). SAE International. <https://doi.org/10.4271/2018-01-1325>
- Mansfield, J., Kwon, H. J., & Kang, Y. S. (2020, April 14). The roles of vehicle seat cushion stiffness and length in child restraint system (CRS) performance. *SAE International Journal of Advances and Current Practices in Mobility 2*(3), 1669–1684. <https://doi.org/10.4271/2020-01-0977>
- Mertz, H. J., Irwin, A. L., & Prasad, P. (2003). Biomechanical and scaling bases for frontal and side impact injury assessment reference values. *Stapp Car Crash J, 47*, 155–188. www.ncbi.nlm.nih.gov/pubmed/17096249
- Mertz, H. J., Irwin, A. L., & Prasad, P. (2016). *Biomechanical and scaling basis for frontal and side impact injury assessment reference values*. 60th Stapp Car Crash Conference. <https://doi.org/10.4271/2016-22-0018>
- Mizuno, K., Iwata, K., Deguchi, T., Ikami, T., & Kubota, M. (2005). Development of a three-year-old child FE model. *Traffic Injury Prevention, 6*(4), 361–371. <https://doi.org/10.1080/15389580500255922>
- Mizuno, K., & Namikiri, T. (2007, June 18-21). *Analysis of child responses in CRS using child human FE model*. 20th International Technical Conference on the Enhanced Safety of Vehicles Conference, Lyon, France.
- Nie, B., Gan, S., Chen, W., & Zhou, Q. (2020). Seating preferences in highly automated vehicles and occupant safety awareness: A national survey of Chinese perceptions. *Traffic Injury Prevention, 21*(4), 247–253. <https://doi.org/10.1080/15389588.2020.1738013>
- O'Donel, C. A. (2017). *The effects of rear facing child restraint system design and installation method on head and neck injury severity in infants involved in rear end collisions*. Master's thesis, Villanova University.
- Park, D.-W., Moon, G.-S., Yoo, W.-S., & Park, S.-J. (2004). Design of a child seat system with multipoint restraints to improve safety. *Proceedings of Asian Conference on Multibody Dynamics*, Seoul, Korea.

- Rola, E., & Wdowicz, D. (2018). Is it safer to transport a three-year-old child in a forward-facing child restraint system or in a rear-facing one while head-on collision? *Institute of Electrical and Electronics Engineers*, 128–130.
<https://doi.org/10.1109/IIPHDW.2018.8388340>
- Sherwood, C. P., Abdelilah, Y., Crandall, J. R., Stevens, S. L., Saggese, J. M., & Eichelberger, M. R. (2004). The performance of various rear facing child restraint systems in a frontal crash. *48th Annual Proceedings, Association for the Advancement of Automobile Medicine*, 8: 303–321.
- Sherwood, C. P., & Crandall, J. R. (2007). Frontal sled tests comparing rear and forward facing child restraints with 1-3 year old dummies. *Annual Proceedings, Association for the Advancement of Automotive Medicine*, 51, 169–180.
- Sherwood, C. P., Gopalan, S., Abdelilah, Y., Marshall, R. J., & Crandall, J. R. (2005). Vehicle interior interactions and kinematics of rear facing child restraints in frontal crashes. *Annual Proceedings, Association for the Advancement of Automotive Medicine*, 41, 215–228.
- Sullivan, L., Loudon, A., & Echemendia, C. (2014, June 15-18). NHTSA's evaluation of a potential child restraint side impact test procedure development. (Paper Number 11-0227). National Highway Traffic Safety Administration. *Proceedings of the 21st International Technical Conference on the Enhanced Safety of Vehicles (ESV)*, Stuttgart, Germany. www-esv.nhtsa.dot.gov/Proceedings/21/09-0539.pdf
- Transport Canada. (2018, July 11). *Occupant crash protection* (Technical Standards Document No. 208, Revision 1R).
- Tylko, S., Bohman, K., & Bussièrès, A. (2015, November). Responses of the Q6/Q6s ATD positioned in booster seats in the far-side seat location of side impact passenger car and sled tests (Technical Paper 2015-22-0012). *59th Stapp Car Crash Conference*, 59, 313–335. <https://doi.org/10.4271/2015-22-0012>
- Tylko S, Locey CM, Garcia-Espana JF, Arbogast KB, Maltese MR. Comparative Performance of Rear Facing Child Restraint Systems on the CMVSS 213 Bench and Vehicle Seats. *Ann Adv Automot Med*. 2013;57:311-28. PMID: 24406967; PMCID: PMC3861808
<https://www.ncbi.nlm.nih.gov/pmc/articles/PMC3861808/>
- Wang, Q., Kapoor, T., & Altenhof, W. (2006, June 4-6). *A numerical investigation into the injury potential of three-year-old children seated in forward facing child safety seats during side impact crashes in far side*. 9th International LS-DYNA Users Conference, Detroit, MI.
- Wang, S., & Li, Z. (2019). Exploring the mechanism of crashes with automated vehicles using statistical modeling approaches. *PLoS ONE*, 14(3), 1–16.
<https://doi.org/10.1371/journal.pone.0214550>
- Wietholter, K., Loudon, A., & Echemendia, C. (2021, June). Development of a representative seat assembly for FMVSS No. 213. (Report No. DOT HS 813 096). National Highway Traffic Safety Administration.
https://rosap.ntl.bts.gov/view/dot/55992/dot_55992_DS1.pdf

- Williams, J. R., O'Donel, C. A., & Leiss, P. J. (2015). Effects of LATCH versus available seatbelt installation of rear facing child restraint systems on head injury criteria for 6 month old infants in rear end collisions. *Traffic Injury Prevention, 16*, S16–S23.
<https://doi.org/10.1080/15389588.2015.1067804>
- Wu, J., Hu, J., Reed, M. P., Klinich, K. D., & Cao, L. (2012). Development and validation of a parametric child anthropomorphic test device model representing 6-12-year-old children. *International Journal of Crashworthiness, 17*(6).
<https://doi.org/10.1080/13588265.2012.703474>
www.tandfonline.com/doi/abs/10.1080/13588265.2012.703474?journalCode=tcrs20
- Yoshida, R., Okada, H., & Nomura, M. (2011, November). *Head impact mechanisms of a child occupant seated in a child restraint system as determined by impact testing*. 55th Stapp Car Crash Conference, Dearborn, MI, 117–139.

Appendix A: ADS-Equipped Highly Automated Vehicles



Tesla Model S



Self-driving taxi BMW in Las Vegas



Amazon/Rivian



Cruise/GM Origin



Ford/Argo AI



First Transit/US Ignite – Polaris GEM shuttle



Volkswagen SEDRIC



Volkswagen ID



Uber



Nissan Easy Ride



May Mobility/Toyota



Nuro delivery vehicle



First Transit/Easy Mile/MnDOT



Milo/First Transit



Waymo/Alphabet Inc.



Olli 2.0 by Beep/Local Motors



Shanghai Automotive Industrial Corp (CA)



Autonom shuttle by Navya/Beep



PonyPilot by Pony.ai



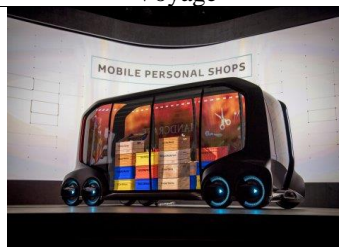
Optimus Ride



Voyage



Drive.ai



e-Palette concept by Toyota













 <p>smart vision EQ fortwo concept by Mercedes-Benz</p>	 <p>Plus.ai</p>
 <p>Volvo Vera</p>	 <p>Freightliner Inspiration</p>
 <p>Tesla Semi</p>	 <p>Ford F-Vision concept</p>
 <p>Tu Simple</p>	 <p>Starsky Robotics</p>
 <p>Daimler/Torc Robotics</p>	 <p>Future Truck by Mercedes-Benz</p>
 <p>Embark Trucks</p>	 <p>Navya Trapezio</p>

Figure A-1. ADS-equipped highly automated vehicles

Appendix B: Differences in Benches

2014 Bench

The 2014 version of the bench was used in the misuse study (Manary et al., 2019). The dynamic tests were performed using a preliminary test bench design (shown in Figure B-1) that has been published as a potential replacement for the FMVSS No. 213 frontal impact bench. It consists of the vehicle seat portion of the side impact buck assembly described in the Notice of Proposed Rulemaking (NPRM) of Federal Docket #NHTSA-2014-0012, except the lower anchors (LAs) were placed 40 mm lower. The bench is mounted to the sled forward-facing without the intruding door assembly but with its height adjusted upward by 50 mm risers. The bench also differs from the NPRM specification in that the seat back has been extended upwards to create a longer/taller seat back support surface. This bench was mounted facing forward on the impact sled at The University of Michigan Transportation Research Institute (UMTRI). It was positioned so excursion measurements of ATDs with this bench would be consistent and comparable with those measured in tests performed on the current FMVSS 213 bench.



Figure B-1. 2014 version of the updated 213 bench used for the test series

2015 Bench

This bench was used to develop a first prototype surrogate retractor (Manary et al., 2018). Most of the tests were performed using a preliminary version of the test bench (shown in Figure B-2) that has been proposed as a potential replacement for the FMVSS 213 frontal impact bench (hereafter referred to as the preliminary 213 bench). It consists of the vehicle seat portion of the buck assembly published in the Federal docket (Federal Docket No. NHTSA-2013-0055-0002, May 17, 2015), except the lower anchors were placed 40 mm lower (per NHTSA's directive). The bench also differs from the NPRM assembly in that the seat back has been extended upwards by 50 mm to create a longer/taller seat back support surface. In addition, the shoulder belt anchor was moved according to the drawings posted in docket NHTSA-2013-0055-0008 (Aug. 25, 2015.) This bench was mounted facing forward on the impact sled at UMTRI. It was positioned so excursion measurements of ATDs with this bench would be consistent with those measured in tests performed on the current FMVSS 213 bench.



Figure B-2. 2015 Version of the updated 213 bench

2018 Bench

This version was used in the Booster Metrics study (Klinich et al., 2020). The test series was performed on an updated version of the preliminary FMVSS No. 213 bench constructed in 2018 and shown in Figure B-3. This seat assembly was constructed using drawings dated July 2017 provided by NHTSA; the final version of these drawings was dated August 2018 and published in NHTSA Docket #2013-0055-0015. The main differences between the 2015 and 2018 seating assemblies were a change in the three-point belt anchoring geometry and the use of a sliding latch plate at the inboard lap belt anchor, as well as an even taller seatback. Of note, the mounting fixture for the 2018 upper shoulder belt D-ring was more rigid than the D-ring mounting fixture used in the 2015 series. When reviewing overhead video, the D-ring fixture in the 2015 series has some visible deflection, which is not present in the D-ring fixture in the 2018 series.

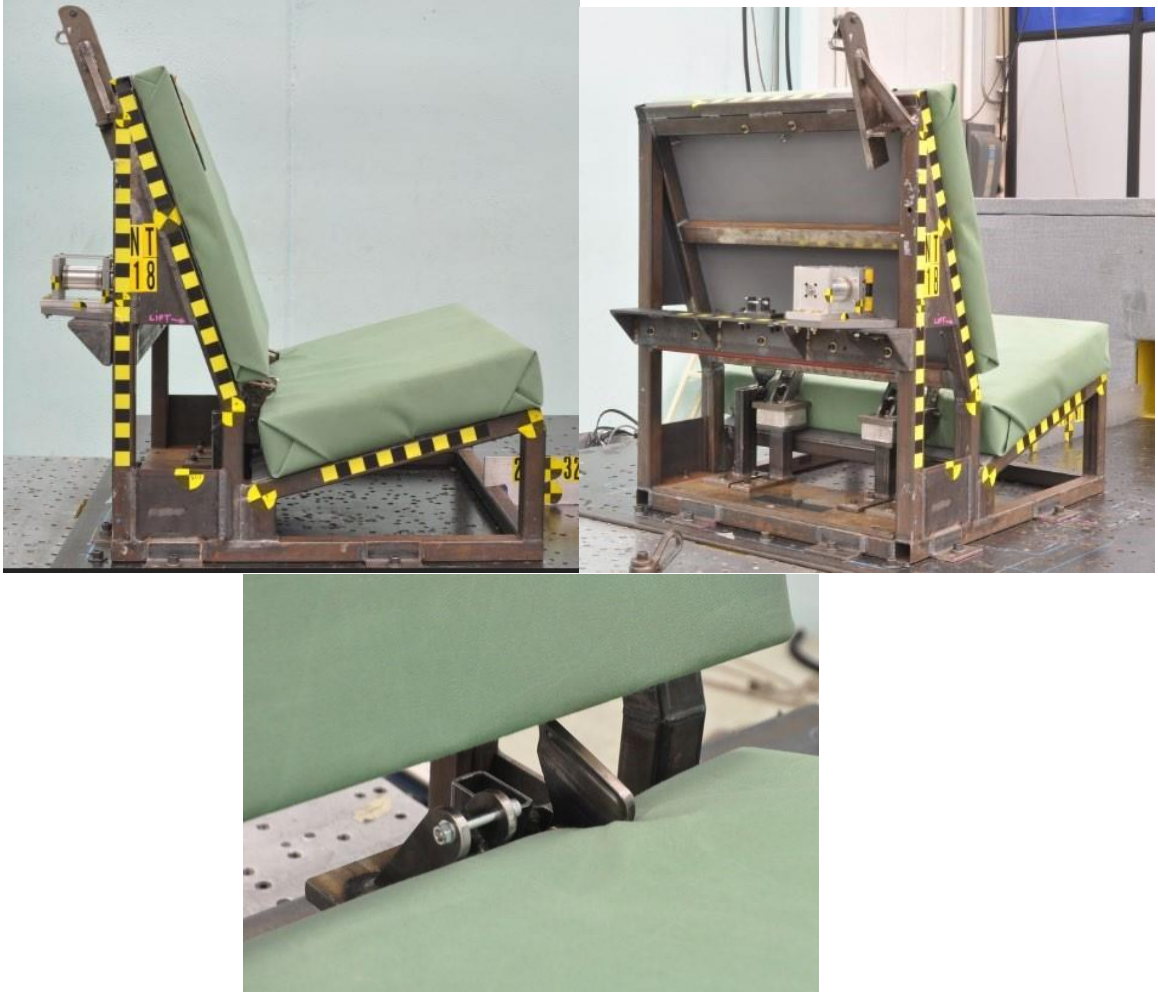


Figure B-3. 2018 version of the updated 213 bench

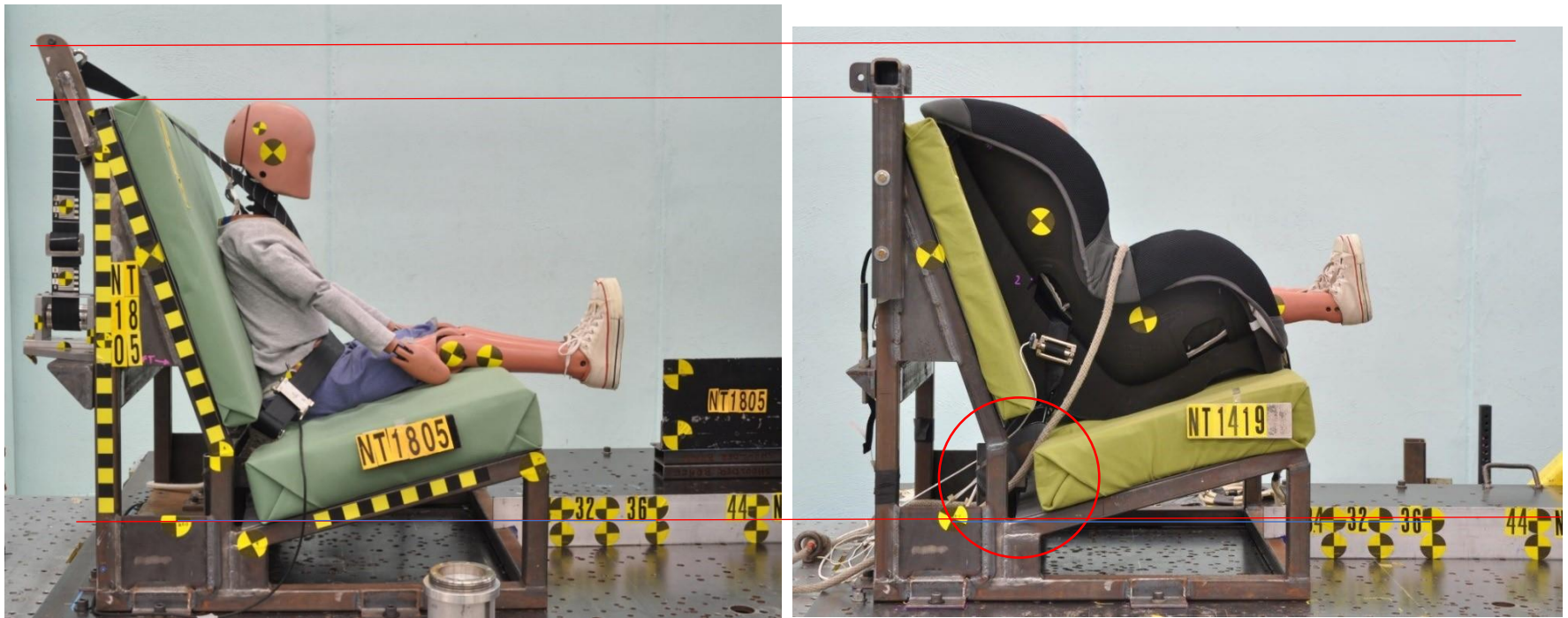


Figure B-4. Comparison of the 213 bench used for booster metrics (left) and misuse (right)

The two photos in Figure B-4 of the 2018 and 2014 versions of the benches are scaled so they match the blue line segment from the Z-point to the 36 inch excursion mark, and are aligned vertically with the Z-point. The main visible differences are the larger gap behind the seat cushion in 2014, the higher seatback height in 2018, and the modified D-ring structure and surrogate retractor.

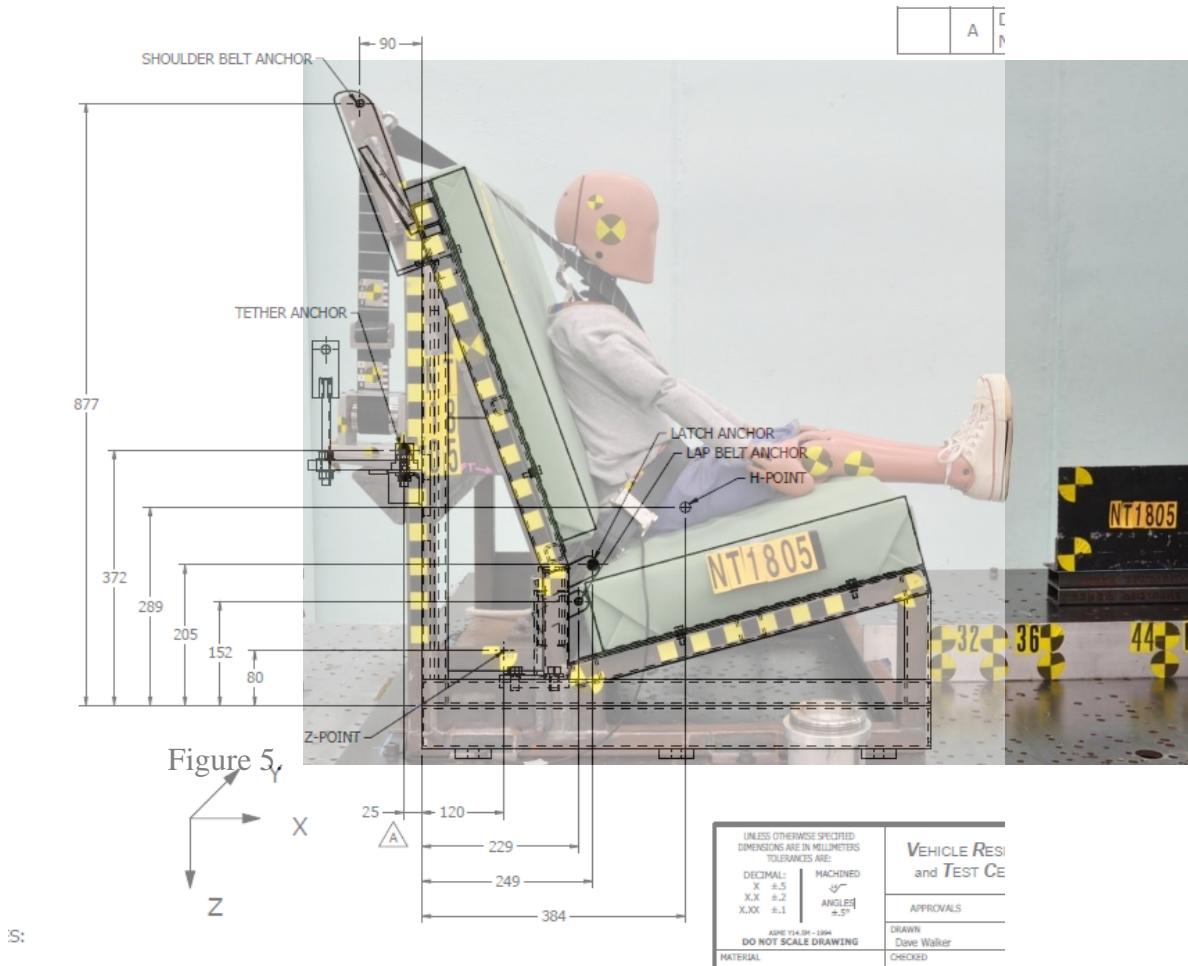


Figure B-5. Overlay of the 2018 bench and 2020 drawing

Figure B-5 shows an overlay of the side view of the 2018 bench and the 2020 drawing. While there is some distortion from parallax, the photos help confirm our assessment that the drawings used to construct the 2018 bench match the drawings published in 2020.

Klinich, K. D., Jones, M. H., Manary, M. A., Ebert, S. H., Boyle, K. J., Malik, L., Orton, N. R., & Reed, M. P. (2020, April). *Investigation of potential design and performance criteria for booster seats through volunteer and dynamic testing* (Report No. DOT HS 812 919). National Highway Traffic Safety Administration. <https://rosap.ntl.bts.gov/view/dot/49119>

Manary, M. A., Flannagan, C. A., Reed, M.P., Orton, N. R., & Klinich, K. D. (2019) Effects of child restraint misuse on dynamic performance. *Traffic Injury Prevention*. 20(8):860-865. doi: 10.1080/15389588.2019.1665177

Manary, M. A., Klinich, K. D., Boyle, K. J., Orton, N. R., Eby, B., & Weir, Q. *Development of a surrogate shoulder belt retractor for sled testing* (Report No. DOT HS 812 660). National Highway Traffic Safety Administration. www.nhtsa.gov/sites/nhtsa.gov/files/documents/812660_development-surrogate-shoulder-belt-retractor-for-sled-testing-of-booster-seats.pdf

Appendix C: Overlay Plots From Validation Tests

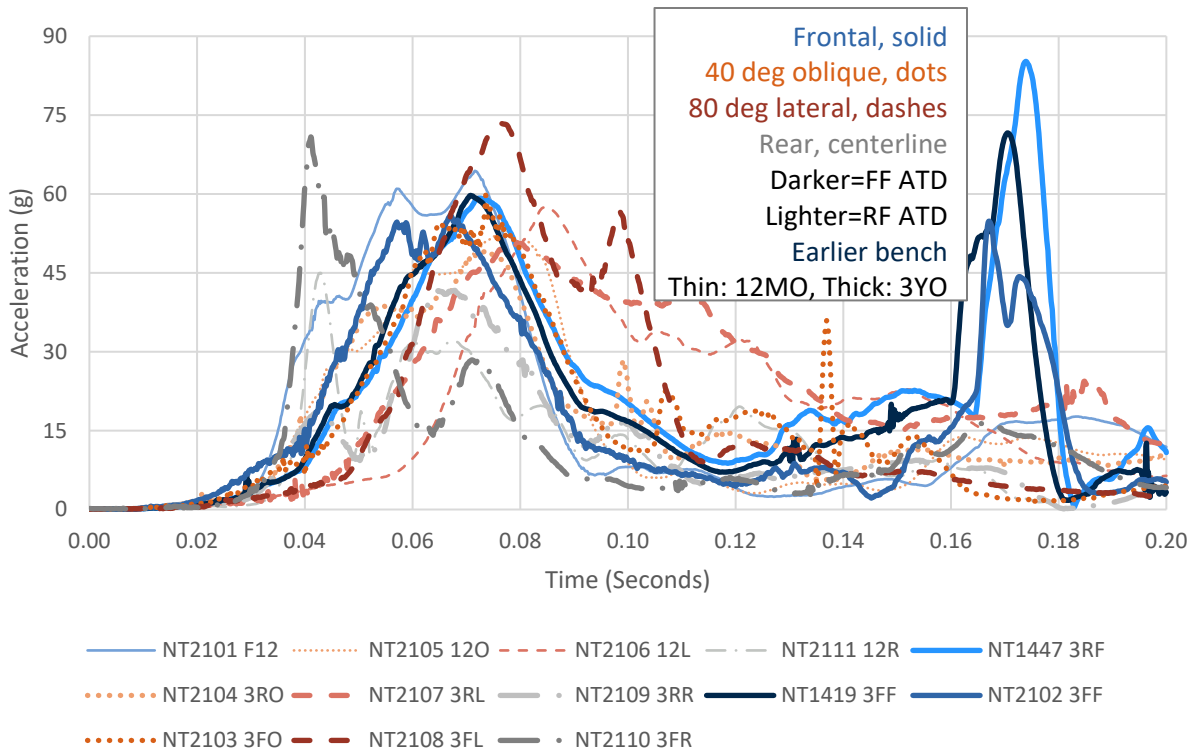


Figure C-1. Head resultant acceleration for tests with CRABI 12MO and H33YO

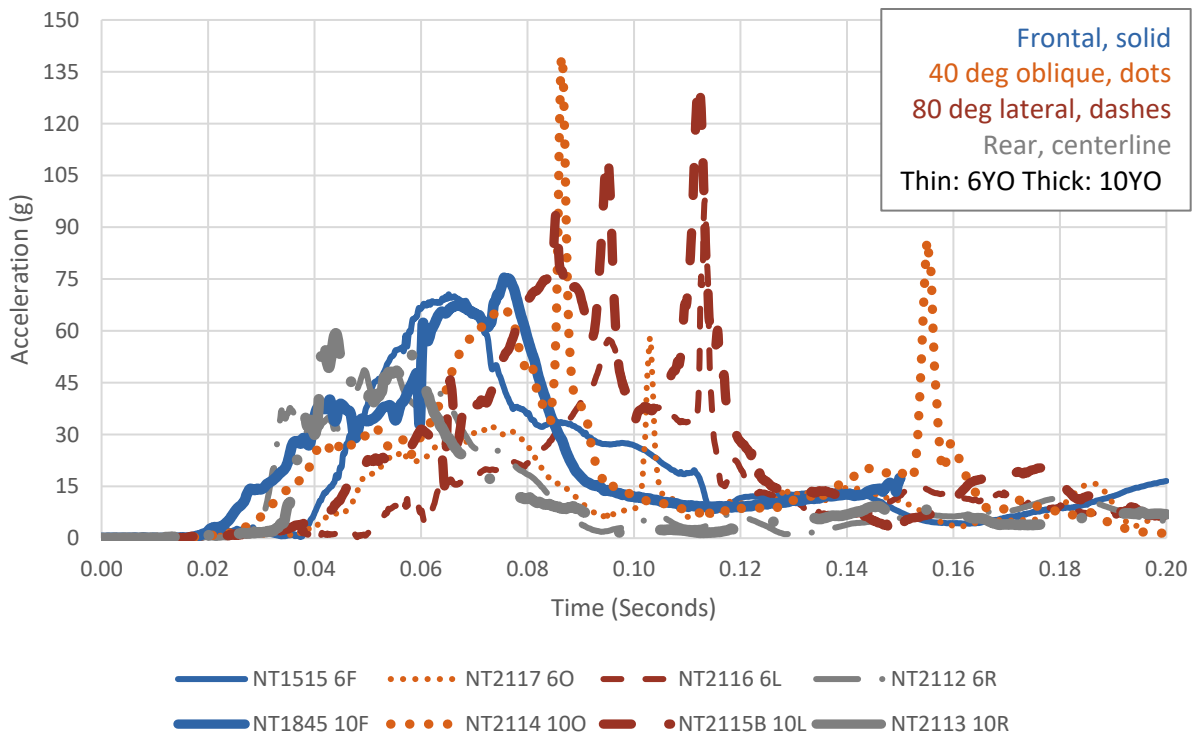


Figure C-2. Head resultant acceleration for tests with H36YO and H310YO

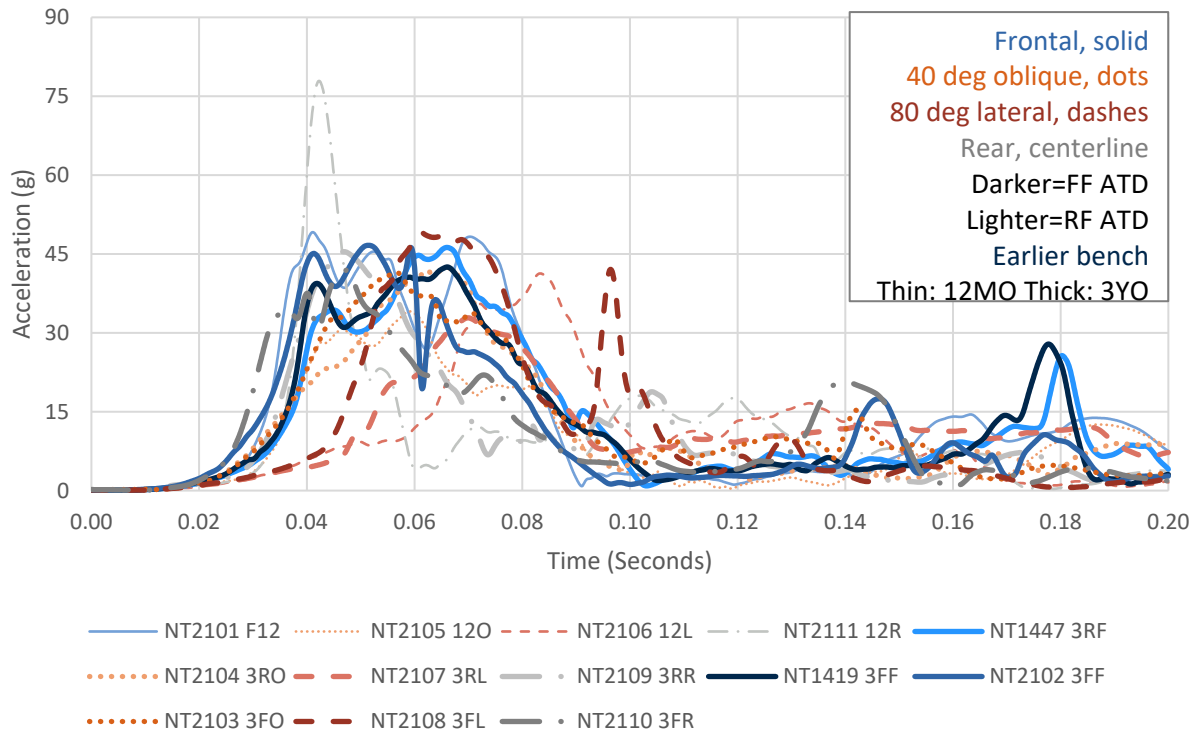


Figure C-3. Chest resultant acceleration for tests with CRABI 12MO and H33YO

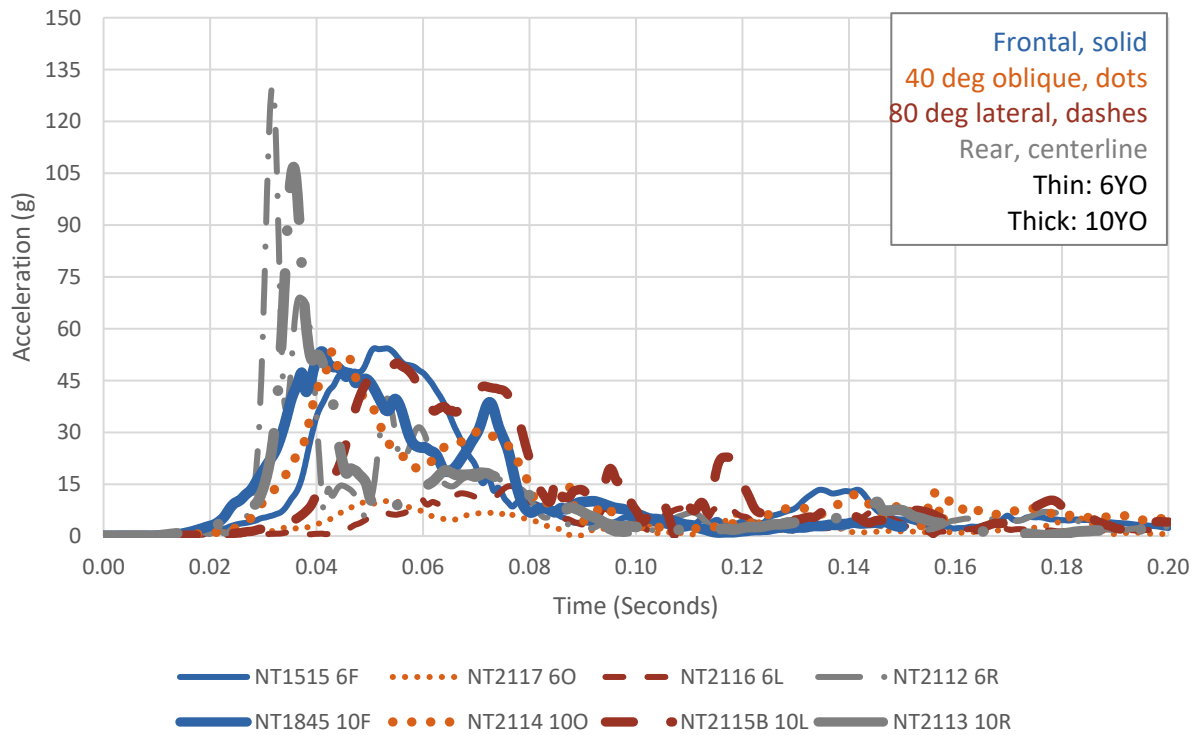


Figure C-4. Chest resultant acceleration for tests with H36YO and H310YO

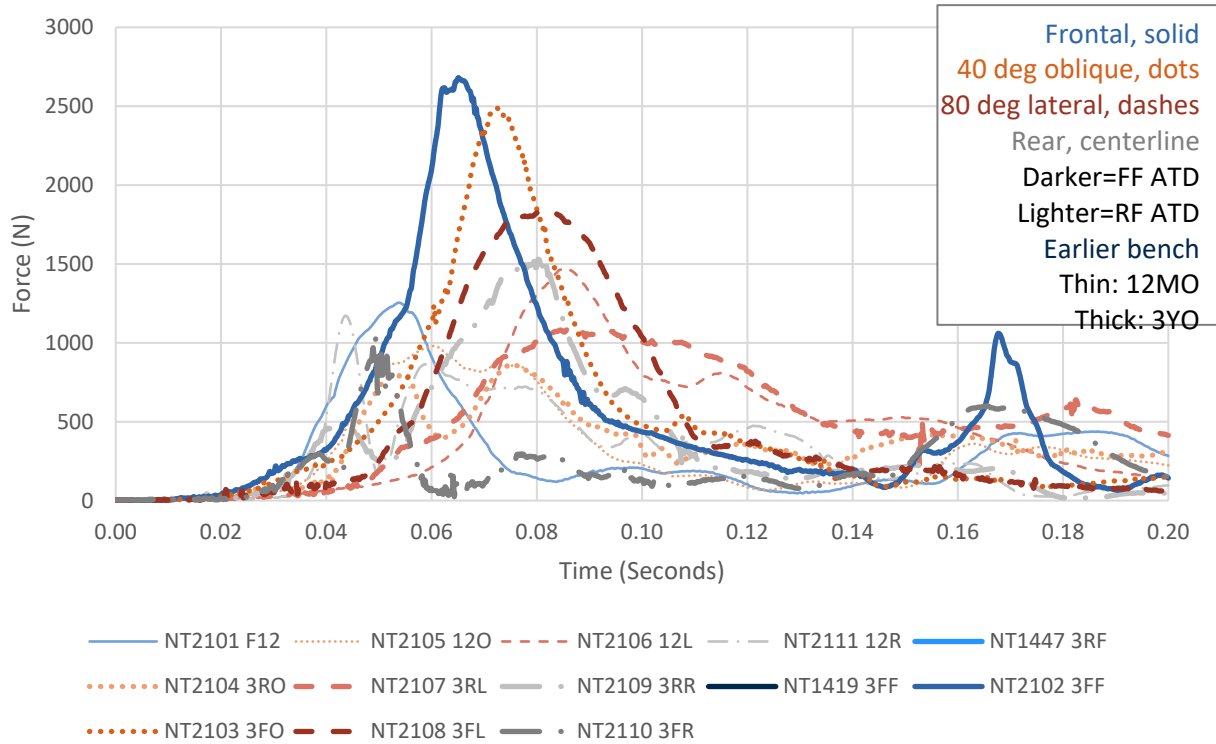


Figure C-5. Neck resultant force for tests with CRABI 12MO and H33YO

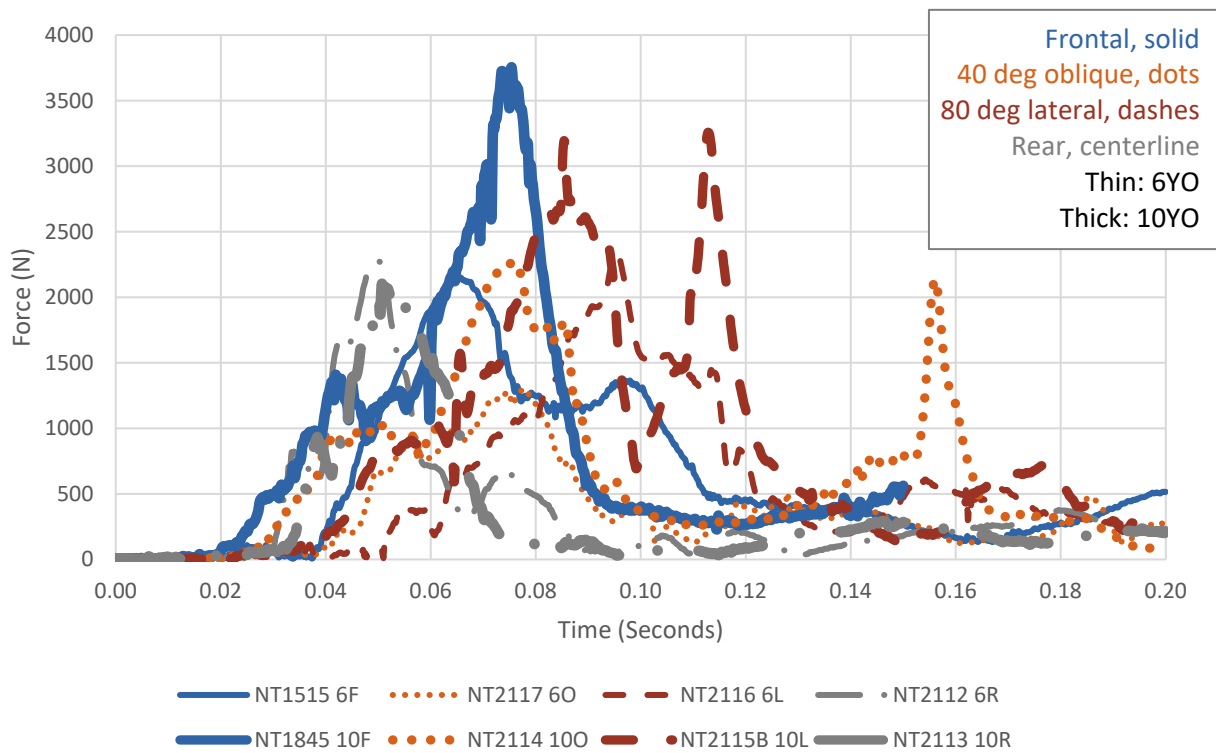


Figure C-6. Neck resultant force for tests with H36YO and H310YO

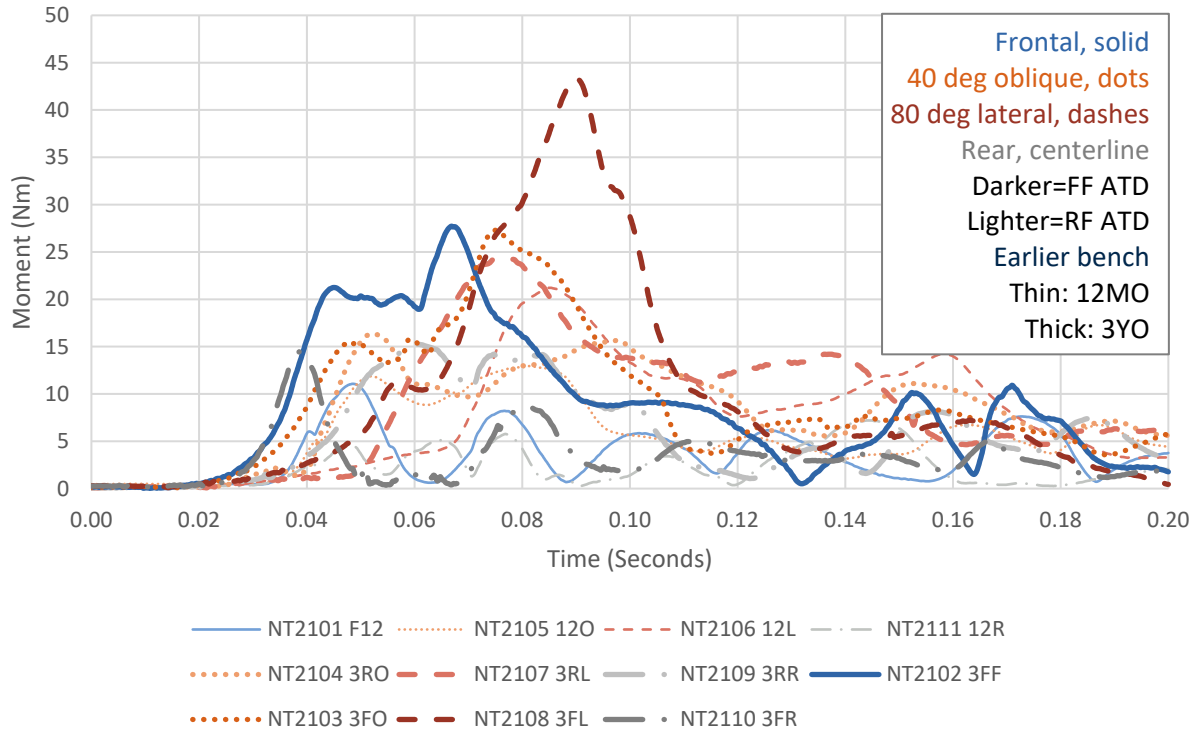


Figure C-7. Neck resultant moment for tests with CRABI 12MO and H33YO

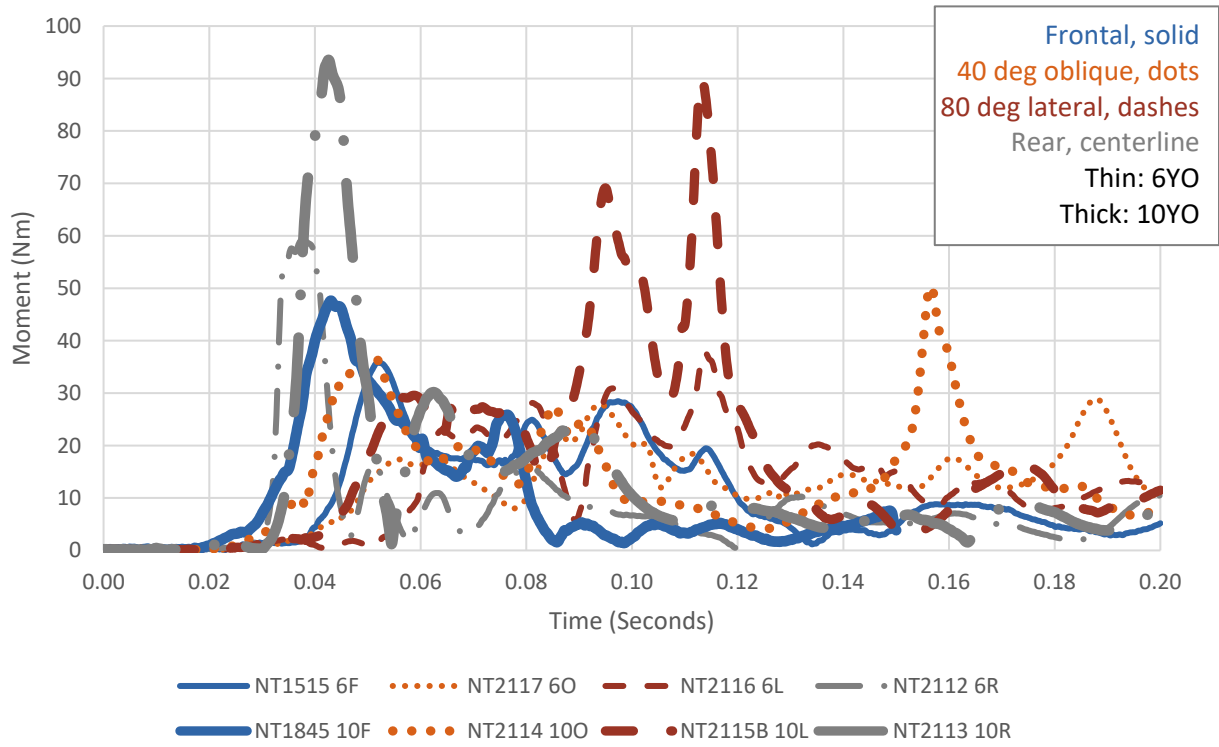


Figure C-8. Neck resultant moment for tests with H36YO and H310YO

DOT HS 813 434
April 2023



U.S. Department
of Transportation
**National Highway
Traffic Safety
Administration**



15821-032923-v3